

REPORT DOCUMENTATION PAGE			Form Approved OMB NO. 0704-0188		
<p>The public reporting burden for this collection of information is estimated to average 1 hour per response, including the time for reviewing instructions, searching existing data sources, gathering and maintaining the data needed, and completing and reviewing the collection of information. Send comments regarding this burden estimate or any other aspect of this collection of information, including suggestions for reducing this burden, to Washington Headquarters Services, Directorate for Information Operations and Reports, 1215 Jefferson Davis Highway, Suite 1204, Arlington VA, 22202-4302. Respondents should be aware that notwithstanding any other provision of law, no person shall be subject to any penalty for failing to comply with a collection of information if it does not display a currently valid OMB control number.</p> <p>PLEASE DO NOT RETURN YOUR FORM TO THE ABOVE ADDRESS.</p>					
1. REPORT DATE (DD-MM-YYYY) 28-03-2013		2. REPORT TYPE Final Report		3. DATES COVERED (From - To) 25-Aug-2009 - 26-Dec-2011	
4. TITLE AND SUBTITLE Center for Alternative Energy Storage Research and Technology - Final Progress Report			5a. CONTRACT NUMBER W911NF-09-1-0451		
			5b. GRANT NUMBER		
			5c. PROGRAM ELEMENT NUMBER 611102		
6. AUTHORS Lawrence T. Drzal, Jeff Sakamoto,			5d. PROJECT NUMBER		
			5e. TASK NUMBER		
			5f. WORK UNIT NUMBER		
7. PERFORMING ORGANIZATION NAMES AND ADDRESSES Michigan State University Hannah Administration Building 426 Auditorium Road, Room 301 East Lansing, MI 48824 -2612			8. PERFORMING ORGANIZATION REPORT NUMBER		
9. SPONSORING/MONITORING AGENCY NAME(S) AND ADDRESS(ES) U.S. Army Research Office P.O. Box 12211 Research Triangle Park, NC 27709-2211			10. SPONSOR/MONITOR'S ACRONYM(S) ARO		
			11. SPONSOR/MONITOR'S REPORT NUMBER(S) 57230-CH.24		
12. DISTRIBUTION AVAILABILITY STATEMENT Approved for Public Release; Distribution Unlimited					
13. SUPPLEMENTARY NOTES The views, opinions and/or findings contained in this report are those of the author(s) and should not be construed as an official Department of the Army position, policy or decision, unless so designated by other documentation.					
14. ABSTRACT Electrolytes, nano-structuring and graphene nanoplatelets for electrodes, and current collectors in batteries and supercapacitors were investigated. The following results were obtained: i) Nano-structuring of graphene nanoplatelets with and without conductive polymers produced supercapacitors with very high specific capacitance (>165 F/gm) and high frequency (>150 Hz) response with low losses; ii) graphene nanoplatelet thin films can replace copper current collectors in energy storage devices and save weight ~80% and reduced cost; iii) a					
15. SUBJECT TERMS alternative energy, batteries, supercapacitors, nanostructured, fault analysis, battery systems control					
16. SECURITY CLASSIFICATION OF:			17. LIMITATION OF ABSTRACT UU	18. NUMBER OF PAGES	19a. NAME OF RESPONSIBLE PERSON Lawrence Drzal
a. REPORT UU	b. ABSTRACT UU	c. THIS PAGE UU			19b. TELEPHONE NUMBER 517-353-7759

Report Title

Center for Alternative Energy Storage Research and Technology - Final Progress Report

ABSTRACT

Electrolytes, nano-structuring and graphene nanoplatelets for electrodes, and current collectors in batteries and supercapacitors were investigated. The following results were obtained: i) Nano-structuring of graphene nanoplatelets with and without conductive polymers produced supercapacitors with very high specific capacitance (>165 F/gm) and high frequency (>150 Hz) response with low losses; ii) graphene nanoplatelet thin films can replace copper current collectors in energy storage devices and save weight $\sim 80\%$ and reduced cost; iii) a relationship between the RTIL type and structure, interfacial capacitance, electron-transfer kinetics and reaction mechanisms of outer- and inner-sphere redox systems for sp^2 and sp^3 carbon electrodes was developed; iv) Reductions of internal resistance of supercapacitors and lithium ion batteries was achieved using silver nanorods 30-100nm in diameter, and approximately 200-300nm in length; v) a new ceramic electrolyte membrane technology, based on LLZO has produced an unprecedented combination of high ionic conductivity (~ 1 mS/cm), and stability against Li and air; vi) infusion of graphene nanoplatelets into carbon aerogel improves both electrical conductivity and mechanical integrity; vii) New balancing and bypassing circuits can maintain the original rated voltage of battery packs even when individual cells fail; and viii) faulty battery performance can be detected using time-frequency representations such as wavelet transforms.

Enter List of papers submitted or published that acknowledge ARO support from the start of the project to the date of this printing. List the papers, including journal references, in the following categories:

(a) Papers published in peer-reviewed journals (N/A for none)

<u>Received</u>	<u>Paper</u>
-----------------	--------------

03/27/2013	8.00	L. T. Drzal, S. Biswas. Multilayered Nano Architecture Of Graphene Nanosheets And Polypyrrole Nanowires For High Performance Supercapacitor Electrodes, Chemical Materials, (09 2010): 5667. doi:
03/28/2013	22.00	Ryan P. Maloney, Hyun Joong Kim, Jeffrey S. Sakamoto. Lithium Titanate Aerogel for Advanced Lithium-Ion Batteries, ACS Applied Materials & Interfaces, (05 2012): 2318. doi: 10.1021/am3002742
03/28/2013	23.00	Jeff Wolfenstine, Jeffrey Sakamoto, Ezhiyl Rangasamy. The role of Al and Li concentration on the formation of cubic garnet solid electrolyte of nominal composition Li ₇ La ₃ Zr ₂ O ₁₂ , Solid State Ionics, (01 2012): 28. doi: 10.1016/j.ssi.2011.10.022
03/28/2013	18.00	Jeff Wolfenstine, Ezhiyl Rangasamy, Jan L. Allen, Jeffrey Sakamoto. High conductivity of dense tetragonal Li ₇ La ₃ Zr ₂ O ₁₂ , Journal of Power Sources, (06 2012): 193. doi: 10.1016/j.jpowsour.2012.02.031
03/28/2013	19.00	J. L. Allen, J. Sakamoto, J. Wolfenstine. Electron microscopy characterization of hot-pressed Al substituted Li ₇ La ₃ Zr ₂ O ₁₂ , Journal of Materials Science, (02 2012): 4428. doi: 10.1007/s10853-012-6300-y
03/28/2013	20.00	Jennifer E. Ni, Eldon D. Case, Jeffrey S. Sakamoto, Ezhiyl Rangasamy, Jeffrey B. Wolfenstine. Room temperature elastic moduli and Vickers hardness of hot-pressed LLZO cubic garnet, Journal of Materials Science, (07 2012): 7978. doi: 10.1007/s10853-012-6687-5
03/28/2013	21.00	Jeff Sakamoto, Yong-Hun Cho, Jeff Wolfenstine, Ezhiylmurugan Rangasamy, Hyunjoong Kim, Heeman Choe. Mechanical properties of the solid Li-ion conducting electrolyte: Li _{0.33} La _{0.57} TiO ₃ , Journal of Materials Science, (04 2012): 5970. doi: 10.1007/s10853-012-6500-5
03/28/2013	5.00	D-Y. Kim, J-C. Yang, H-W. Kim, G. M. Swain. Heterogeneous electron-transfer rate constants for ferrocene and ferrocene carboxylic acid at boron-doped diamond electrodes in a room temperature ionic liquid, Electrochimica Acta, (04 2013): 49. doi:
03/28/2013	7.00	S. Biswas, L. T. Drzal. Multilayered Nano-Architecture of Variable Sized Graphene Nanosheets for Enhanced Supercapacitor Electrode Performance, ACS Applied Materials and Interfaces, (06 2010): 2293. doi:
03/28/2013	17.00	J.L. Allen, J. Wolfenstine, E. Rangasamy, J. Sakamoto. Effect of substitution (Ta, Al, Ga) on the conductivity of Li ₇ La ₃ Zr ₂ O ₁₂ , Journal of Power Sources, (05 2012): 315. doi: 10.1016/j.jpowsour.2012.01.131

TOTAL: 10

Number of Papers published in peer-reviewed journals:

(b) Papers published in non-peer-reviewed journals (N/A for none)

03/28/2013 2.00 E. Rangasamy, J. Wolfenstine, J. Allen, J. Sakamoto. The effect of 24c-site (A) cation substitution on the tetragonal-cubic phase transition in $\text{Li7-xLa3-xAxZr2O12}$ garnet-based ceramic electrolyte, J Power Sources, (01 2013): 261. doi:

TOTAL: **1**

Number of Papers published in non peer-reviewed journals:

(c) Presentations

J. Sakamoto, Invited presentation: "Keeping up with the increasing demands for electrochemical energy storage", National Academy of Engineering, Frontiers of Engineering, Vehicle Electrification Symposium, Warren, MI (2012).

J. Sakamoto, Invited presentation: "Fast ion conducting ceramic electrolyte based on Li7La3Zr2O12 garnet", Department Seminar, University of California, Los Angeles, CA (2012).

J. Sakamoto, "Invited presentation: Improving charge acceptance and safety through the development of highly-ordered and hierarchical electrodes for lithium ion batteries & Fast ion conducting ceramic electrolyte based Li7La3Zr2O12 garnet", Dow Distinguished Guest Lecture Series speaker, Dow Chemical Company, Midland, MI (2012).

J. Sakamoto, Invited presentation: "Fast ion conducting ceramic electrolyte based on Li7La3Zr2O12 garnet", Department Seminar, University of Michigan, Ann Arbor, MI (2012).

Invited presentation: J. Sakamoto, "Fast ion conducting ceramic electrolyte based on Li7La3Zr2O12 garnet", MSU, Bioeconomy Institute speaker, Holland, MI (2012).

J. Sakamoto, Invited presentation: "Fast ion conducting ceramic electrolyte based on Li7La3Zr2O12 garnet", American Ceramic Society, Electronic Materials and Application Symposium, Orlando, FL (2012).

J. Sakamoto, Invited presentation: "Fast ion conducting ceramic electrolyte based on Li7La3Zr2O12 garnet", Naval Research Laboratory, Anacostia, VA (2012).

J. Sakamoto, Invited presentation: "Improving charge acceptance and safety through the development of highly-ordered and hierarchical electrodes for lithium ion batteries & Fast ion conducting ceramic electrolyte based Li7La3Zr2O12 garnet", Ford Research Center, Dearborn, MI (2011).

Ezhiyl Rangasamy, Jeff Wolfenstine, Jeff Sakamoto "Fast ionic conducting Li7La3Zr2O12 " Presented at the Spring Materials Research Society Meeting in San Francisco, CA.

Hyun Joong Kim, Ryan Maloney, Inhwan Do, Hiroyuki Fukushima, Larry Drzal and Jeff Sakamoto, "Synthesis of exfoliated graphite nanoplatelet (xGnP) composite carbon aerogels for use in supercapacitors," oral presentation at the Spring, Materials Research Society Meeting in San Francisco, CA.

W. Qian, J. Cintron-Rivera, S. Han, X. Lu and F. Z. Peng, "Management and control of energy storage systems," presentation at the Joint 2010 IEEE Nanotechnology Materials and Devices Conference and 1st IEEE International Symposium on Energy, Environment, Safety and Security, Monterey, CA, USA, Oct., 2010.

Lawrence T. Drzal, "Exfoliated Graphite Nanoplatelets (xGnP): A Graphene Based Alternative for Improved Structural, Energy, Power, Barrier, and Thermal Applications", Carbon Nanotubes for Space Applications, Aerospace Corporation, El Segundo, CA, March 16, 2010.

Lawrence T. Drzal, (Invited) "Graphene Nanoplatelets (GnP) for Multifunctional polymers and Composites & Energy Generation and Storage Applications" DARPA-MITRE meeting Wash DC March 6-7, 2012

Lawrence T. Drzal, Biswas, S., "Layered Composite of Graphite Nanoplatelet and Polypyrrole for Supercapacitor Application" CERMACS ACS Meeting 2009, Cleveland, Ohio

Anchita Monga & Lawrence T. Drzal, "Metal oxide -graphite nanoplatelets composite as anode material for lithium ion batteries" SPE Automotive Composites Conference & Exhibition (ACCE), Troy MI September 2011)

Anchita Monga & Lawrence T. Drzal, "Nanostructured Metal doped Graphite Nanoplatelets as Anode Material for Lithium Ion Battery"

Anchita Monga, Lawrence T. Drzal, Oral presentation at Materials Research Society (MRS) Spring, 2011, San Francisco, CA (April 2011)

Anchita Monga & Lawrence T. Drzal, "Metal doped nanostructured graphite nanoplatelets as anode for lithium ion battery" "The 15th International Meeting on Lithium Batteries-2010", Montreal, Canada (June 2010)

Debkumar Saha and Lawrence T. Drzal, Performance Optimization of Graphite Nanoplatelet Based Electrode in Lithium Oxygen Battery, MRS Spring Meeting (2012).

Number of Presentations: 17.00

Non Peer-Reviewed Conference Proceeding publications (other than abstracts):

Received Paper

TOTAL:

Number of Non Peer-Reviewed Conference Proceeding publications (other than abstracts):

Peer-Reviewed Conference Proceeding publications (other than abstracts):

Received Paper

03/28/2013	14.00	J.Weigui , L. Xi , J. Yuan, T. Yingbin, F. Ran, F. Z. Peng. Low cost battery equalizer using buck-boost and series LC converter with synchronous phase-shift control, Applied Power and Electronics Conference, IEEE . 2013/03/06 00:00:00, . : ,
03/28/2013	15.00	X. Lu, W. Qian, F. Z. Peng. Modularized buck-boost + Cuk converter for high voltage series connected battery cells, IEEE Applied Power Electronics Conference and Exposition. 2012/03/14 00:00:00, . : ,

TOTAL: 2

Number of Peer-Reviewed Conference Proceeding publications (other than abstracts):

(d) Manuscripts

Received Paper

TOTAL:

Number of Manuscripts:

Books

Received

Paper

TOTAL:

Patents Submitted

J. Sakamoto, E. Rangasamy, H. Kim, R. Maloney, Y. Kim, "Methods of making and using oxide ceramic solids and products and devices related thereto", Filed non-Provisional Patent, 3000.048US1 MSU (2012)

Patents Awarded

Awards

Anchita Monga, "Metal Doped Nanostructured Graphite Nanoplatelets as Anode Material For Lithium Ion Batteries" 2nd Place Student Poster Award, 2011 Automotive Composites Conference and Exposition, September 13, 2011.

Anchita Monga "Replacement of Metal Current Collectors with Graphene Nanoplatelets in Advanced Lithium Ion Battery Electrodes" Research Translation Award at the 2012 MSU Engineering Graduate Research Symposium, 2012.

Graduate Students

<u>NAME</u>	<u>PERCENT SUPPORTED</u>	Discipline
Hui Zhao	0.50	
Gregory Spahlinger	0.50	
Sanjib Biswas	0.20	
Anchita Monga	0.50	
Debkumar Saha	0.50	
Ju Chan Yang	0.50	
Susan Farhat	0.50	
Ezhiyl Rangasamy	0.50	
Wei Qian	0.50	
Xi Lu	0.50	
Shuai Jiang	0.50	
Ramin Amiri	0.50	
FTE Equivalent:	5.70	
Total Number:	12	

Names of Post Doctorates

<u>NAME</u>	<u>PERCENT SUPPORTED</u>
Hyun Joong Kim	0.50
Hyouun Woo Kim	0.50
Chun-I Wu	0.50
Hyun Joong Kim	0.50
FTE Equivalent:	2.00
Total Number:	4

Names of Faculty Supported

<u>NAME</u>	<u>PERCENT SUPPORTED</u>	National Academy Member
Lawrence T. Drzal	0.05	
Jeffrey Sakamoto	0.05	
Greg Baker	0.05	
Greg Swain	0.05	
Martin Hawley	0.05	
Tim Hogan	0.05	
Elias Strangas	0.05	
Feng Peng	0.05	
FTE Equivalent:	0.40	
Total Number:	8	

Names of Under Graduate students supported

<u>NAME</u>	<u>PERCENT SUPPORTED</u>	Discipline
Anna Y. Cho	0.10	Chemistry
Jorge Cintron-Rivera	0.10	Electrical Engineering
FTE Equivalent:	0.20	
Total Number:	2	

Student Metrics

This section only applies to graduating undergraduates supported by this agreement in this reporting period

The number of undergraduates funded by this agreement who graduated during this period: 0.00

The number of undergraduates funded by this agreement who graduated during this period with a degree in science, mathematics, engineering, or technology fields:..... 0.00

The number of undergraduates funded by your agreement who graduated during this period and will continue to pursue a graduate or Ph.D. degree in science, mathematics, engineering, or technology fields:..... 0.00

Number of graduating undergraduates who achieved a 3.5 GPA to 4.0 (4.0 max scale):..... 0.00

Number of graduating undergraduates funded by a DoD funded Center of Excellence grant for Education, Research and Engineering:..... 0.00

The number of undergraduates funded by your agreement who graduated during this period and intend to work for the Department of Defense 0.00

The number of undergraduates funded by your agreement who graduated during this period and will receive scholarships or fellowships for further studies in science, mathematics, engineering or technology fields: 0.00

Names of Personnel receiving masters degrees

NAME

Total Number:

Names of personnel receiving PHDs

NAME

Susan Farhat

Sanjib Biswas

Ezhiyl Rangasamy

Xi Lu

Total Number:

4

Names of other research staff

<u>NAME</u>	<u>PERCENT SUPPORTED</u>
Karl Dersch	0.10
FTE Equivalent:	0.10
Total Number:	1

Sub Contractors (DD882)

Inventions (DD882)

Scientific Progress

See Attachment

Technology Transfer

ARO FINAL PROGRESS MarchREPORT

08/25/2009-12/26/2011

Proposal 57230CH, Agreement No. W911NF-0910451

Center for Alternative Energy Storage

Research and Technology

MICHIGAN STATE UNIVERSITY

Lawrence T. Drzal, PI

Tel. 517-353-5466 Email: drzal@egr.msu.edu

Abstract. Electrolytes, nano-structuring and graphene nanoplatelets for electrodes, and current collectors in batteries and supercapacitors were investigated. The following results were obtained: *i)* Nano-structuring of graphene nanoplatelets with and without conductive polymers produced supercapacitors with very high specific capacitance (>165 F/gm) and high frequency (>150 Hz) response with low losses; *ii)* graphene nanoplatelet thin films can replace copper current collectors in energy storage devices and save weight $\sim 80\%$ and reduced cost; *iii)* a relationship between the RTIL type and structure, interfacial capacitance, electron-transfer kinetics and reaction mechanisms of outer- and inner-sphere redox systems for sp^2 and sp^3 carbon electrodes was developed; *iv)* Reductions of internal resistance of supercapacitors and lithium ion batteries was achieved using silver nanorods 30-100nm in diameter, and approximately 200-300nm in length; *v)* a new ceramic electrolyte membrane technology, based on LLZO has produced an unprecedented combination of high ionic conductivity ($\sim 1\text{mS/cm}$), and stability against Li and air; *vi)* infusion of graphene nanoplatelets into carbon aerogel improves both electrical conductivity and mechanical integrity; *vii)* New balancing and bypassing circuits can maintain the original rated voltage of battery packs even when individual cells fail; and *viii)* faulty battery performance can be detected using time-frequency representations such as wavelet transforms.

Title and Abstract.....	1
Table of Contents	2
List of Figures	4
List of Tables.....	5
Abstract and Executive Summary.....	6
CAESRT Objectives	7
Research Participants	8
Research Organization.....	9
Scientific and Technical Goals and Objectives.....	9
Project Scientific Progress and Accomplishments.....	11
1. Polymer Electrolyte Membranes (G.Baker).....	11
Objectives.....	11
Description of Research Tasks.....	11
Summary of Baker Group Scientific Progress and Accomplishments.	12
I. Electrolyte Synthesis.....	12
2. Nanostructured Graphene Nanoplatelet Electrodes for Li Ion Batteries and Supercapacitors (L. T. Drzal).....	15
Objectives.....	15
Description of Research Tasks.....	15
Summary of Drzal Group Scientific Progress and Accomplishments.	15
I. Multilayered Nano Architecture of Graphene Nanosheets and Polypyrrole Nanowire for High Performance Supercapacitor Electrode	16
II. Replacement of Metal Current Collectors with Graphene Nanoplatelets in Advanced Lithium Ion Battery Electrodes	20
III. Metal Doped Graphene Nanoplatelets as Anode Material.....	26
IV. Graphene Nanoplatelets for the Fabrication of Lithium-Air Battery Cathode.....	31
3. Microstructure, Surface Chemistry and Properties of sp ² and sp ³ Carbons (G.Swain).38	
Objectives.....	38
Description of Research Tasks.....	41
Summary of Swain Group Scientific Progress and Accomplishments.....	42
I. Heterogeneous Electron-Transfer Kinetics in RTILs	43
II. Double-Layer Effects on ET Kinetics at Diamond Electrodes	43
III. Diamond Powders as New EDLC Electrodes	44
IV. Double Layer Capacitance of Graphene - Effect of Electrolyte Species	45
4. High Surface Area Electrodes as Electrodes (T.Hogan)	46
Objectives.....	46

Description of Research Tasks.....	46
Summary of Hogan Group Scientific Progress and Accomplishments.....	47
I. Growth of Nanowires for High Surface Area Electrodes	47
5. Composites with Dielectric Properties and Capacitive Density for Applications as Embedded Capacitors (M. Hawley)	49
Objectives.....	49
Description of Research Tasks.....	51
Summary of Hawley Group Scientific Progress and Accomplishments.....	53
I. Magneto-Dielectric Materials for Wireless Energy Transport	53
6. Graphene Nanoplatelets (GnP) for Applications in Lithium Ion Batteries and Supercapacitors (J. Sakamoto)	56
Objectives.....	56
Description of Research Tasks.....	58
Summary of Sakamoto Group Scientific Progress and Accomplishments.....	58
I. Synthesis of Exfoliated Graphite Nanoplatelet (GnP) Composite Carbon Aerogels	59
II. Synthesis and Characterization of Sol-Gel Ceramic Oxides for Lithium-Air Batteries	60
7. Novel Management and Control Approaches for Battery System (F. Peng)	61
Objectives.....	61
Description of Research Tasks.....	61
Summary of Peng Group Scientific Progress and Accomplishments.....	62
I. Balancing and Bypassing Circuits to Provide Fail Safe Battery Ssystem Operation	63
8. Online and Precise Health Monitoring of Batteries Under Thermal Abuse Conditions (E. Strangas).....	65
Objectives.....	65
Description of Research Tasks.....	67
Summary of Strangas Group Scientific Progress and Accomplishments.....	68
I. Healthy Mode Operation.....	68
II. Fault Diagnosis and Prognosis.....	69
Publications and Presentations from ARO Support	70
Students Supported	71
Technology Transfer.....	71
References	72

List of Figures and Illustrations

Figure 1. Graphical representation of Li ion nanoparticles self-assembled into a conducting network.

Figure 2. Temperature dependent conductivity of polymeric TFSI analogues grown from modified silica nanoparticles in PEG500-DM. The carrier concentration (Li^+) is expressed as the ratio between the ether oxygen atoms of the PEG500-DM.

Figure 3. Monolayer of GnP showing conductivity and transparency.

Figure 4: Morphology of polypyrrole nanowire: A highly dispersed network polypyrrole nanowire with an average diameter of 40 to 60 nm is attached to the large basal plane of graphene nanosheets in figure a,b. With multilayer deposition, the highly fibrous morphology of these nanowires is shown in figure c,d.

Figure 5: Electrochemical characterization: Cyclic voltammetric characteristics of multilayer composite of polypyrrole / graphene nanosheets and control polypyrrole sample at increasing voltage scanning rate from 25 to 100 mv/sec

Figure 6. Cyclic stability: At 1 A/gm constant current density, the multilayer composite of polypyrrole and graphene nanosheets continues to maintain a highly symmetric charge discharge characteristics from 100th to 1000th electrochemical cycles with a potential drop of only 30 mv

Figure 7. SEM Images of the GnP paper (as made) at different magnifications

Figure 8: Testing protocol of galvanostatic cycling for performance evaluation

Figure 9. Cross-sectional SEM Images of the electrode at different magnifications (a) & (b), followed by high mag images of (c) GnP paper (d) active material region

Figure 10. SEM images of X-sectional view of (a) current collector GnP paper, (b) the unpressed and (c) pressed electrodes.

Figure 11. SEM images showing cross-sectional view of GnP-15 electrode on different current collectors: (a) Copper (b) GnP paper

Figure 12. Representative Galvanostatic Performance of GnP-15 at different charge rates (a) Active material (b) Total weight including the substrate weight of GnP paper

Figure 13. EIS Analysis of GnP electrodes on cycling (a) Copper current collector (b) GnP Paper as current collector; Comparison of (c) uncycled electrodes (d) after 5 cycles

Figure 14. Electrochemical Performance of LTO electrodes casted on different current collectors (a) On copper (b) On GnP Paper

Figure 15. Schematic showing the potential of metal doped carbon as anodes for lithium ion batteries

Figure 16. Nickel nanoparticle doped GnP platelets (Scale bar- a: 20 nm, b & c: 1 μm)

Figure 17. XRD pattern of nickel doped materials in comparison with undoped GnP (a) Full spectra (b) Ni peaks

Figure 18. Galvanostatic performance of nickel doped materials in comparison with undoped GnP (a) Protocol (b) Undoped GnP (c) GnP_Ni-60 (d) GnP_Ni-30c

Figure 19. Cyclic Voltammogram of Ni doped materials

Figure 20. Tin based nanoparticle doped GnP platelets (Scale bar- a: 5 nm, b: 2nm)

Figure 11. Working principle of a non-aqueous Lithium-air battery

Figure 2 Average discharge performances of GNP paper electrodes ('a', 'b', and 'c' from table 2)

Figure 3 A typical discharge profile of a GnP paper electrode

Figure 24. Comparison of discharge performances of GnP paper electrodes ('a', 'b', and 'c' from table 1) and GNP coated stainless steel cloth electrode along with material loading on each electrode

Figure 25 Comparison of discharge performances of GNP paper electrodes ('a', 'b' and 'c' from table 2; 'd' from table 3) along with material loading on each electrode

Figure 26 Comparison of discharge performances of GNP paper electrodes ('a', 'b' and 'c' from table 1; 'd' from table 2) along with thickness of each electrode

Figure 27. Electrochemical property characterization (cyclic voltammetry) and the microstructure (Raman Spectroscopy) of electrically conducting diamond powder and graphene.

Figure 28. Silver nanorod growth on metal substrates to be used as an electrode for carbon nanoparticle decoration and supercapacitor applications (scale bars are 1 μ m in the top two images, and 100nm for the bottom two images).

Figure 29. Coins placed closer to the evaporation source showed little, or no metal nanorod growth.

Figure 30. Illustration of Periodic FSS Layers

Figure 31. Illustration of Composite Geometry and FSS Arrays

Figure 32. Permittivity and Permeability Illustrations

Figure 33. Li diffusivity during de-intercalation from graphite is slow below -20 $^{\circ}$ C, thus causing cell polarization

Figure 34. SEM of carbon aerogel with 2 wt% GnP. The red circles highlight the GnP embedded in the carbon aerogel

Figure 35. Test results for battery cell charge/discharge with/without balance circuit

Figure 36. Test configuration of the defective cell bypass using the modular buck-boost balance circuit

LIST of TABLES

Table 1. Comparison of properties of copper foil and GnP paper as current collectors

Table 2. Different categories of GNP papers

Table 3. GNP-M/C hybrid bilayer paper specifications

TABLE 4. Test Data With Two Defective Cells

ARO FINAL REPORT
08/25/2009-12/26/2011
Proposal 57230CH, Agreement No. W911NF-0910451

Center for Alternative Energy Storage
Research and Technology
MICHIGAN STATE UNIVERSITY

Lawrence T. Drzal, PI
Tel. 517-353-5466 Email: drzal@egr.msu.edu

Abstract. Electrolytes, nano-structuring and graphene nanoplatelets for electrodes, and current collectors in batteries and supercapacitors were investigated. The following results were obtained: *i)* Nano-structuring of graphene nanoplatelets with and without conductive polymers produced supercapacitors with very high specific capacitance (>165 F/gm) and high frequency (>150 Hz) response with low losses; *ii)* graphene nanoplatelet thin films can replace copper current collectors in energy storage devices and save weight $\sim 80\%$ and reduced cost; *iii)* a relationship between the RTIL type and structure, interfacial capacitance, electron-transfer kinetics and reaction mechanisms of outer- and inner-sphere redox systems for sp^2 and sp^3 carbon electrodes was developed; *iv)* Reductions of internal resistance of supercapacitors and lithium ion batteries was achieved using silver nanorods 30-100nm in diameter, and approximately 200-300nm in length; *v)* a new ceramic electrolyte membrane technology, based on LLZO has produced an unprecedented combination of high ionic conductivity ($\sim 1\text{mS/cm}$), and stability against Li and air; *vi)* infusion of graphene nanoplatelets into carbon aerogel improves both electrical conductivity and mechanical integrity; *vii)* New balancing and bypassing circuits can maintain the original rated voltage of battery packs even when individual cells fail; and *viii)* faulty battery performance can be detected using time-frequency representations such as wavelet transforms.

Executive Summary

The Center for Alternative Energy Storage Research and Technology (CAESRT) has been established* to conduct innovative, high impact, fundamental and applied research in materials, technology and systems for storing and retrieving energy. CAESRT will achieve this goal through developing the next generation of energy storage batteries and electrochemical capacitors through the use of nanomaterials and nanoarchitectures to overcome existing limitations with current designs.

The goal is the synthesis, design and validation of energy storage devices and systems that have high power densities; are durable, safe, light-weight, and environment-friendly; are scalable in size for specific applications; and are relevant to both DoD and civilian markets. Research at CAESRT has been directed primarily at Defense Department (Army) applications to provide effective technology transfer to government and industry.

Effective energy storage is a critical technology for alternative energy since it facilitates load management and exploitation of diurnal cost differentials as well as ability to utilize non-stationary sources of alternative energy such as wind and solar energy. Concurrently, the national effort at developing alternative energy generation options relies critically on the ability to store and retrieve energy as well. CAESRT has focused its research efforts in energy storage to:

- Nanomaterials for High Performance Energy Storage Devices,
- Nanostructuring of Materials for High Energy and High Power Devices
- Identification of Device Failure Mechanisms during System Performance
- Multi-level Modeling and Simulation, Incorporating Self-diagnostics for Energy Storage System Design

CAESRT OBJECTIVES

The objectives of the CAESRT research program are to: *i)* gain a fundamental understanding of the atomic and molecular level processes that govern the operation, performance and failure mechanisms of energy storage systems; *ii)* design and investigate nanostructured materials with the goal of increasing the performance, durability and reliability of batteries and supercapacitors; *iii)* explore nanostructuring of materials for battery and supercapacitor materials to facilitate fast electron and ion transport and *iv)* develop systems level control and operation paradigms (with a focus on batteries and supercapacitors;

The objectives of CAESRT are achieved through fundamental research directed at understanding the atomic and molecular level processes that govern the operation, performance and failure of current materials used in energy storage devices and identifying the underlying principles that govern these complex and interrelated phenomena. To achieve these requirements, fundamental research must be conducted on energy storage materials, device design, and system-level operational strategies.

Specifically, CAESRT has conducted interrelated research on: nanostructured battery and capacitor electrodes that are sustainable, failure-tolerant and reliable; new innovative hierarchically structured polymer electrolytes with high conductivities, excellent mechanical properties, as well fabrication and cost advantages; development of in-situ analysis and characterization techniques at the micro and mesoscopic levels to observe the dynamic structure and composition of at an

electrode surface in real time during charge transport and transfer; and systems level analysis, modeling, and experimental investigation of the interaction of energy storage parameters and dynamics, load demand and the dynamics of the prime energy sources. As a result of the synergy between these research areas, the ability to monitor the health, diagnose faults and predict system, subsystem and component failures under different operating conditions is also being developed.

**CAESRT was originally proposed as a three year program after which its operation would be self-sufficient and funded through industry, state and other sources. Because of changes that took place at the federal level, funding for this program consisted of one year plus a no-cost time extension.*

RESEARCH PARTICIPANTS

The research under the Center for Alternative Energy Storage Research and Technology (CAESRT) has been conducted in facilities in the Colleges of Engineering and Natural Sciences. Faculties from the College of Engineering (Chemical Engineering, Materials Science and Electrical and Computer Engineering) as well as the College of Natural Science (Chemistry) were the participants in this program. The research program was led by a senior faculty member (Prof. Lawrence Drzal) of the College of Engineering who reported to the Associate Dean for Research (Dr. Leo Kempel). The group of faculty researchers has expertise in: nanomaterials and nanoarchitectures for energy storage devices, power conditioning, intelligent storage technologies, and potential user technologies will be part of the research mission. The faculty participants and their expertise are:

Gregory L. Baker**, PhD., Chemistry. Electrolyte membranes for batteries and fuel cells, controlled polymerizations from surfaces

Lawrence T. Drzal, PhD., Chemical Engineering and Materials Science. Graphene nanoplatelets; nanostructuring of materials; and surface functionalization of materials for energy storage

Martin C. Hawley, PhD., Chemical Engineering and Materials Science. Carbon nanotube synthesis; Chemical kinetics; transport phenomena; plasma reactions; electromagnetic processing of materials;

Timothy Hogan, PhD., Electrical and Computer Engineering. Charge transport measurements, pulse laser deposition of new electronic materials, and synthesis of nanowires

Fang Z. Peng, PhD., Electrical and Computer Engineering. Power electronics, motor drives, hybrid electric vehicles, renewable energy interface systems

Jeffrey Sakamoto, PhD., Chemical Engineering and Materials Science. Materials for energy and medical technology: nanostructured device fab and testing, aerogel-based thermal insulation, lithium-ion battery research

Elias Strangas, PhD., Electrical and Computer Engineering, Electrical machines and drives, Electromechanical Systems

Greg M. Swain, PhD., Chemistry. Electrochemistry, and advanced sp^2 - and sp^3 -bonded carbon materials for energy storage and conversion

**** Tragically, Professor Greg Baker passed away unexpectedly.**

RESEARCH ORGANIZATION

The goals of CAESRT are to be pursued by the faculty participants through simultaneous investigations of several interrelated research areas. While each researcher has responsibility in his area of expertise, the operational mode of CAESRT will be highly interactive and collaborative. The materials synthesis, characterization and device fabrication activity will advance from the laboratory stage to the systems level through fabrication of devices to be tested in the 1.2 kWh battery/super-cap energy storage system test-bed under the direction of Professor Peng. Post failure analysis will be provided to the nanomaterials and nano-architecture activities for modification and optimization in order to verify the nanostructuring approach and achieve systems level success.

Experimental Tasks (Participants/Responsibilities)

- Polymer Electrolyte Development (Baker)
- Nanomaterial Synthesis and Functionalization (Hawley, Hogan, Sakamoto, Swain, Drzal, Baker)
- Battery and Supercapacitor Fabrication (Sakamoto, Drzal, Swain, Hawley)
- Nanostructured Material Characterization (Hogan, Sakamoto, Drzal, Swain)
- Electrochemical Characterization (Swain, Sakamoto, Hogan, Drzal)
- Battery and Supercapacitor Testing and Evaluation (Peng, Sakamoto)
- Simulation And Design Tools For Materials Selection (Hawley)
- Failure, Fault Analysis and Prognosis under Load, (Strangas, Peng)
- Systems Level Management and Control Issue Identification and Improvement (Peng)

SCIENTIFIC AND TECHNICAL GOALS AND OBJECTIVES:

The CAESRT Research program has as its objectives to: *i)* nanostructure the battery anode, cathode, and electrolyte materials as well as supercapacitor electrode materials in order to extend their performance, durability and reliability and *ii)* to develop systems level health monitoring and fault analysis technology coupled with management and control methodology for optimized system level performance under operational conditions.

Specific Aims:

Nanostructured Electrodes and Electrolytes for Batteries and Supercapacitors:

Supercapacitors: High surface area metal electrodes modified by coatings of graphene nanoplatelets and/or carbon aerogel and graphene nanoplatelet multilayered nano-architecture to provide high frequency capacitive response, small equivalent series resistance losses at 1000 mV/sec scanning rate, and fast ionic diffusion for high power electrical double layer capacitor applications

Preparation, characterization and determination of the relationship between the physical, chemical and microstructural properties and the capacitance and heterogeneous rates of electron transfer of high surface area, electrically conducting diamond powders and graphene nanoplatelets in aqueous-based redox systems

Design and development of novel two dimensional periodic metallic arrays of selected shape particles nanostructured into multilayered composites to produce frequency selective surface multilayers for embedded capacitors having high dielectric constant, low dielectric loss (low dissipation factor), increased capacitive density, wideband performance, and simple processability. The capacitive and inductive elements will be selected based on the desired reflection and transmission characteristics as well as the desired bandwidth.

Batteries: Synthesis of ceramic electrolytes and catalyst supports for metal-air, solid-state batteries and supercapacitors. New process for synthesis of LiLaTiO_3 for use in lithium batteries. Highly conductive polymer based nanoparticle systems with lithium counter-ions immobilized on their surfaces to produce high conductivity solid electrolytes.

System Level Health Monitoring and Management and Control: Development of different classification algorithms from the high-frequency portion of the current signal to detect the on-line condition of batteries under thermal abuse conditions using time-frequency representations (e.g. wavelet transform features).

Identify and address the management and control issues in existing energy storage systems. Initial focus is on: the characteristics of different Li-ion batteries; the problems of using low-voltage battery cells in a high voltage battery pack; the present circuits and charge methods to increase the battery capacity utilization and lifetime; the defective cell bypass protective method to ensure reliable long-term operation; the hybrid combination of batteries and supercapacitors to optimize the dynamic performance; investigation of highly efficient bidirectional dc-dc converter topologies for voltage boosting.

PROJECT SCIENTIFIC PROGRESS AND ACCOMPLISHMENTS

1. Polymer Electrolyte Membranes- Gregory L. Baker

Objective:

- To develop mechanically robust ion electrolytes with Li^+ conductivities $>10^{-4}$ S/cm.
- To improve the stability of the SEI and inhibit dendrite formation.

Background: Among the various existing energy storage technologies, rechargeable lithium and lithium ion batteries are an effective solution for high-energy density electrochemical power sources. However, lithium metal anodes react with conventional liquid electrolytes to form a passivation layer that limits electrode utilization, and the formation of lithium dendrites during charging leads to safety concerns. Liquid electrolytes

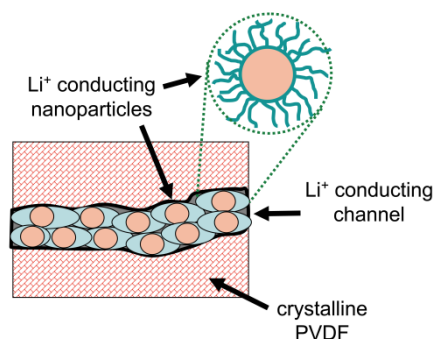


Figure 1. Graphical representation of Li ion nanoparticles self-assembled into a conducting network.

also suffer from problems such as electrolyte leakage, flammability, and electrolytic degradation of the organic electrolyte. Solid polymer electrolytes could overcome these problems, and provide lithium batteries with better stability and longer cycle life. Although the potential benefits of polymer electrolytes are well recognized, the optimization of mutually exclusive properties such as high conductivity, good mechanical strength, and easy processing, has not been achieved.

We will synthesize Li^+ conducting nanoparticles that self-assemble into conducting networks within hydrophobic polymers *Figure 1*. The resulting

composites will have superior single-ion conductivities and mechanical properties. Since we will use rigid poly(vinylidene fluoride) (PVDF) as the hydrophobic polymer, we also expect that this approach will greatly limit dendrite formation and provide mechanical and dimensional stability up to the melting point of PVDF ($>160^\circ\text{C}$). Finally, the two-phase approach to membrane design promises to reduce the cost of membrane manufacturing costs, since the particles and the hydrophobic polymer can be independently optimized.

Description of Research Tasks:

Task 1: Nanoparticle synthesis and formation of conducting membranes. We will use standard chemistry to modify the surface of silica nanoparticles (10-30 nm diameter). We previously used the same techniques to modify fumed silica and silica nanoparticles for proton conductors. Rather than simply attaching acids groups to the nanoparticle surface, we will use atom transfer radical polymerization (ATRP) to grow polystyrene chains from

the nanoparticle, and then sulfonated the polystyrene to obtain particles suitable for ion transport. Using sulfonic acid-containing *polymers* greatly amplifies the number of groups that can be anchored to a nanoparticle. Loading the particles into a DMF solution of polyvinylidene fluoride (PVDF) and evaporation of the solvent at $\sim 50\text{ }^{\circ}\text{C}$ will provide mechanically robust (comparable to PVDF) electrolytes with high single ion Li^+ conductivities.

Task 2: Characterization of electrolytes. Characterization of the electrolytes will focus on understanding the relationship between the bulk conductivity and the bicontinuous network formed by dispersing nanoparticles in PVDF. Various microscopy techniques (SEM, TEM, confocal) will be used to elucidate the conducting channels in the PVDF matrix. In situ analysis by X-ray tomography would be particularly useful. Basic electrochemical characterization such as impedance spectroscopy will be measured in the Baker lab. Cycling experiments designed to test for dendrite formation and stable SEI layers will be carried out in collaboration with Professor Jeff Sakamoto in the Department of Chemical Engineering and Materials Science.

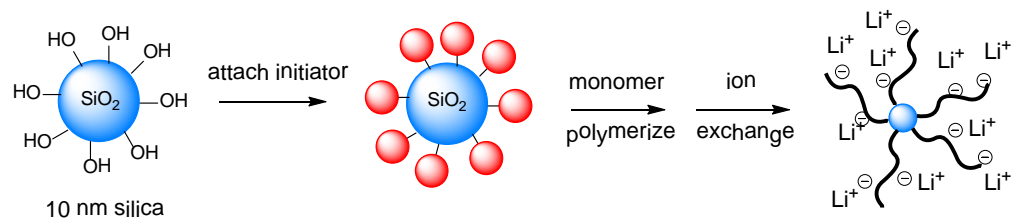
Summary of Baker Group Scientific Progress and Accomplishments.

When a lithium ion battery is discharged, electrons flow from the anode to the cathode through the external circuit, while inside the cell, lithium cations, formed at the anode, migrate and intercalate into the cathode. Typical measurements of the Li^+ transference number (T_{Li^+}) in typical electrolytes range from 0.2-0.3, which indicates the anion as the dominant species in Li^+ transport. Since a low T_{Li^+} limits a battery's power density and often affects the chemical stability of electrolytes, development of electrolytes with near-unity lithium ion transference numbers is important. In the research accomplished in this project, polymer grafted nanoparticles systems were developed where the anions are immobilized. However, their conductivity never exceeded 10^{-4} S/cm . Current work explores structure-function relationships in the conductivity of polymer architectures, targeting new designs for high Li^+ transference electrolytes.

I. Electrolyte Synthesis

Several nanoparticle systems were investigated where lithium counterion grafted polymers were attached to nanoparticles. Since the process is similar for all monomers, the example of sodium polystyrene sulfate is described and is indicative of all of the results. As shown in *Scheme 1*, initiators were attached to 10 nm silica nanoparticles, and using Atom Transfer Radical Polymerization (ATRP), a controlled method useful for growing polymers from the surfaces, sodium styrene sulfonate was polymerized from the particles. After polymerization and purification, the sodium sulfonate groups were converted to the corresponding lithium salt by an ion exchange process.

Scheme 1



Electrolytes were prepared from the purified particles and low-molecular weight (~ 500 g/mol) polyethylene glycol dimethyl ether. (PEG500-DM) The conductivity data, shown in *Figure 2*, show the temperature-dependent conductivity as measured by impedance spectroscopy. The data show the characteristic increase in conductivity with temperature, as expected for thermally activated ion transport. In addition, the conductivity increased with the concentration of the lithium salt (plotted as the O:Li ratio, equivalent to the volume fraction of the modified nanoparticles). The maximum conductivity occurred at

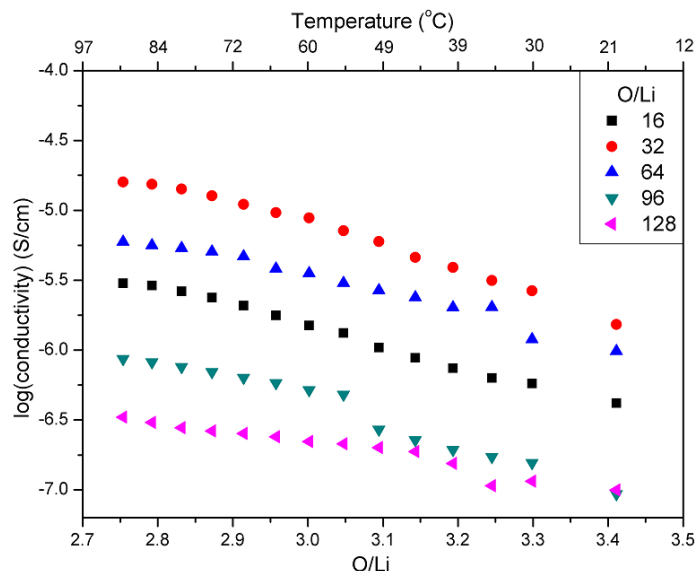


Figure 2. Temperature dependent conductivity of polymeric TFSI analogues grown from modified silica nanoparticles in PEG500-DM. The carrier concentration (Li^+) is expressed as the ratio between the ether oxygen atoms of the PEG500-DM.

O:Li = 16; materials prepared with higher particle contents were poorly mixed and were discontinuous due to the low volume fraction of the PEG500-DM. The absolute conductivity is comparable to the single ion conductors described in the literature. The low conductivities for aryl sulfonate modified particles are not discouraging on their own, since aryl sulfonates generally provide electrolytes with modest conductivities.

High conductivity requires dissociation of the Li^+ from the anion. Anions such as ClO_4^- , PF_6^- and bis(trifluoromethylsulfonyl amide) (TFSI) are therefore commonly used in electrolytes. A polymerizable analogue of TFSI was synthesized and the corresponding polymers were grown from silica nanoparticles. As shown in *Figure 2*, electrolytes prepared from the particles gave the highest conductivities. The conductivity at 30°C does not exceed 10^{-5} S/cm, which is typical for polymer-based single ion conductors. A lack of promising results caused us to reconsider and modify our approach in the present project.

Copper-catalyzed alkyne azide cycloaddition (CuAAC) is a powerful method for coupling and for post-synthetic modification of polymers and has become a staple of modern polymer chemistry. However, CuAAC has rarely been used in the synthesis of polymer electrolyte materials. It was intended to investigate alkynylated nanoparticles as CuAAC tunable single ion conductors previously; however, it was decided to investigate oligomer model compounds to discern the impact of the resulting triazole moieties on ionic conductivity.

Oligomer model compounds with ether oxygen to triazole ratios of 6:2, 8:2 and 8:1 and molecular weights close to 500g/mol were designed and synthesized. Conductivity in the salt complexes of these compounds was as many as 10 times lower than that of poly(ethylene glycol) 500 dimethyl ether, at 30°C and nearly the same in all compounds at 85°C. Additionally, conductivity was found to correlate more strongly with glass transition temperature (T_g) than with triazole content. Electronic structure calculations at the G3(MP2) level have shown that while the triazole moiety is a stronger binder of Li^+ in a monocoordinate complexes, the difference decreases with coordination number and becomes trivial ($\sim 3\text{kJ/mol}$) in 4 coordinate complexes. The crystallization behavior of the 6:2 model enabled single crystal XRD analysis, which showed dipole-dipole interactions to be the main intermolecular force. The decrease in conductivity observed in the model compounds is hypothesized to be an effect of chain dynamics. Bipolar pulse pair stimulated echo NMR experiments have been proposed to measure the coefficients of self diffusion and charge carrier diffusion in the oligomer model compounds, which should enable a complete analysis, and publication. These efforts are ongoing.

A final direction is the proposal and synthesis of ionic liquid conductors with 3 tethered charges: two anions and one cation. Theoretically these should have a lower T_{Li^+} than true single ion conductors, but may be conductive enough for application.

2. Nanostructured Graphene Nanoplatelet Electrodes for Li Ion Batteries and Supercapacitors - Lawrence T. Drzal

Objectives:

- To synthesize graphene nanoplatelets (GnP) with controlled edge chemistry for electrode applications in lithium ion batteries and supercapacitors
- To optimize nanostructured morphology and GnP size and surface chemistry to achieve energy and power metrics
- To fabricate nanostructured electrodes, Li ion batteries and supercapacitors using GnP in sizes and at scales suitable for energy storage devices in a 1.2 kWh battery/super-cap system

Description of Research Tasks:

Task 1. Electrode structure can be manipulated through control of graphene nanoplatelet thickness, platelet separation, graphene surface chemistry, conductive polymer morphology, etc., to achieve minimum ESR with high energy and power density at high cyclic stability. Chemical functionalization of the graphene nanoplatelets can take place on the edges of the platelets (with ease) and the graphene surface (with difficulty). Reduction of contact resistance between particles while assuring high conductivity within the graphene nanoplatelets is the key to achieving high performance. Gas phase reduction of the GnP will be used to remove unwanted edge and surface groups such as hydroxyl and carboxylic acid groups and replace them with either hydrogen or desirable functional groups. By tailoring the surface chemistry, the compatibility of the GnP with various liquids will also be altered to insure optimum dispersion and controlling the self-assembly into monolayers. The self-assembly of graphene nanoplatelets with different nanostructures of conductive polymers and the application of this graphene nanosheet-polypyrrole electrode as a free standing supercapacitor film in a liquid electrolyte is also to be investigated.

Task 2. High resolution SEM, XPS, EDX and AFM will be used to quantify the resulting electrodes and assembled cells. Cyclic voltammetry, constant current chronopotentiometry and impedance spectroscopy will be used to characterize the electrochemical performance of the batteries and supercapacitors.

Summary of Drzal Group Scientific Progress and Accomplishments

Background: Recently, a process has been developed in the Drzal Group for quickly and reproducibly depositing large areas of monolayers of thin sheets of graphene on any surface. The graphene sheets are synthesized into nanoplatelets shape by an intercalation and exfoliation process which directly produces graphene nanoplatelets with dimensions

ranging from 50 microns to 0.1 micron in diameter and controllable thicknesses ranging from 20 nm to < 1 nm. Graphene is a highly attractive new form of graphite. Graphene has the inherent stability of graphite along with exceptional thermal and electrical conductivity. The edge sites of the nanoplatelets are locations for the formation of a variety of carbon-oxygen functional groups that strongly influence the GnP polarity.

A new method of fabrication of graphene nanosheets into large area planar nanometer thin films has been developed based on the self-assembly of conductive polymer and graphene nanosheets resulting in exquisite control over the orientation and the alignment of the nanosheets within the film. [1] *Figure 3* shows results for a monolayer made by this process with thicknesses of 4, 10 and 20 nm made from 1 micron graphene

Glass slide coated with xGnP with ~80% transmission in visible spectrum

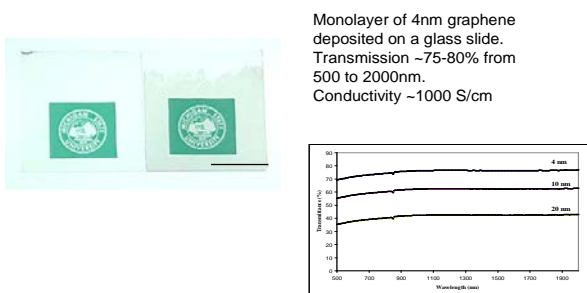


Figure 3. Monolayer of GnP showing conductivity and transparency.

nanosheets on a glass slide. The surface conductivity of this film is about 1,000 S/cm. The transparency of this monolayer varies with the thickness of the graphene nanosheet as shown. The 4 nm film has a transparency over the visible range of approximately 80%. Thinner monolayers are expected to have higher transparency and the same conductivity. The level of transparency and conductivity for the 4nm film equals that of conventional ITO and FTP coatings. The process for producing these monolayers films of graphene nanoplatelets is robust and fast. It is

scalable to any lateral dimension.

I. Multilayered Nano Architecture of Graphene Nanosheets and Polypyrrole Nanowire for High Performance Supercapacitor Electrode

A novel nano architecture has been developed by combining the nanostructured conductive polymer polypyrrole with highly electrically conductive graphene nanosheets in a multilayered configuration to achieve high specific capacitance and low electronic resistance for supercapacitor electrode application. Fibrous network of polypyrrole nanowire with high electrolyte ionic accessibility was interspersed with electrically conductive monolayers of highly dispersed and aligned network of large sized graphene nanosheets as a series of current collectors within the macroscopic configuration for enhanced electronic charge transport inside the bulk electrode. Capillary force and drying induced self-assembly coupled with the strong van der Waals force of attraction between highly aromatic graphene basal plane and π conjugated conductive polymer chains was employed to create a 100% binder free multilayered stacking of these two distinct

nanostructured elements to construct the electrode. This multilayer composite electrode exhibits a high specific capacitance 165 F/gm with a nearly ideal rectangular cyclic voltammogram at increasing voltage scanning rate and high electrochemical cyclic stability.

Results and discussion: Fabrication of multilayered nano architecture with large and small sized nanosheets of graphene nanosheets from the liquid-liquid interfacial approach have been demonstrated to develop a supercapacitor electrode with enhanced capacitance and improved rate capabilities. In this approach, the use of monolayers of highly electrically conductive large sized graphene nanosheets served as a series of current collectors within the multilayer configuration to achieve rapid charge discharge characteristics with minimum equivalent series resistance. In a similar approach large sized graphene nanoplatelet sheets have been integrated with polypyrrole nanowires to reduce electronic resistance and increased ionic accessibility from the presence of fibrous network of nanowires on the electrochemical energy storage, rate capability and cyclic stability of this new composite supercapacitor electrode. A surfactant assisted soft template approach was employed to prepare polypyrrole nanowire with an average diameter from 40 to 60 nm.

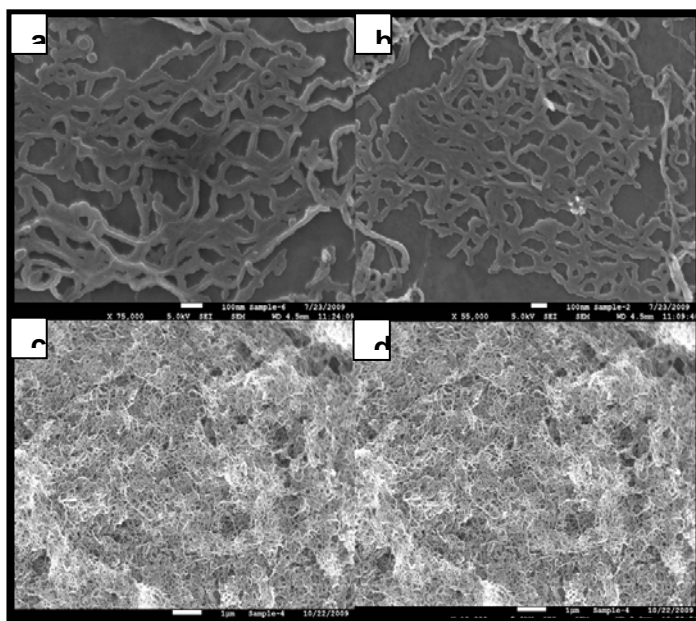


Figure 4: Morphology of polypyrrole nanowire: A highly dispersed network polypyrrole nanowire with an average diameter of 40 to 60 nm is attached to the large basal plane of graphene nanosheets in figure a,b. With multilayer deposition, the highly fibrous morphology of these nanowires is shown in figure c,d

To investigate the morphology and dispersion of polypyrrole nanowire on the graphene nanosheets, a thin film of nanowire was first transferred on a substrate coated with a monolayer film of graphene nanosheets. On complete liquid evaporation, strong van der Waal's force of attraction between the highly aromatic graphene basal plane and the π conjugated polymer film adheres these two nanostructures one on top of another. The attachment of nanowires on the graphene nanosheets was found to be strong enough that the dry film could not be washed away with flowing water. FESEM micrographs in Figure 1a,b clearly demonstrate the highly dispersed network of polypyrrole nanowire deposited on the graphene nanosheet.

The electrical conductivity of the polypyrrole nanofibrous film was 65 S/m measured by using a four point probe technique. The graphene nanosheet film on the other hand exhibited a two order of magnitude higher electrical conductivity of the order of 1.25×10^4 S/m. In order to exploit this high electrical conductivity of graphene nanosheets, these are interspersed with polypyrrole nanowire in a multilayer configuration for supercapacitor electrode formation. These nanosheets are not only connected with each other near their edges but also interact with the polypyrrole nanowire from strong van der Waal's force of attraction with the highly aromatic graphene basal plane. The large sized nanosheets are firmly attached to the current collector surface to serve like series of current collectors within this multilayer configuration.

The electrochemical properties of this multilayered film were characterized using a two electrode cell immersed in 1 M aqueous NaCl solution. Figure 5 compares the cyclic voltammetry characteristics of layered composite of polypyrrole nanowire and graphene nanosheets with the control polypyrrole nanowire sample. A nearly ideal rectangular shaped CV for the aligned composite at increasing voltage scanning rate from 10 to 100 mv/sec clearly demonstrates excellent ionic and electronic transport within the bulk multilayered configuration of polypyrrole nanowires and graphene nanosheets. Under similar measurement conditions, the fibrous network of the control polypyrrole sample failed to maintain the capacitive response with increasing voltage scanning rate.

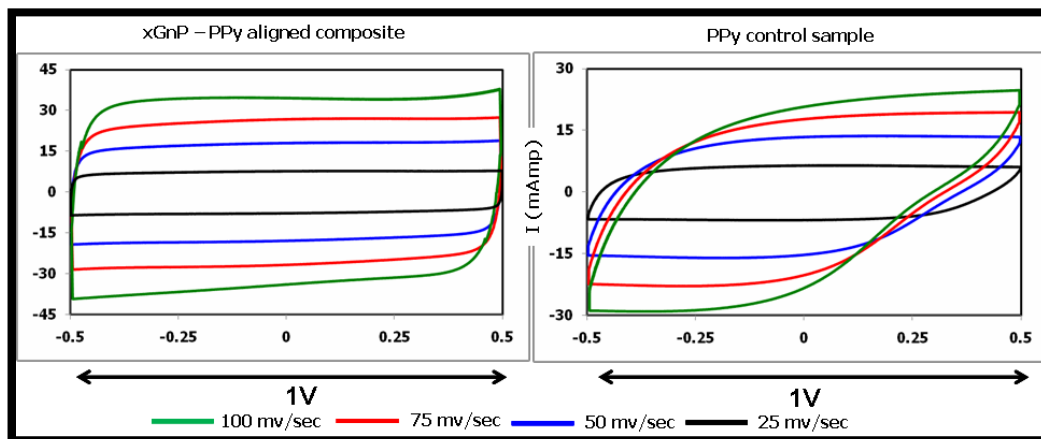


Figure 5: Electrochemical characterization: Cyclic voltammetric characteristics of multilayer composite of polypyrrole / graphene nanosheets and control polypyrrole sample at increasing voltage scanning rate from 25 to 100 mv/sec

The enhanced electronic transport with the incorporation of aligned graphene nanosheets is also evident from the impedance analysis. The contact interface resistance R_c for the aligned composite is more than one order of magnitude smaller than the control polypyrrole sample. This clearly demonstrates the reduced interfacial contact resistance between the active electrode materials inside the bulk electrode and minimum interfacial contact resistance of two dimensional large sized graphene nanosheets with the current

collector surface. Moreover, the above analysis points to the strength of the underlying van der Waal's force of interaction between the polypyrrole nanowire and large aromatic graphene basal plane for facile interlayer charge transport within the composite multilayer configuration. Instead of encapsulating the graphene nanosheets with thick polymer coating by chemical or electro polymerization process, in this new approach an edge shared network of series of highly aligned monolayer films were incorporated inside this multilayer electrode configuration not only to reduce the electronic resistance between the active electrode materials but also to enhance the charge transport from the interior of the bulk electrode to the current collector surface through strongly attached graphene nanosheets at the top section of the electrode. The higher rate capability of the aligned composite is evident from a knee frequency close to 50 Hz.

The increase in the charge transport also had a stabilizing effect on the capacity retention of polypyrrole nanowire under continuous electrochemical cycling. As shown in *Figure 6* at the end of thousand cycles, the aligned composite electrode maintains a symmetric charge discharge characteristics with more than 92% capacitance retention at 1 A/gm cyclic discharge current density. With increasing voltage drop (IR drop) the control specimen of polypyrrole nanowire failed to maintain the capacitive response in less than 250 electrochemical cycles at 1 A/gm discharge current densities.

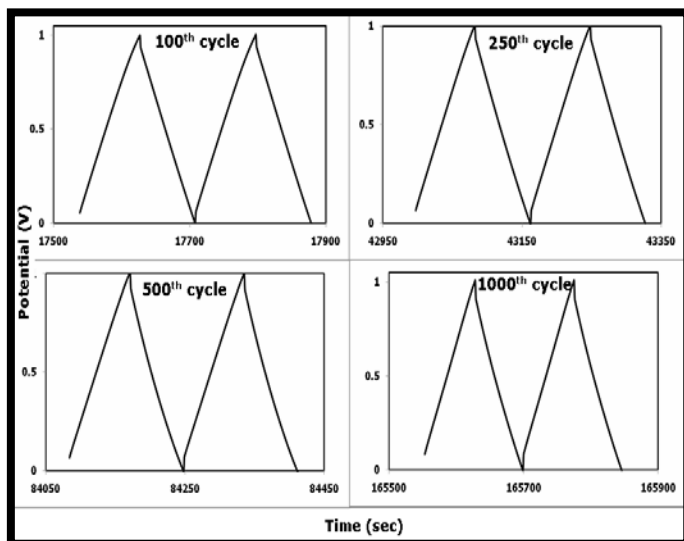


Figure 6. Cyclic stability: At 1 A/gm constant current density, the multilayer composite of polypyrrole and graphene nanosheets continues to maintain a highly symmetric charge discharge characteristics from 100th to 1000th electrochemical cycles with a potential drop of only 30 mv.

The specific capacitance obtained from the discharge slope of constant current galvanostatic technique was 165 F/gm at the end of 1000 cycles at 1 A/gm discharge current density.

Summary: Electro-polymerization was used to uniformly cover graphene nanosheets with a polymer coating to prepare composite electrodes for supercapacitor applications. Instead

of using chemical or electro polymerization technique to wrap the nanosheets completely, aligned monolayers of graphene nanosheets in this new approach are interspersed within the fibrous network of polypyrrole as a series of current collectors inside the multilayer bulk electrode configuration. This nanostructured electrode exhibits high ionic and electronic transport attributed to the presence of fibrous network or polypyrrole and electrically conductive graphene nanosheets. Impedance analysis clearly demonstrated the low equivalent series resistance obtained from the inter layer charge transport of graphene nanosheets and polypyrrole nanowire from strong van der Waals force of attraction between the large graphene basal plane and the π conjugated polymer chain. The facile electronic charge transport from the presence of graphene nanosheets also had a stabilizing effect on the electrochemical cyclic stability of this composite electrode. This multilayer film electrode displays symmetric charge discharge characteristics and a nearly ideal rectangular cyclic voltammogram with increasing voltage scanning rate from 10 to 100 mV/sec. Maintaining a high frequency capacitive response with a knee frequency close to 50 Hz this nano architecture exhibits 165 F/gm specific capacitance at 1A/gm discharge current density at the end of 1000th electrochemical cycles.

II. Replacement of Metal Current Collectors with Graphene Nanoplatelets in Advanced Lithium Ion Battery Electrodes

For high performance compact batteries, improvements in all components are being sought, and this need motivates the exploration of alternate current collectors which reduces the weight to the battery setup without increasing any cost. Currently, copper foils of $\sim 10\ \mu\text{m}$ thickness are used as a standard current collector for the anode side of lithium ion batteries. This current collector is a substantial component which contributes nearly 12 % of the total weight and 5% of the total cost of the cell¹. To increase the energy density and reduce the cost contribution of the current collector, various alternatives are being explored. One approach is generally to make self-supporting films of the electrode material, so that there is no need for a current collector. But such methodologies are restricted by the morphology and properties of the active electrode materials which are either limited to certain kinds of materials or require addition of conductive fillers and binders.

Conductive graphitic films are attractive because of their low density, good electrical properties and good electrochemical stability. Copper has a density of 9 g/cc while graphene has a density of $\sim 2\ \text{g/cc}$. The material used here is exfoliated graphite nanoplatelets (GnP), which is an inexpensive nanographitic material synthesized by acid intercalation and microwave exfoliation technique. This material had been found to be a good anode material and shows a reversible intercalation capacity of $\sim 370\text{mAh/g}$, which is higher, compared to commercial anode materials. The focus of this work is to use exfoliated graphite nanoplatelets (GnP) in the form of a self –standing paper, with

attractive electrical and mechanical properties as an alternative to copper films for the role of current collector.

GnP paper. GnP paper is a binder-free self-standing, flexible and porous paper prepared by a simple filtration process using aqueous suspension of GnP ¹⁴. This paper can be made in controlled porosities (ranging from 30-90 %) and thickness using different sizes of GnP materials. This paper has very good electrical conductivity which ranges from 500-2000 S/cm depending on the size of platelets, porosity and thickness of paper. *Figure 7* below shows the cross-sectional morphology of GnP paper at different magnifications. As can be seen from the high magnification images, the paper is a very ordered network of GnP platelets having a high degree of in-plane alignment and connected together contributing to the good electrical conductivity.

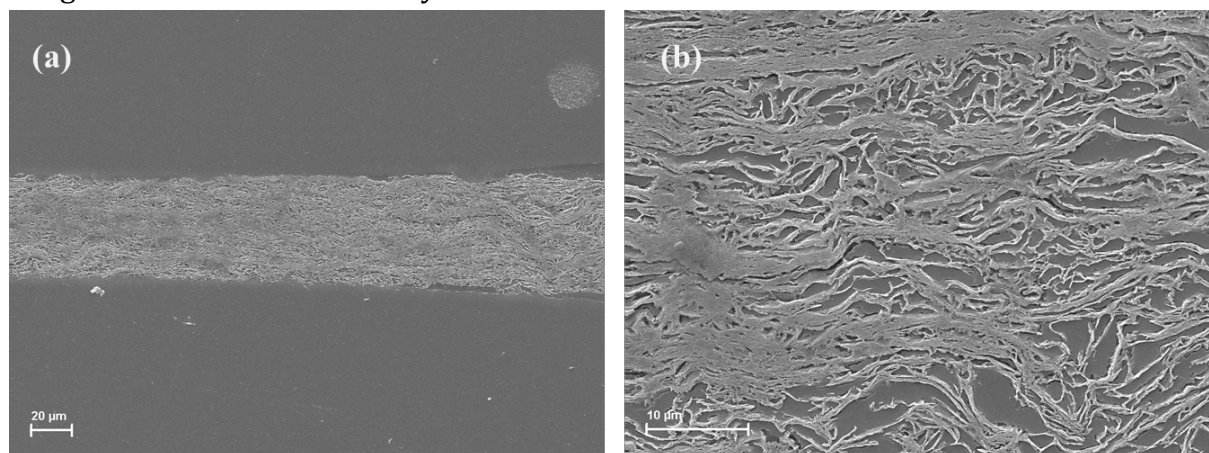


Figure 7. SEM Images of the GnP paper (as made) at different magnifications

Electrode Preparation. The evaluation of GnP Paper was done by using the same procedure of electrode preparation as done with copper as current collector. The anode is prepared by coating the slurry of active anode material with N-Methyl-2-pyrrolidone and PVDF as the binder on the GnP Paper as substrate using the microfilm applicator on an automatic electrode coating instrument. Different anode materials GnP-15, Timcal SLP 30 and LTO, were evaluated in terms of its cyclability and impedance analysis. The anode material was tested in a three electrode half-cell Swagelok setup (for GnP electrodes) or Coin cell setup (for LTO) with Ethylene Carbonate-Dimethyl carbonate-Lithium hexafluorophosphate as electrolyte and lithium foil as counter and reference electrodes. The relative loading of active material on the electrode was kept around 4-5 mg/cm². Fundamental performance characterization at different charge rates was done to assess the response of this electrode. The protocol adopted to evaluate the performance at different charge rates is shown in *Figure 8*. The galvanostatic cycling was done at different rates for every 5 cycles, keeping the rate same for both charge and discharge. Charge rate C corresponds to a charge or discharge rate equal to the theoretical capacity of a battery in one hour.

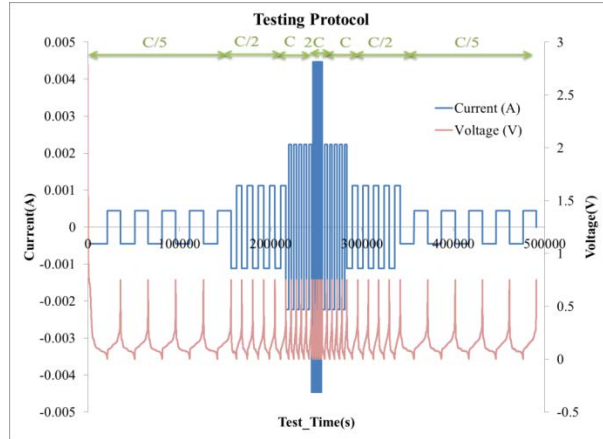


Figure 8: Testing protocol of galvanostatic cycling for performance evaluation.

GnP Electrode on GnP Paper. The first material under investigation here is an electrode of graphene nanoplatelets of 15 μm diameter on GnP Paper by the procedure described above. Figure 9 shows the SEM images of the cross-section of electrodes at different locations and magnifications.

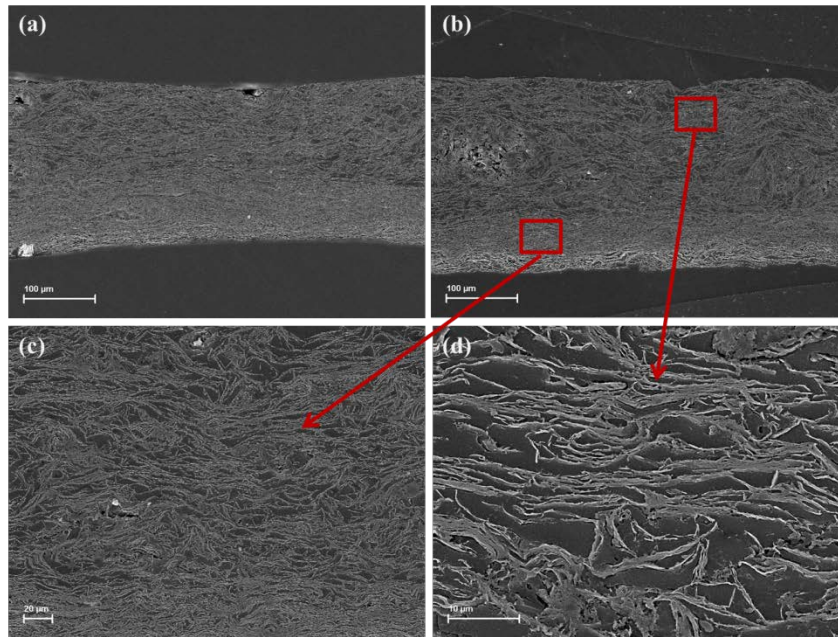


Figure 9. Cross-sectional SEM Images of the electrode at different magnifications (a) & (b), followed by high mag images of (c) GnP paper (d) active material region

From the cross-sectional SEM images, we can see that there is good adhesion between the GnP paper and the electrode material coated on top of it. The high resolution images shown in Figure 9(c) and (d) show that the morphology of both the paper and electrode active material indicating a highly porous well-arranged network, although the GnP paper is more compacted dense than the electrode coated above it, which is the result of the preparation procedure.

For electrochemical testing, the electrode was pressed at 0.1 MPa to produce the controlled porosity. SEM images in *Figure 10* show the changes that the GnP paper morphology undergoes in the process of electrode coating, and battery anode fabrication.

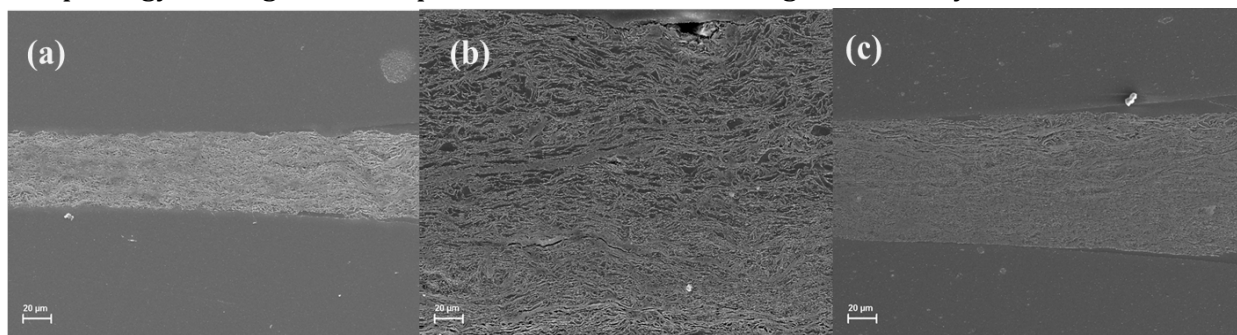


Figure 10. SEM images of X-sectional view of (a) current collector GnP paper, (b) the unpressed and (c) pressed electrodes.

Comparison of GnP Paper and Cu as current collectors. *Figure 11* compares the electrode made by GnP-15 as active material on two different substrates, viz. copper and GnP Paper.

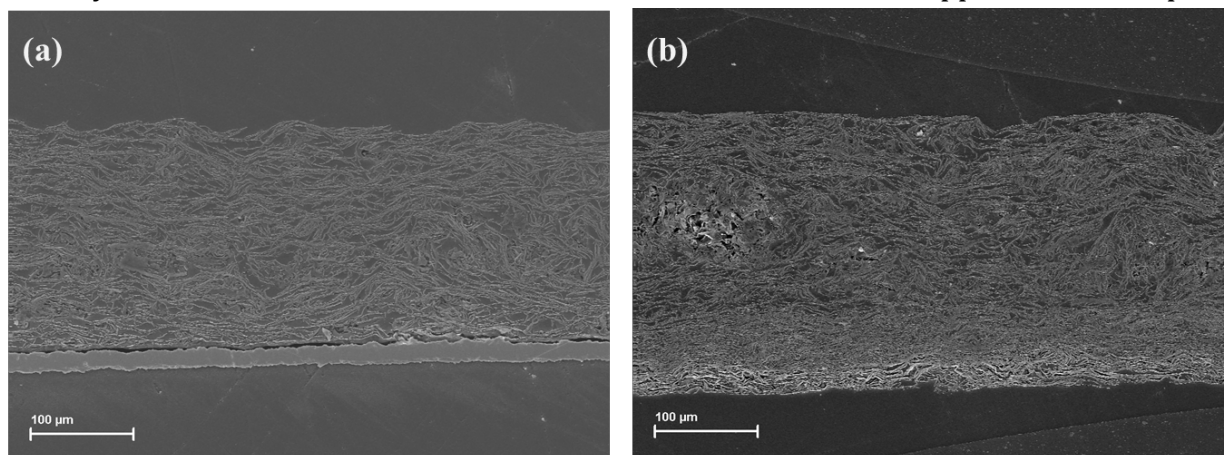


Figure 11. SEM images showing cross-sectional view of GnP-15 electrode on different current collectors: (a) Copper (b) GnP paper

The results of the performance testing are shown in *Figure 12*, calculated based on the weight of just the active material coated on GnP paper (*Figure 12 (a)*) and also using the complete weight including that of GnP paper *Figure 12 (b)*.

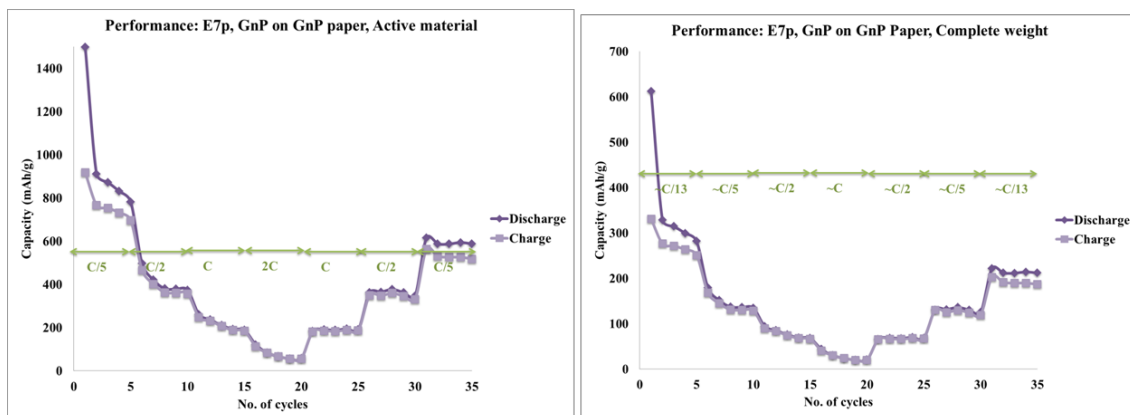


Figure 12. Representative Galvanostatic Performance of GnP-15 at different charge rates (a) Active material (b) Total weight including the substrate weight of GnP paper

As expected, GnP paper itself contributes towards lithium storage; hence calculations based on weight of active material indicate exceptional performance. However, in a real system, considering the weight of GnP paper as a contribution to electrode weight, the storage capability of the material is not completely utilized. This can be attributed to incomplete access of material because of very high loading 7-8 mg/cm². EIS (*Figure 13*) was conducted on the GnP electrodes made on Copper and GnP paper as current collector as a function of cycling. From the plots, we can conclude that GnP paper offers comparable conductivity and performance as copper current collector.

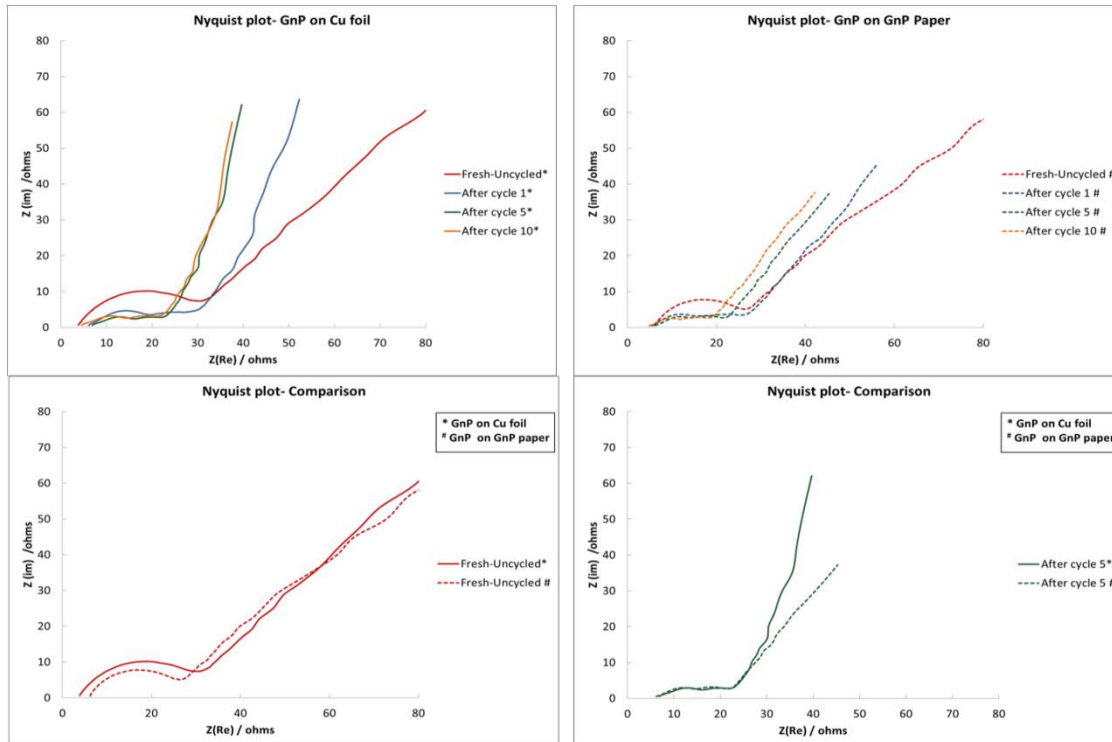


Figure 13. EIS Analysis of GnP electrodes on cycling (a) Copper current collector (b) GnP Paper as current collector; Comparison of (c) uncycled electrodes (d) after 5 cycles

Lithium Titanate (LTO) Electrode on GnP Paper. The use of these GnP Papers as current collector is not restricted to carbon based anode materials, and this was verified by using it as current collector for Lithium Titanate (LTO) as anode material. The electrodes were casted by coating NMP based slurry by similar procedures as described above.

The analysis in *Figure 14* compares the electrochemical performance of LTO electrodes cast on copper foil vs. GnP Paper. From this we can observe that the GnP paper performs very well with LTO as anode material, in fact a little better than the electrode made on copper. Such an improvement can be a consequence of improved conduction due to better adhesion of electrode with current collector thus providing good electronic conduction.

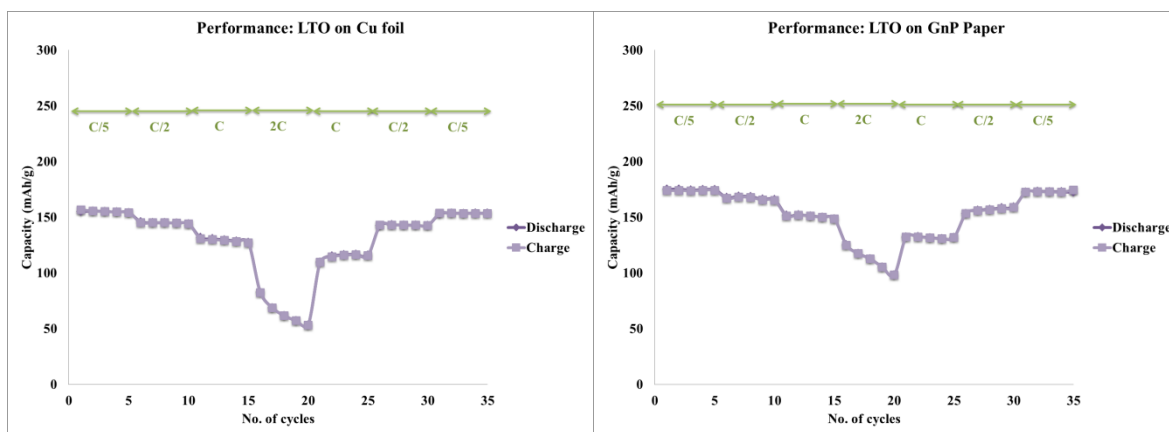


Figure 14. Electrochemical Performance of LTO electrodes casted on different current collectors
(a) On copper (b) On GnP Paper

This analysis with a non-graphitic anode material operates above the potential range in which carbon gets involved in any interaction with lithium. The results clearly demonstrate the diversity of use of GnP Paper as current collector even in situations, where it has no active electrochemical role to play.

Summary. We have demonstrated that the GnP paper has potential to replace copper as current collector and can serve the necessary role in terms of imparting electrical conductivity to the anode material. Interpreting from the performance data, it can be asserted that GnP Paper can match and potentially replace the use of copper as current collector. Table 1 shows the relative comparison of properties of the two current collectors.

Properties	Copper Current Collector	GnP paper Current Collector
Areal density	8.6 mg/cm ²	4.3 mg/cm ²
Electrical Conductivity (4 probe measurements)	8*10 ⁵ S/cm	750 S/cm
Tensile Strength	70 Mpa (Yield)	2.85 +/- 0.30 Mpa

Table 1. Comparison of properties of copper foil and GnP paper as current collectors

In summary, it is advantageous to use GnP Paper as a current collector over copper because of its light weight, reduced cost and positive contribution towards energy density. Also, this paper can easily be scaled up by using simple methods like by using paper making machines. Certain challenges that need to be addressed include GnP paper mechanical strength and ductility to allow its versatility for industrial scale continuous, roll to roll and calendaring processing.

III. Metal Doped Graphene Nanoplatelets as Anode Material

Nanographitic materials such as nanotubes and graphene nanosheets have gained considerable attention as potential energy storage materials, because of their desirable properties such as high surface area, good conductivity, and significant mechanical and electrochemical stability. Particularly, anodes made of graphene nanoplatelets and their composites have shown a significant increase in specific capacity (nearly 100%) by careful control of interlayer spacing ¹⁶.

Another category of anode material which is of prime significance is the metal nanoparticles which have excellent catalytic properties but are restricted in their use due to poor mechanical integrity and high cost. Research supported by the ARO grant for lithium ion batteries has focused on integrating two different materials, and developing a metal-nanographite composite as electrode to capitalize on the high lithium storage capability from metals and their oxides and combine it with excellent conductivity and mechanical robustness of graphitic systems.

There are numerous reports on combining SnO₂ , silicon and other metal oxides with graphene to form a high capacity nanostructure with highly conductive support, capable of sustaining the strain due to lithium alloying/dealloying process of metal component ¹⁷⁻²⁰ .

Our approach is to develop a 3 dimensional layered graphite nanoplatelets structure where the addition of metal nanoparticles allows the potential for a tailorable architecture. The schematic shown in *Figure 15* gives an overview of the concept behind the technique.

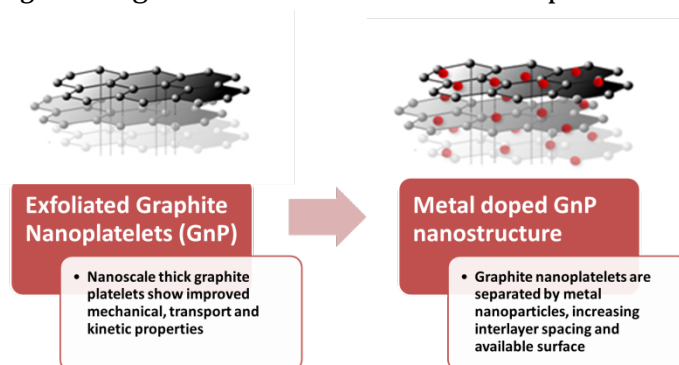


Figure 15. Schematic showing the potential of metal doped carbon as anodes for lithium ion batteries

A nanostructured electrode will have the benefits of fast diffusion and better mechanical robustness. In particular the addition of these nanoscale metal particles can result in a structured nanographite assembly that has the following:

- Metal nanoparticles can act as spacers, increasing interlayer spacing and thus allowing easy diffusion of lithium ions in and out of the electrode thereby enhancing the reaction rate.
- Metal nanoparticles can act as conducting additive, thereby reducing the electric resistance of the electrode.
- Use of appropriate metal dopants, such as nickel, tin and antimony, can contribute to the capacity because of their inherent interaction with lithium, thereby augmenting the specific capacity of the anode
- Improved cycle life as compared to metal anodes, by restricting the extent of volume expansion in the nanographitic matrix.
- Possibly reducing the SEI layer formation by covering active graphitic sites by metal dopants.

Nickel Doped GnP. To understand the effect of size of dopant, nickel nanoparticles of different sized has been developed by different approaches. The synthesis of small size metal doped GnP (< 5nm) is done by microwave assisted polyol process, in which glycols of different compositions can be used to synthesize metal nanoparticles by reducing them from their salts, with occasional modifications induced by use of reducing agents and stabilizers. This technique offers the advantages of rapid, homogeneous heating coupled with enhanced reaction rates, thus facilitating synthesis of metal nanoparticles of controlled size and morphology.

The other nickel nanoparticle doped GnP materials were developed by a simple procedure involving reduction of nickel salts on graphene surface by heat treatment in inert environment. *Figure 16* shows the images of nickel nanoparticle doped GnP-15 platelets with different sizes of metal nanoparticles ranging from <5 nm to 30 nm - 60 nm.

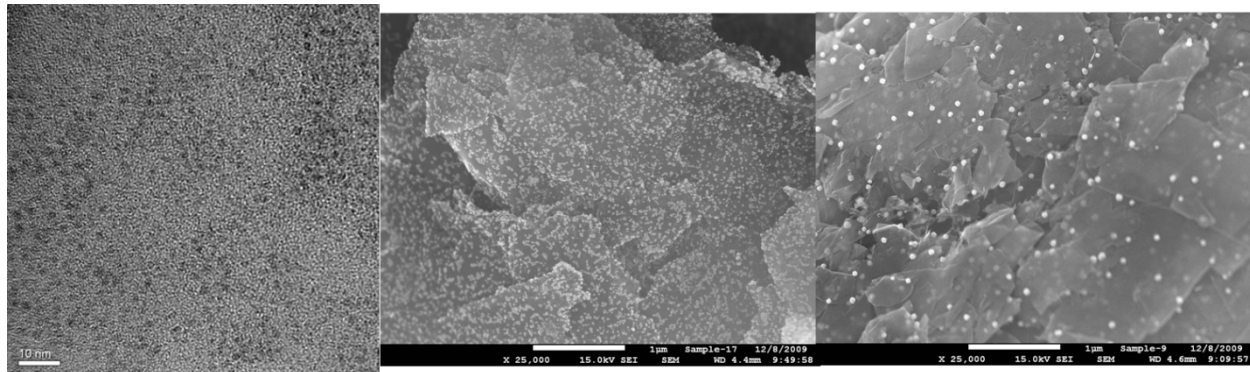


Figure 16. Nickel nanoparticle doped GnP platelets (Scale bar- a: 20 nm, b & c: 1 µm)

XRD pattern for different nickel doped materials is shown in *Figure 17* compared with undoped GnP. As seen from characteristic graphitic peaks at 26° and 55° are observed in all the materials. The characteristic peaks of Ni occur at $2\theta = 44.5^\circ, 51.86^\circ, 76.39^\circ$, and for NiO at $2\theta: 37.26^\circ, 43.29^\circ, 62.88^\circ, 75.42^\circ, 79.41^\circ$. From *Figure 18(b)*, we can see that all the materials show a mixture of Ni/NiO peaks, which indicates the possibility of partial oxidation of the nanoparticles. From the analysis, presence of metal nanoparticles is very clearly distinguishable with the peak widths in correspondence to the Scherrer equation, according to which broader the peak, smaller the size of the crystallite.

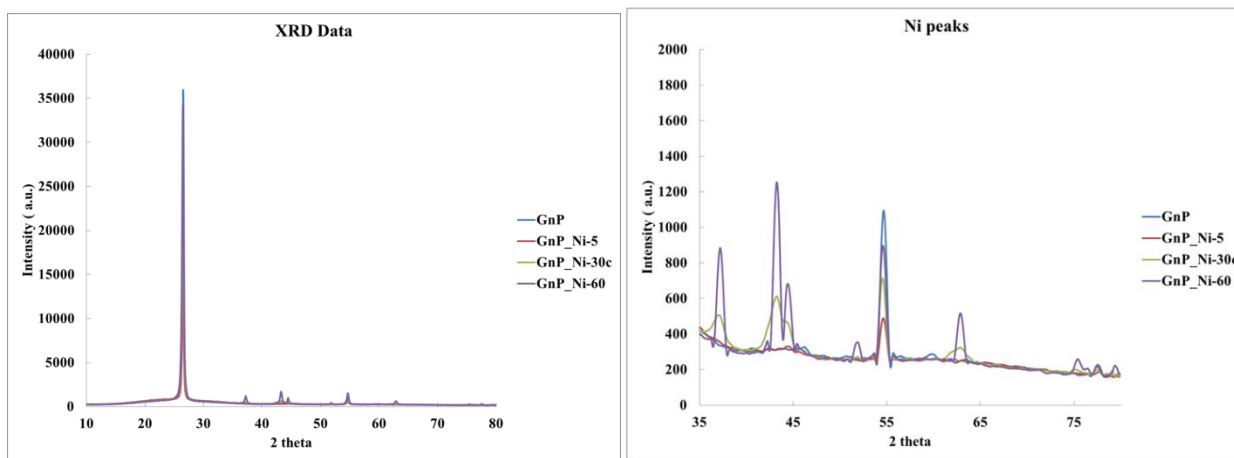


Figure 17. XRD pattern of nickel doped materials in comparison with undoped GnP
(a) Full spectra (b) Ni peaks

The performance of these metal doped nanographitic materials was evaluated at different charge rates by adopting the protocol shown in *Figure 18(a)*. The galvanostatic cycling was done at different rates for every 5 cycles, keeping the rate same for both charge and discharge. *Figure 18 (b)*, shows that the capacity values of base material undoped GnP-15 at

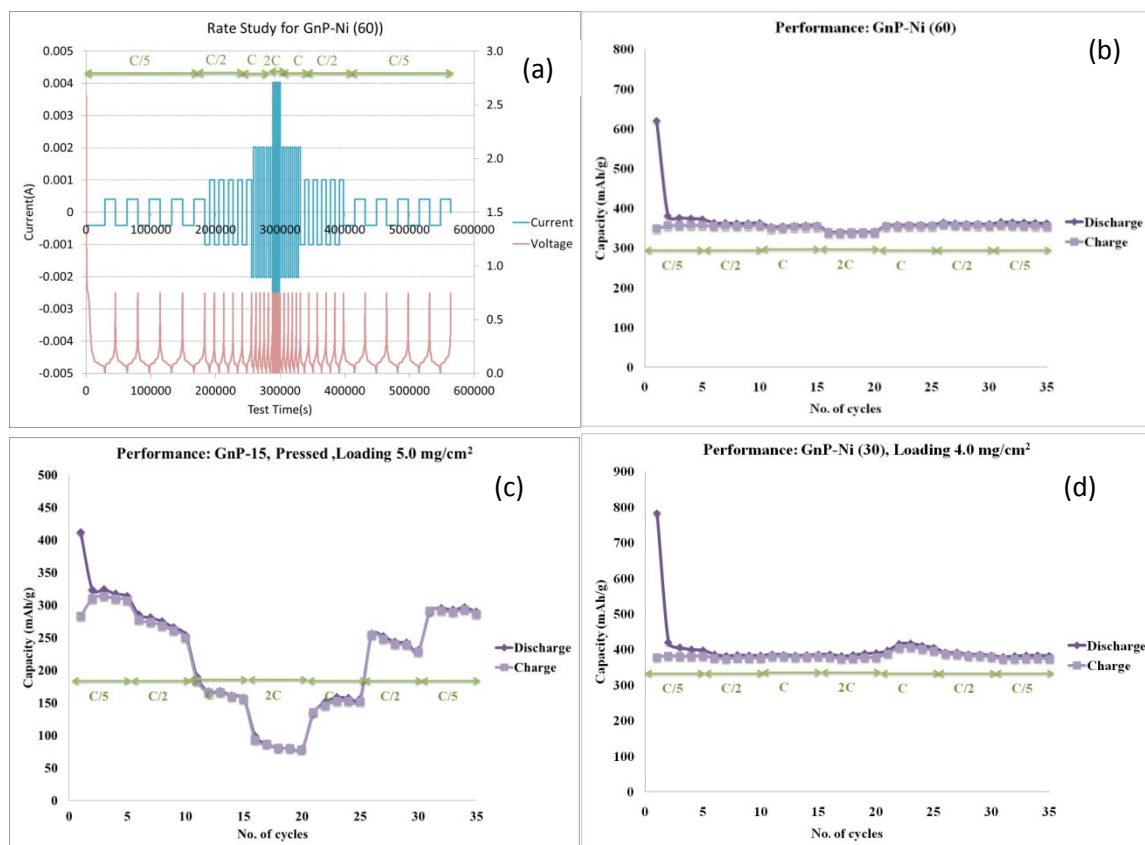


Figure 18. Galvanostatic performance of nickel doped materials in comparison with undoped GnP (a) Protocol (b) Undoped GnP (c) GnP_Ni-60 (d) GnP_Ni-30c

different charge rates as per the protocol. We can see there is a decrease in the capacity values at faster charge rates, as expected in graphitic systems. For Ni doped systems mentioned above, the performance is shown in *Figure 18 (c) and (d)* for GnP_Ni-60 and GnP_Ni-30 respectively. The capacity of the electrode was maintained at the same value even when the charge rate was varied from C/5 to C/2, C and 2C. This demonstrates the potential of the metal doped material to perform very well even at faster charge rates.

To understand the mechanism behind the improved performance at faster charge rates, a cyclic voltammogram at low scan rate (0.05 mV/s) was done to see the role of Ni in the system. From the CV shown in *Figure 19* we can observe that there are no distinct Ni peaks (expected at 0.34V reduction peak, and 1.75V oxidation peak).

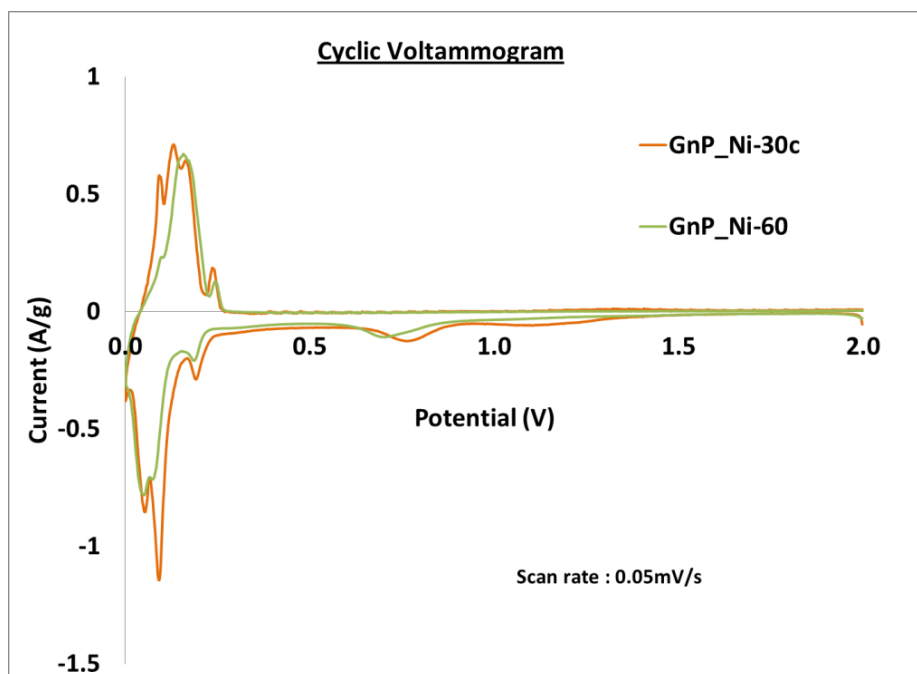


Figure 19. Cyclic Voltammogram of Ni doped materials

All the peaks observed correspond to different stages of lithium intercalation in to graphitic materials. This indicates that nickel plays an electrochemically inactive role here, and does not participate in any direct conversion reaction with lithium. If nickel does not contribute itself to capacity storage, as per our proposed concept, the improved capacity values can be an indication of improved diffusion due to metal spacers, resulting in improved performance at faster charge-discharge conditions.

Summary. The methodology described here resulted in development of metal doped graphene surfaces, stacked together to form an organized/layered structure, allowing flexibility for easy diffusion of lithium in and out of anodes, aiming at high reversible capacity for batteries. Although there are several research articles which have demonstrated that Ni dopants are electrochemically active and synthesizing NiO-graphene composites in a 3-D arrangement can enhance the performance of the anode ^{20,21}. However, in our case, the nickel dopants appear to be passivated and have no significant contribution to the capacity of the anode material. The increase in performance at faster charge rate can be inferred as an effect of facile diffusion of ions.

Future Work. The future plan is to develop nanostructured GnP electrode with dopants having some contribution to the capacity because of its inherent interaction with lithium, which is expected to increase the capacity of the anode material. Sn doped GnP platelets were synthesized by polyol based microwave reduction methodology, which resulted in very small size nanoparticles as shown by the TEM images in *Figure 20*.

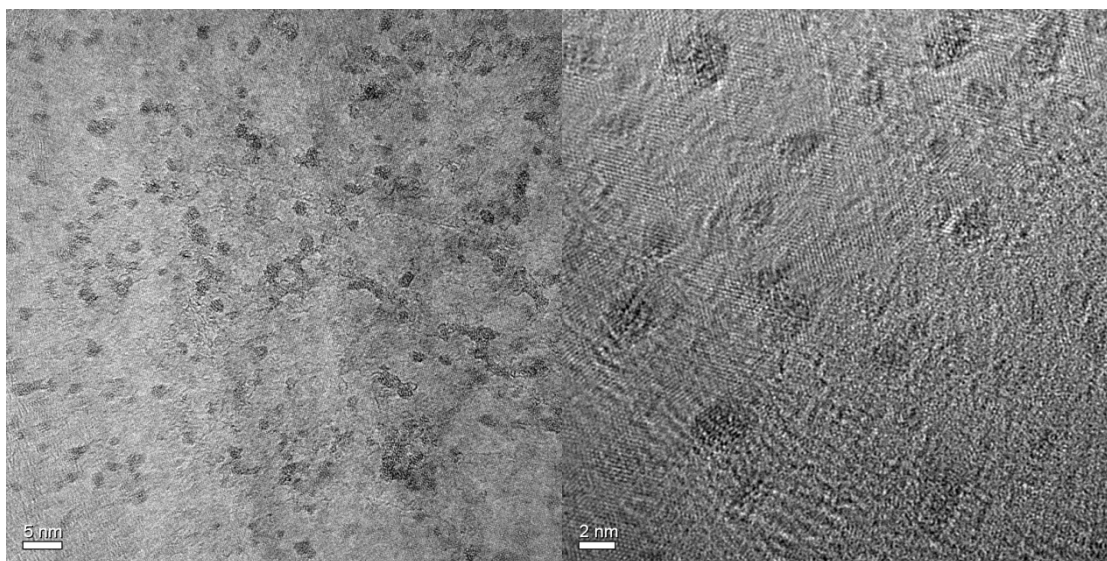


Figure 20. Tin based nanoparticle doped GnP platelets (Scale bar- a: 5 nm, b: 2nm)

IV. Graphene Nanoplatelets for the Fabrication of Lithium-Air Battery Cathode

This research focuses on Lithium-air batteries. Traditionally, Graphite has been the anode active material of choice for Lithium-ion batteries. Hence, it would be interesting to look at GnPs as an alternative to graphite. Most of the research conducted in the area of Lithium-air batteries has used porous, high surface area materials. GnPs with high open surface area may be an alternative to porous materials that may come with a disadvantage as will be discussed later. Also, GnPs are oxidation resistant, thus making them a more suitable choice for the Lithium-air cathode where Oxygen Reduction Reaction (ORR) takes place.

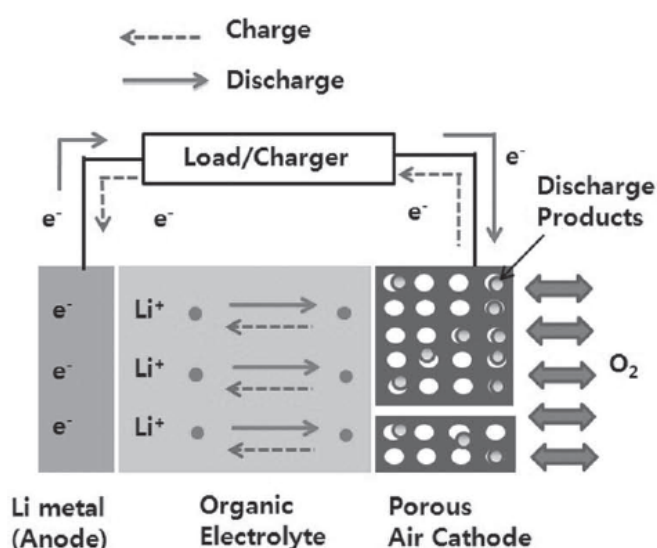


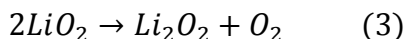
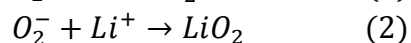
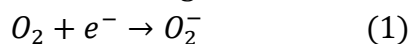
Figure 41. Working principle of a non-aqueous Lithium-air battery

Figure 21 shows the working principle of a non-aqueous Lithium-air battery.²⁶ On discharge, lithium ions are formed at the lithium metal anode and are transported across the electrolyte into the pores of the oxygen-cathode. The cathode breathes oxygen from the atmosphere and dissolves into the electrolyte present within the pores of the cathode. The dissolved oxygen is reduced at the porous electrode surface by electrons from external circuit and combines with Li^+ from the electrolyte to form oxide(s) of lithium as the final discharge product.¹⁸ If an

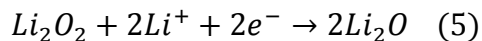
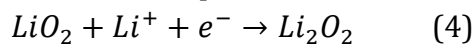
oxide or oxides of lithium have been formed during discharge, the oxide(s) should release oxygen gas upon charging and thus current flow in the external circuit. Whether or not and what type of lithium oxide(s) are formed during discharge are debatable at this time. It is important to note that by non-aqueous we refer to ‘aprotic’ organic solvent electrolyte. Depending upon the nature of the electrolyte, lithium-air batteries can have four different architectures.¹⁹ Likewise; the chemistry of reactions may be different at the oxygen cathode depending upon the architecture of the cell. It is important to note that although we refer to the battery as ‘Lithium-air’, only the oxygen takes part in the reaction. Thus, the battery could be called ‘Lithium-oxygen’ as well.

The reactions relevant to a non-aqueous system are described below¹⁸:

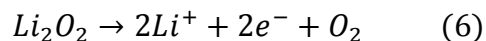
The mechanism of oxygen reduction on discharge is:



Some studies suggest an alternative set of equation¹⁸:



Most literature support reaction mechanism (1) to (3). The reaction upon charge will be as follows¹⁸:



Reaction set (1) to (3) and reaction (6), together, constitute a reversible energy storage system.

An electrolyte must exhibit sufficient Li^+ ion conductivity, O_2 solubility and diffusion to ensure rate capability. These desired properties can be achieved by optimizing the composition of the electrolyte. This involves a large permutation of salts, solvents, and additives¹⁷

The challenges of Lithium-air battery are related to having an open system. As already discussed, most prototype ‘Lithium-air’ research batteries could be considered as ‘Lithium-oxygen’ batteries. The batteries are fed with pure oxygen instead of air to avoid contamination from moisture and other components of air. To produce Lithium-air batteries at commercial level, membranes would need to be developed that selectively allow oxygen in the battery. Protective coatings could be developed to protect lithium from atmospheric moisture and to consider the probability of a hybrid aqueous/non-aqueous system.

Graphene nanoplatelet as an alternative to porous high surface area carbon materials. The materials investigated in prototype Lithium-air research batteries have mostly been porous materials.¹⁷ Porous materials may come with disadvantages either due to the clogging of

the pore orifice or due to the insulating nature of the discharge products.¹⁷ Pore clogging blocks Li⁺ ion and oxygen transport. Insulating nature of the discharge product inhibits electron transport. Both of them result in unused volume of the pore; thus, lowering discharge capacity. Materials with meso-pores exhibit relatively higher capacity compared to materials with micro-pores¹⁶ due to less pore blockage and more utilization of pore volume. However, meso-pore means lower surface area material in comparison to a material with micro-pore. Graphene nanoplatelet has high open surface area without any inherent pores as the material is prepared by thermal exfoliation of intercalated graphite. High open surface area material may be an alternative to porous materials as it provides enough surfaces for discharge product to deposit without the negative aspects of pores.

Results. Fabrication of GnP paper electrodes and discharge performance. Binder free, self-standing, flexible papers consisting of GnPs have been prepared.²¹ The GnP papers have been investigated as air-electrodes in Lithium-air batteries. Lithium-air battery performance is determined by the amount of reaction product deposited within the cathode structure; hence, it is reasonable to assume that the percentage of open areas within the structure; the shape and size of the openings as well as the thickness of the cathode will affect how much reaction product could be deposited. Therefore, it is required that a method be adopted for cathode fabrication which allows us to control and tailor the cathode structure in terms of parameters that are assumed to affect reaction products deposition. GnP paper is such a tailorable structure that has the potential to be used as an air cathode. GnP being a much less expensive material, it is reasonable to explore GnP paper as an alternative. The GnP paper is fabricated by filtration of a dispersion of GnP (M-grade, 120-150m²/g, average 15µm particle size, XG Sciences) in water. GnP is hydrophobic and doesn't disperse well in water. Polyethylenimine (PEI) is first dissolved in

Table 2. Different categories of GNP papers

Paper Category	GnP (M) (gm)	PEI (gm)	Dispersion volume (ml.)	Electrode loading (mg)	Thickness (micron)
Paper 'a'	0.2	0.2	200	6	114
Paper 'b'	0.1	0.1	100	3	67
Paper 'c'	0.7	0.7	700	21	488

water followed by the addition of GnP, sonication for 2 minutes and overnight stirring. PEI modifies the surface of GnP to make it hydrophilic. After overnight stirring a dispersion of GnP in water is obtained. The dispersion is then filtered through a filter paper under vacuum. The deposit of GnPs could be peeled off from the filter as a whole (paper

structure) after overnight drying. Most of the PEI is washed away during the filtration process. The residual amount of PEI is removed after heat treatment at 340°C which is the decomposition temperature of PEI. Three different types of papers were prepared as shown in table 1 and designated as paper 'a', 'b', and 'c'. An image of a Graphene paper is shown in fig. 9. Circular electrodes of 0.5" diameter were punched from the papers and investigated as air-electrodes in Lithium-air batteries. The average material loading and thickness for a 0.5" diameter electrode is indicated in the Table 2.

Lithium-air cells were assembled with 0.5" diameter circular electrodes punched from the papers and discharged. The electrolyte used was 1(M) solution of LiPF_6 in propylene carbonate (PC). The rate of discharge was $0.05\text{mA}/\text{cm}^2$ with a cut-off discharge potential of 2V. The potential of a cell immediately after assembly was above 3V. *Figure 22* shows the average discharge performances of three paper categories as described in Table 2. The average discharge time increases as we go from a thicker paper/higher material loading (paper 'a') to a thinner paper/lower material loading (paper 'b'). The average discharge time increases further as thickness/material loading are increased several times (paper 'c'). Several cells were assembled to obtain the average discharge performance. *Figure 23* shows a typical discharge profile of the paper electrodes.

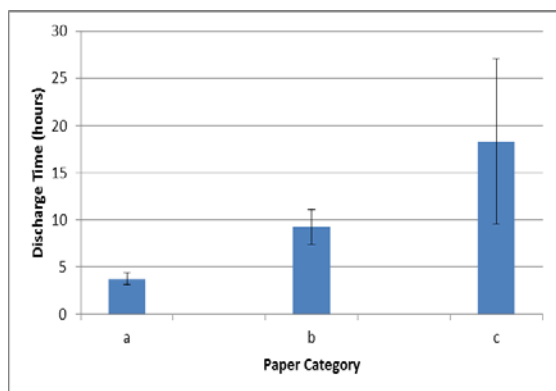


Figure 6 Average discharge performances of GNP paper electrodes ('a', 'b', and 'c' from table 2)

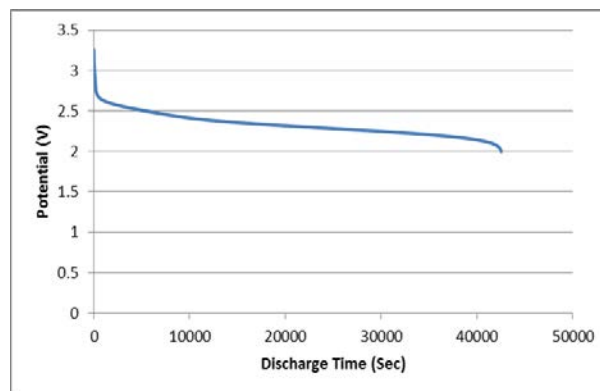


Figure 5 A typical discharge profile of a GNP paper electrode

Comparison of the discharge performances of GnP coated stainless steel cloth electrode and GnP paper electrodes. *Figure 24* compares the average discharge performances of three GnP paper electrodes and GnP coated stainless steel cloth electrode along with the material loading of each of the electrodes. The GnP coated stainless steel cloth electrode has a discharge time almost equivalent to that of the thickest paper electrode (paper 'c') although material loading is much lower (only about 3.46mg for the GnP coated stainless steel cloth electrode compared to 21mg for the paper electrode 'c'). This observation is of significance

for gravimetric energy density. Although it appears from this observation that GnP paper shows poorer performance, there are certain advantages of using a paper structured electrode.

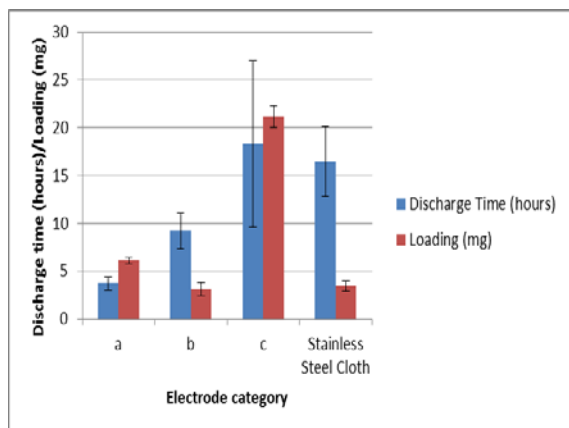


Figure 24. Comparison of discharge performances of GnP paper electrodes ('a', 'b', and 'c' from table 1) and GNP coated stainless steel cloth electrode along with material loading on each electrode

Fabrication of Bilayer Hybrid GnP Paper and Discharge Performance. The main assumption behind investigating GnP as a potential alternative to porous material is that the high open surface area of GnP could be utilized as reaction product deposition sites. Currently GnP is available with surface area as high as $750\text{m}^2/\text{g}$ (Grade-C, $<2\mu\text{m}$ particle size, XG Sciences). It would be interesting to investigate how this material performs compared to the M-grade GnP. However, this material poses significant challenges when trying to fabricate electrodes. Coating on stainless steel cloth hasn't been a viable option as most of the material filters through the openings. Coating on Nickel foam has been tried as suggested in some literature²⁴, however, some other literature has suggested that the foam itself takes part in reaction²⁵. Fabrication of GnP (grade-C) paper has been tried following the same process as that of the GnP (grade-M). However, the deposit of GnP could not be peeled off as a whole in the form of a paper structure. Instead of fabricating a GnP paper with 100wt% grade-C material, we have tried to fabricate a paper with 50wt% M-grade, 50wt% C-grade material by mixing them together when forming the dispersion. However, the GnP separates into two layers during filtration with C-grade being the bottom layer and M-grade being the top layer and the problem with peeling persists.

However, an alternative is to prepare a bilayer hybrid GnP M/C paper with bottom grade-M layer and a top grade-C layer by subsequent filtration of two dispersions of GnP-M and GnP-C on top of each other. The paper structure is expected separate from the filter as GnP-M is the bottom layer. Also, the GnP-M layer in the paper acts as support for the smaller particle size GnP-C layer. GnP-C having a higher surface area, most of the discharge capacity is expected to come from it. First, a GnP-M layer is deposited on the filter; dried overnight; and the same filter is reused to deposit a second layer of GnP-C on top of the already deposited M-layer. This is followed by overnight drying; peeling off the composite layer from filter; and the removal of residual PEI as discussed previously. The two layer deposit

can be peeled off nicely as a paper structure. Circular electrodes of 0.5" diameter were punched from the papers and investigated as air-electrodes in Lithium-air batteries. The composition of the dispersions and the average material loading and thickness for a 0.5" diameter electrode is indicated in the Table 3. This paper has been designated as paper'd'.

A Lithium-air cell was assembled with a 0.5" diameter circular electrode and discharged as previously described. The electrolyte used was 1(M) solution of LiPF_6 in propylene carbonate (PC). The rate of discharge was $0.05\text{mA}/\text{cm}^2$ with a cut-off discharge potential of 2V. The potential of a cell immediately after assembly was above 3V. Several cells were assembled with circular electrodes punched from the original electrode to obtain the average discharge time was 30 hours.

Table 3. GNP-M/C hybrid bilayer paper specifications

Paper Category	GNP (M) (gm)	GNP (C) (gm)	PEI (gm)	Dispersion volume (ml.)	Electrode loading (mg)	Thickness (micron)
'd'	0.1	0.1	0.2	200	5.12	143.4

Comparison of discharge performances of GnP papers. Figure 26 compares the discharge performances of four paper electrodes (i.e. single layer papers 'a', 'b', 'c' and bilayer paper 'd') along with the material loading. Figure 27 compares the discharge performances of the same paper electrodes along with the paper thicknesses. Comparison of Figures 25 and 26 shows that both (discharge time/material loading) ratio and (discharge time/paper thickness) ratio are highest for the bilayer hybrid GnP-M/GnP-C paper. These observations are of significance for both gravimetric and volumetric energy densities.

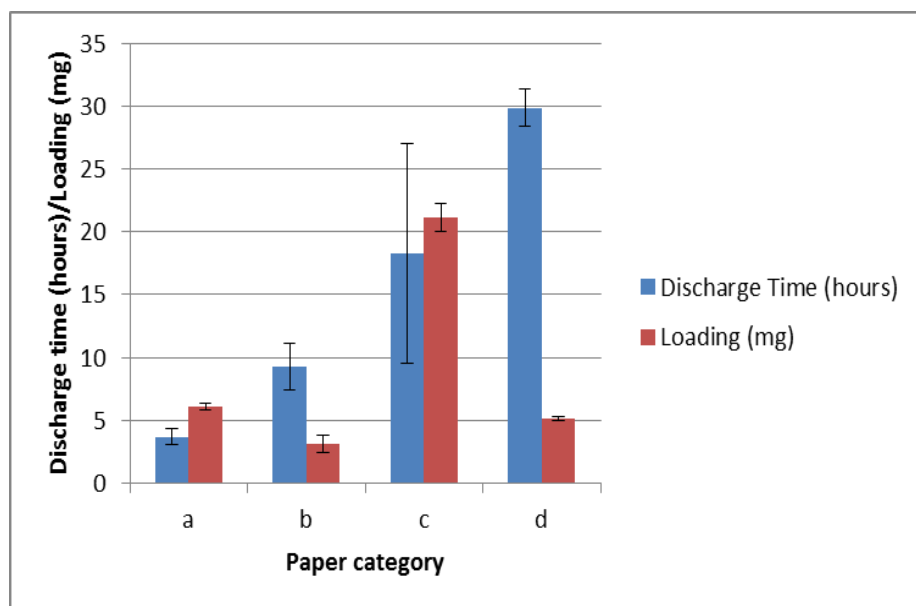


Figure 25 Comparison of discharge performances of GNP paper electrodes ('a', 'b' and 'c' from table 2; 'd' from table 3) along with material loading on each electrode

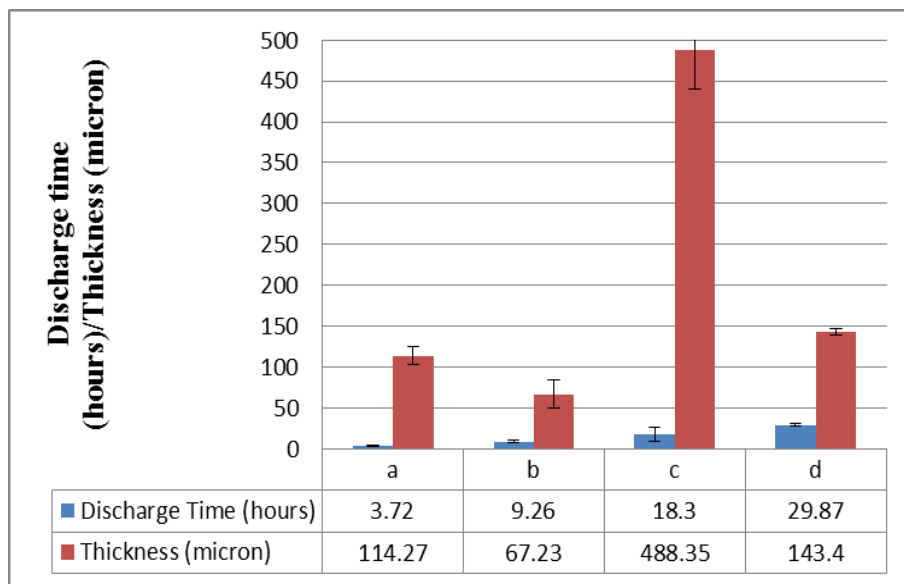


Figure 26 Comparison of discharge performances of GNP paper electrodes ('a', 'b' and 'c' from table 1; 'd' from table 2) along with thickness of each electrode

Summary. The primary goal of this research has been to determine the viability of GnP as a potential alternative to conventionally researched porous materials and contribute to one of the challenges of Lithium-air system; which is, to obtain high capacity by avoiding pore clogging and the early termination of discharge.

GnP paper was investigated as an alternative electrode due to better control over its structure. The difference in performances of various categories of GnP paper electrodes ('a', 'b' and 'c' table 2) and the difference in performances of paper electrodes and GnP coated stainless steel cloth electrode led into looking at performance in terms of electrode structure. As thickness is increased several fold, the discharge performance increases; contrary to the expectation that the discharge time will be reduced (paper 'c'). This might be due to the availability of a higher amount of GnP wetted by the electrolyte; however, the ratio of discharge time to the amount of material in a single electrode is low suggesting poor utilization of material and hence lower energy density.

Higher surface area GnP (C-grade) material was investigated to verify the assumption that availability of higher open surface area contributes to high discharge time and hence is a potential alternative to porous materials. The C-grade GnP material having a small particle size, an electrode with a conventional method couldn't be prepared. Incorporation of high surface area material in a paper structure could increase the net discharge performance compensating for the performance reduction due to poor transport properties. However, due to difference in morphologies and other unknown factors, a paper structure with a homogeneous mixture of two grades of GNPs could not be prepared. An alternative method was adopted to prepare a bilayer paper with a high surface area/small particle size GnP-C layer and a relatively low surface area/large particle size GnP-M layer as support. A bilayer

GnP-M/C electrode with a thickness and material loading equivalent to that of a single layer GnP-M electrode exhibits much improved performance in spite of the possible transportation limitations imparted by the GnP-M support layer. Thus, not only that high surface area GnP contributes to better discharge performance, but energy density is enhanced too.

3. Microstructure, Surface Chemistry and Electronic Properties of sp^2 and sp^3 Carbons - Greg M. Swain

Objectives:

- To study the fundamental relationships between the microstructure, surface chemistry and electronic properties of novel sp^2 and sp^3 -bonded carbon electrode materials and their basic electrochemical properties and performance,
- To investigate how the chemical, electronic and electrochemical properties of single and multilayer graphene films can be tailored for electrical storage applications through controlled chemical modification of the surface

Background:

Research has been conducted to gain more fundamental insight the atomic and molecular processes that govern the performance of carbon-based energy storage systems. The work was conducted using electrically conducting and high surface area sp^2 carbon materials (graphite, glassy carbon, nanotubes) and advanced sp^3 (boron-doped diamond and diamond-like carbon) and sp^2/sp^3 composite materials (graphite nanoplatelets/nanocrystalline diamond and graphite nanoplatelet/nanocrystalline diamond/metal oxide). The sp^3 -bonded carbons offer greater microstructural stability, a wider working potential window and potentially higher rates of charge and discharge compared to presently used sp^2 carbons. Thin films and pellets of the powders were prepared and cyclic voltammetry, capacitance-potential and impedance-potential curves will be recorded in various aqueous and non-aqueous electrolyte solutions, and ionic liquids. The measurements are made at variable temperatures. The goal of the work is to compare and contrast the basic electrochemical properties of the sp^2 and sp^3 carbon materials with controlled microstructure and surface chemistry. Electrical conductivity and BET surface area measurements, as well as SEM, XRD, Raman spectroscopy and XPS, have been employed pre- and post-polarization to determine the extent of any microstructural, chemical or electrical property changes. *In situ* Raman spectroscopy was used during the polarization measurements to investigate the time dependence of any microstructural changes of the different powders. Impedance analysis was used to assess changes in the ohmic resistance, polarization resistance and capacitance.

Research has also been conducted to better understand the microstructural stability of the

nanostructured carbon materials (conducting diamond and diamond-like carbon powders, graphite nanoplatelet/diamond composites and graphite/nanoplatelet/metal oxide composited during charge/discharge cycling (e.g., D. Y. Kim, B. Merzougui and G. M. Swain, Chem. Mater. 2009). The measurements are made in various aqueous and non-aqueous electrolyte solutions, and ionic liquids. These materials have high surface area (50-200 m²/g) and short charge transport lengths from the active carbon to the current collector. Electrical conductivity and BET surface area measurements, as well as SEM, XRD, Raman spectroscopy and XPS, are employed pre- and post-polarization to determine the extent of any microstructural, chemical or electrical property changes. *In situ* Raman spectroscopy is also used during the polarization measurements to investigate the time dependence of any microstructural changes.

Carbon electrodes (e.g., graphite, glassy carbon and carbon fiber) have been used as electrochemical electrodes for over 50 years now. Much of what is understood about structure-function relationships has come from studies using well-defined highly oriented pyrolytic graphite. It is well established that there are major differences between the electrical, chemical and electrochemical properties of the edge plane sites compared to basal planes of graphitic carbons. The density of electronic states near the edges is significantly greater than the surrounding basal plane, adsorption of polar molecules near these edges tends to be stronger than on the surrounding basal plane, and the heterogeneous electron-transfer rate constant for many redox reactions is orders of magnitude greater at the edge versus basal plane sites. The effect of chemical modification of the edges on the heterogeneous rate of electron transfer is also well understood.

Graphene is a flat monolayer of carbon atoms firmly packed into a 2-D honeycomb-like crystalline lattice (S. Park and R. S. Ruoff, Nano Technol. 2009, 4, 217). Unmodified and chemically-modified forms of the material are promising candidates as components in energy storage and conversion devices. To achieve this promise, fundamental research is needed on how to tailor the electronic and chemical properties of the material through controlled chemical modification. To learn more about structure-function relationships at this material, the some same approaches that have been successfully used in the past to characterize HOPG and various amorphous carbons are applied. (R. J. Rice, N. M. Pontikos, and R. L. McCreery, J. Am. Chem. Soc. 1990, 112, 4617; A. E. Fischer, Y. Show and G. M. Swain, Anal. Chem. 2004, 76, 2553). The goal is to better understanding of electron transfer at electrified graphene interfaces and how the capacitance of single and multilayer graphene films can be altered through controlled chemical modification. The Swain Group has extensive experience with modifying sp² and sp³ carbon electrodes using the electrochemically-assisted derivatization of substituted aryl diazonium salts (T.C. Kuo, R. L. McCreery and G. M. Swain, Electrochem. Solid-State Lett. 1999, 2, 288; R. L. McCreery, Chem. Rev. 2008, 198, 2646). Furthermore, the role that the substrate has on the

electrochemical properties of the carbon is being investigated.

Figure 27 typifies the characterization approach being utilized. Electrochemical methods are used extensively to probe the activity of the edge and basal plane sites using a suite of inner-sphere and outer-sphere redox analytes. Graphene layers with controlled levels of edge states have been produced for these studies. The fraction of edge versus basal plane present in a layer have been probed by *in situ* Raman spectroscopy. The heterogeneous rates of electron transfer are correlated with the carrier mobility and concentration, as determined from Hall Effect measurements. The relationship between the applied potential and the capacitance has been studied in aqueous and non-aqueous solutions and ionic liquids. Scanning electrochemical microscopy (SECM) is being used *in situ* to provide spatial information about the electrochemical activity across the graphene film surface (*i.e.*, local electronic properties). Electrochemical STM has been used *in situ* to learn how the local atomic structure and density of states change as a function of the applied potential. Transparent forms of graphene deposited on optically transparent substrates are being used in transmission spectroelectrochemical measurements (Y. Dai, G. M. Swain, M. D. Porter and J. Zak, Anal. Chem. 2008, 80, 14). These hybrid techniques can provide dual information about the electronic and optical properties of the material as a function of the electrochemical conditions.

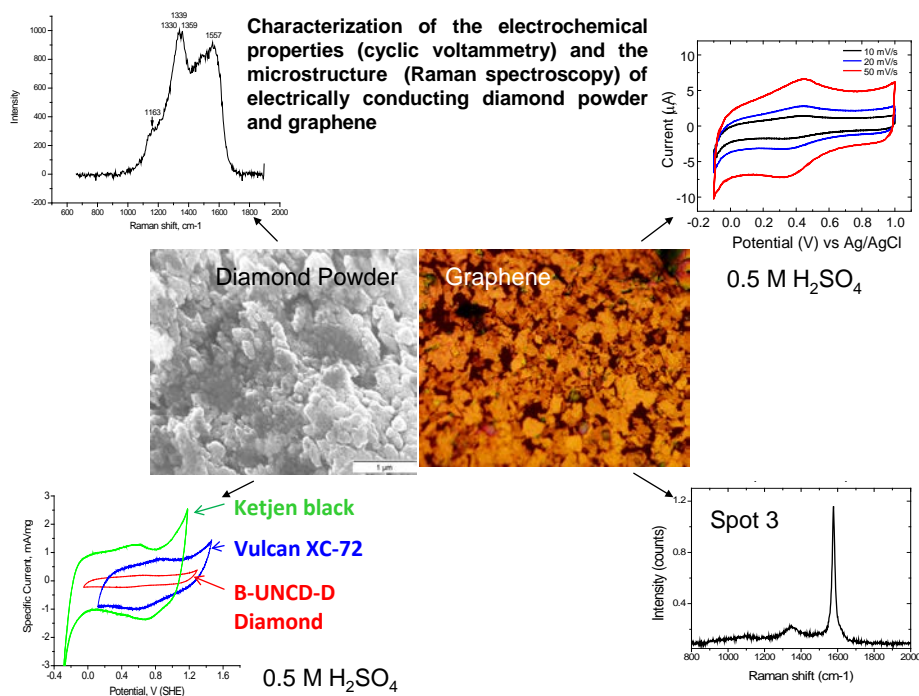


Figure 27. Electrochemical property characterization (cyclic voltammetry) and the microstructure (Raman Spectroscopy) of electrically conducting diamond powder and graphene.

These hybrid techniques are also useful for characterizing chemically-modified graphene

surfaces as well as molecular adsorption on the modified surfaces. Molecular adsorption or covalent modification of the graphene surface could have a striking influence on the electronic and optical properties. The above work utilizes low-oxygen graphene. An important fabrication step for making graphene-based electrodes is chemical modification of the edges, basal plane, or both. Robust devices are best fabricated with covalent bonding to conducting “contacts”, most likely through edge-bonding to graphene plates. Basal plane modification has been shown to change a graphene sheet from metallic to semiconducting, with a significant decrease in conductivity. The Swain Group has extensive experience with covalent modification of carbon materials via reduction of diazonium reagents, which react significantly faster with graphite edges than with basal plane. Diazonium-mediated bonding to graphene has been reported recently, but only in preliminary form. By monitoring the process spectroscopically, where the diazonium-generated radical attaches to the graphene can be determined, and also assess the spectroscopic consequences of covalent modification. Raman spectroscopy should be particularly informative, since it can reveal disordering of the graphene by basal attack, and also verify the presence of newly formed functional groups on the graphene edge.

Description of Research Tasks:

Task 1. We will study the fundamental the relationships between the microstructure, surface chemistry and electronic properties of novel sp^2 and sp^3 -bonded carbon electrode materials and their basic electrochemical properties (e.g., charge storage and electron transfer). We will prepare high surface area and electrically conducting sp^2 (graphite, glassy carbon, carbon black, nanotubes), sp^3 (diamond and diamond-like carbon) and sp^2/sp^3 composite carbon materials for use in electrochemical double layer capacitors (EDLCs) and study their stability, potential window and capacitance in aqueous and non-aqueous electrolyte solutions, and ionic liquids. The goal will be to gain a fundamental understanding of the atomic and molecular processes governing the performance of energy storage devices made with these carbons. We anticipate development of more dimensionally-stable carbons for EDLCs that possess improved cycle life as well as improved energy and or power densities. This work will be collaborative with the Baker, Drzal, Hawley and Sakamoto groups.

Task 2: We will investigate the properties of unmodified and chemically-modified single and multilayer graphene films. The surface chemistry will be controlled systematically using aryl diazonium chemistry that results in the covalent attachment of phenyl-substituted moieties. Various *in situ* methods will be used to probe the surface chemistry and microstructure, and their effect on the electron transfer and capacitance. Microstructural changes in the material as a function of the applied potential and electrolyte solution will be assessed using Raman microprobe spectroscopy. It will be

important to learn how these structural changes affect electron transfer and capacitance. The heterogeneous rates of electron transfer for multiple test redox systems will be correlated with the carrier mobility and concentration, as determined from Hall Effect measurements. The effect of the applied potential on the capacitance will also be studied. Scanning electrochemical microscopy (SECM) will be used *in situ* to provide spatial information about the electrochemical activity across the graphene film surface (i.e., local electronic properties). Electrochemical STM will be used *in situ* to learn how the local atomic structure and density of states changes as a function of the applied potential. Transparent forms of graphene deposited on optically transparent substrates will be used in spectroelectrochemical measurements. These hybrid techniques can provide dual information about the electronic and optical properties of the material as a function of the electrochemical conditions. These hybrid techniques will also be useful for characterizing chemically-modified graphene surfaces as well as molecular adsorption on the modified surfaces. Molecular adsorption or covalent modification of the graphene surface could have a striking influence on the electronic and optical properties. This work will be collaborative with the Drzal and Hogan groups.

Summary of Swain Group Scientific Progress and Accomplishments.

Fundamental research was carried out to understand the basic processes governing redox reactions as well as the interfacial organization at nanostructured sp^2 , sp^3 and hybrid sp^2/sp^3 carbon materials in room temperature ionic liquids (RTILs). Comparison studies were performed in aqueous electrolyte solutions. RTILs are emerging as a new medium for redox processes as these liquids possess high solubilizing power, electrical conductivity, wide breakdown voltage and low volatility. The more extensively studied sp^2 carbon materials (glassy carbon, highly oriented pyrolytic graphite and graphene) with the less studied sp^3 materials (single and polycrystalline diamond, tetrahedral amorphous carbon films, and hybrid composite nanographene/nanodiamond powders) were compared and contrasted in order to delineate, among other things, the role of the extended π -electron system, which exists in the former but not the latter materials. **The new science in this work was the focus on the relationship between the RTIL type and structure, and the interfacial capacitance, electron-transfer kinetics and reaction mechanisms of outer- and inner-sphere redox systems at well characterized sp^2 and sp^3 carbon electrodes. The work is significant because it provides new insight on structure-function relationships at sp^2 and sp^3 carbon electrodes in these technologically-important electrolytes.**

Generally, it has been found that electrochemical reactions and mechanisms of organic redox systems in RTILs are the same as those in conventional aprotic solvents. The differences rest mainly in the higher viscosity of the RTILs, hence the lower diffusion

coefficients of the redox species. However, studies of reactions and mechanisms of inorganic redox systems in RTILs are not widely reported especially at sp^3 -bonded carbon electrodes.

This research has two aims. **Aim 1:** detailed characterization of the structure and chemical composition (bulk and surface) of the different carbon materials enabling correlations to be made between the physical, chemical and electrical properties and the electrochemical performance. **Aim 2:** basic studies of the interfacial properties and electrochemical activity of the different carbon electrodes in RTILs including; capacitance-potential curves, heterogeneous electron-transfer rate constant determinations of various inner and outer-sphere redox systems and distance effects on ET for the different redox systems. The sp^3 carbon materials offer two major advantages over conventional sp^2 carbons: (i) significantly improved structural stability and (ii) a wider working potential window. Combining these new electrode materials with RTILs will lead to the development of an advanced class of materials for charge storage devices that provide increased lifetimes, improved cyclability, and higher energy and power densities.

I. Heterogeneous Electron-Transfer Kinetics in RTILs (Electrochimica Acta, 2013)

Heterogeneous electron-transfer rate constants were determined for ferrocene and ferrocene carboxylic acid (FCA) in the room temperature ionic liquid (RTIL), 1-butyl-3-methylimidazolium tetrafluoroborate (BMIMBF₄), at boron-doped microcrystalline diamond thin-film electrodes. Comparison data for FCA in 1 M KCl were also obtained. The apparent heterogeneous electron-transfer rate constant, k_{app}^o , for FCA was 10x lower in the RTIL $(1.5 \pm 1.1) \times 10^{-3} \text{ cm s}^{-1}$ as compared to KCl $(4.6 \pm 1.3) \times 10^{-2} \text{ cm s}^{-1}$. The k_{app}^o for ferrocene was also 10x lower in the RTIL $(5.0 \pm 1.2) \times 10^{-3} \text{ cm s}^{-1}$ as compared to a common organic electrolyte solution $(5.5 \pm 1.2) \times 10^{-2} \text{ cm s}^{-1}$. The diffusion coefficient for FCA (D_{red}) was determined by chronoamperometry to be $1.3 \times 10^{-7} \text{ cm}^2 \text{ s}^{-1}$, *ca.* 100x lower than the value $(1.9 \times 10^{-5} \text{ cm}^2 \text{ s}^{-1})$ in KCl. The lower diffusion coefficient is consistent with the 100x greater viscosity of the RTIL. The lower k_{app}^o values for these outer-sphere redox systems is attributed, at least in part, to a reduced number of attempts to surmount the activation barrier (*i.e.*, a reduced nuclear frequency factor, ν_n) due to the more viscous medium.

II. Double-Layer Effects on ET Kinetics at Diamond Electrodes (J. Phys. Chem. C, 2011).

Cyclic and linear sweep voltammetry were used to investigate the effects of the electrolyte composition and temperature on the electron-transfer kinetics of $\text{Fe}(\text{CN})_6^{3-/4-}$ at well characterized, boron-doped diamond thin-film electrodes. This redox system is highly sensitive to the surface cleanliness, microstructure and chemistry of carbon electrodes! Highly conductive films were employed, which were first cleaned of any adventitious

nondiamond carbon impurity by a two-step chemical oxidation and subsequently hydrogenated in hydrogen microwave plasma. The apparent heterogeneous electron-transfer rate constant, k^o_{app} , depended on the electrolyte concentration and the electrolyte cation type, increasing in order of $\text{Li}^+ < \text{Na}^+ < \text{K}^+ < \text{Cs}^+$. However, the dependence of k^o_{app} on the electrolyte cation was less than the dependence observed for other electrodes, such as glassy carbon and gold. For example, k^o_{app} at the 1.0 M concentration was only a factor of 1.6 greater in KCl than in LiCl for diamond. This is less than the factor of approximately 10 observed for glassy carbon and gold. The transfer coefficient for the oxidation reaction was relatively independent of the temperature and the electrolyte composition with a value ranging from 0.52-0.55. The activation energy for electron transfer was found to be 14.3, 15.6 and 16.5 kJ/mol, respectively, for KCl, NaCl and LiCl. The results suggest that the electric double layer structure at diamond is distinctly different from than at sp^2 carbon electrodes, such as glassy carbon.

III. Diamond Powders as New EDLC Electrodes.

The voltammetric response and electrode capacitance of high surface area, electrically conducting diamond powder were investigated by cyclic voltammetry and ac impedance analysis, respectively. Conducting diamond powder is of interest as a corrosion-resistant electrocatalyst support for fuel cells and a dimensionally-stable EDLC electrode material. The wider working potential window (3-3.5 V in aqueous media) and superior microstructural and morphological stability at high potentials and currents, as compared to conventional sp^2 carbon electrode materials, make diamond an attractive new electrode for EDLC applications. The goal of this work was to gain a better fundamental understanding of how aqueous acid and an ionic liquid affect the electrochemical performance of this material in terms of the background voltammetric current and the capacitance.

The diamond powder was prepared by overcoating inexpensive diamond grit (3-6 nm diam., 220 m^2/g) with a layer of boron-doped ultrananocrystalline diamond (B-UNCD). The coated powder had a specific surface area of $\sim 170 \text{ m}^2/\text{g}$ and an electrical conductivity of $\geq 0.4 \text{ S/cm}$. The electrochemical properties were evaluated in two media: 0.5 M H_2SO_4 and the ionic liquid, 1-butyl-3-methylimidazolium tetrafluoroborate (BMIMBF₄). Comparison measurements were made using several microstructurally-distinct sp^2 carbon powders. The B-UNCD-diamond powder exhibited a flat and featureless voltammetric current response in both media. The voltammetric response was stable during extended potential cycling in both media with a potential window approaching 3 V in H_2SO_4 and over 4 V in BMIMBF₄. The specific capacitance of B-UNCD-diamond was $\sim 22 \text{ F/g}$ in both media. Furthermore, the specific capacitance varied from 12-22 F/g in H_2SO_4 and from 15-25 F/g in BMIMBF₄ between -0.2 and 0.8 V vs. Ag/AgCl. The key findings were that the B-UNCD-diamond powder exhibits good cycling characteristics in media, excellent microstructural

and chemical stability during extended cycling in both media, and a specific capacitance that depends on the specific surface area. Comparable specific capacitance values were observed for diamond in the two media.

The preparation and initial material characterization of a hybrid sp^2/sp^3 carbon powder was initiated but not completed as a result of the termination of the project funding. This composite powder possesses a diamond core with an overcoating of boron-doped ultrananocrystalline diamond (B-UNCD). The surface of the B-UNCD layer contains nanographene platelets.

IV. Double Layer Capacitance of Graphene - Effect of Electrolyte Species.

This task has been a collaborative one with the Drzal Group at MSU and with Dr. Paul Sheehan (Naval Research Laboratory), who is a world leader in the preparation, characterization and application of well-defined, single layer graphene. The single and multilayer graphene samples were characterized by *ex situ* AFM. Individual graphene segments, 5 ~ 20 nm thick and 10-20 μm wide, were observed, in good agreement with the optical transmittance of the samples in the UV/Vis ($\%T \propto l$ (thickness)). The samples generally exhibited uniform transparency indicating the thickness is uniform over large areas. Visible Raman spectra showed an I_D/I_G intensity ratio of <0.08 , and relatively sharp 2D peak, indicating the graphene is thin. AFM revealed the graphene layers have many wrinkles, formed during sample preparation, with a stair-step edge structure. Background cyclic voltammetric *i-E* curves in 0.5 M H_2SO_4 revealed a pseudocapacitance with a redox peak centered at ~ 0.4 V. These peaks are probably due to the redox behavior of quinone/hydroquinone functional groups existing at the edge plane sites. The background voltammetric current in just supporting electrolyte solutions, at potentials away from the redox peaks, increased proportionally with the scan rate and the immersed sample area. This indicates the currents result from the charging and discharging of the electric double layer. The double layer capacitance (C_{dl}) was calculated from background current at 0.6 V, and was found to be $\sim 12 \mu\text{F}/\text{cm}^2$. Using BET surface area, it can be converted into specific capacitance. For example, using this capacitance and assuming a BET surface area of 700 m^2/g , C_{dl} is calculated to be *ca.* 85 F/g.

The single and multilayer graphene samples were chemically modified using the electrochemically-assisted reduction of diazonium salts. Specifically, the ad molecule was anchored to edge plane sites of the graphene samples. The ad molecule reduced voltammetric background currents consistent with a lowered capacitance. The apparent rate of electron transfer for the inner sphere, $\text{Fe}(\text{CN})_6^{-3/-4}$, was significantly reduced in the presence of the ad layer while the rate for the outer-sphere, $\text{Ru}(\text{NH}_3)_6^{+3/+2}$, was much less affected. The results indicate that, like HOPG, electron transfer for $\text{Fe}(\text{CN})_6^{-3/-4}$ occurs

primarily through edge plane sites while electron transfer for $\text{Ru}(\text{NH}_3)_6^{+3/+2}$ occurs at both edge and basal plane sites.

4. High Surface Area Electrodes as Electrodes - Timothy Hogan

Objectives:

- Develop high surface area electrodes as substrates for nano-graphene sheets.
- Assemble systems for characterization of the nano-graphene decorated electrodes and measurements of cyclic voltammetry, electrochemical impedance spectroscopy, time dependent measurements for RC time constant and total capacity of the electrodes.

Background:

Commercially available supercapacitors are commonly made with activated carbon to fabricate electrical double-layer capacitors. To obtain large charge storage capacities, highly porous carbons are commonly used in various forms. The low electrical conductivity of highly porous carbon, unfortunately can lead to excessive loss and heating during charging and discharging [1]. Optimal structures might be found through minimizing the path from the electrolyte solution to the metal electrode, while maintaining a large surface area. To achieve this, a high surface area metal structure is proposed as the electrode on which a highly porous thin film of nano-graphene is coated. The short path through the thin carbon structures is expected to help minimize the electrical resistance losses in the carbon, while the high surface area of the thin carbon film maintains the high specific capacitance of the structure.

Several groups have recently shown nanowire structures that exhibit promising properties for use in lithium ion batteries, including ZnO [2, 3, 4], SnO_2 [5, 6, 7], Si [8], and Ge [9]. Aligned nanowires have shown increases in the capacity and less degradation of the capacity upon charge-discharge cycling. Such alignment is found with nanowires grown using the vapor-liquid-solid technique (VLS). Aligned nanowires can accommodate significant expansion and contraction of the nanowires while maintaining a connection to a metal electrode substrate. We will use our expertise of the VLS growth of ZnO and GeO_2 to investigate these materials as possible electrodes for lithium ion batteries.

Description of Research Tasks:

Task 1. Fabricate various metal and metal-oxide nanowires and measure the properties of the corresponding samples as potential electrodes for supercapacitors or lithium ion batteries.

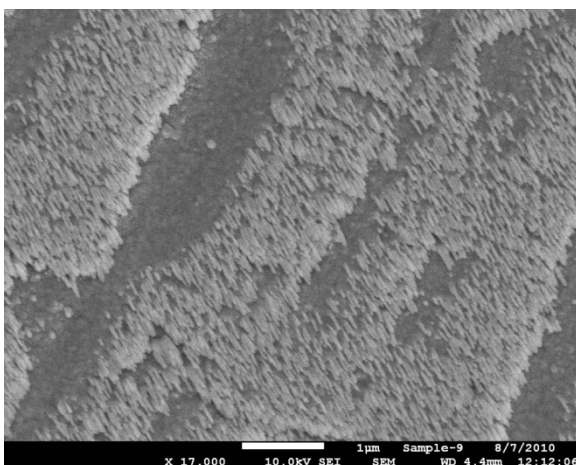
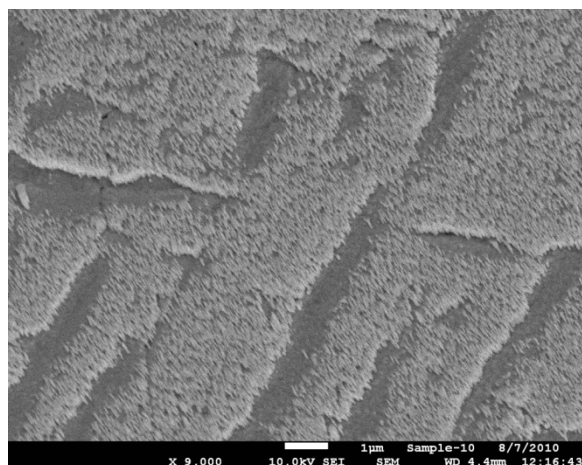
Task 2. Assemble measurement systems needed for characterization of the resulting exfoliated graphite coated metal nanowires for their evaluation in supercapacitors.

Summary of Hogan Group Scientific Progress and Accomplishments.

The goals of this research were to utilize expertise in nanowire growth to develop high surface area electrodes with low electrical resistance. Through collaborative efforts these electrodes would be used with high surface area carbon based materials to make supercapacitor and lithium ion battery structures.

I. Growth of Nanowires for High Surface Area Electrodes

For compliance with the measurement systems, 0.5" diameter metal disks were used as a substrate, and a 21 sample holder was developed for a physical vapor deposition system. An oblique angle deposition technique was used where $\sim 50\text{nm}$ of silver is first deposited on the substrates at normal incidence. After this initial layer, the substrate stage is tilted at a high angle relative to the source metal ($\sim 80^\circ$ tilt), and the rotation of the substrate is stopped. As the metal is deposited, small surface outgrowth leads to shadowing affects that can be used to form metal nanorods growing out of the surface at an angle. The grown silver nanorods were approximately 30-100nm in diameter, and approximately 200-300nm in length. Regions of several square microns showed nanorod "forests". Gaps in the surface coverage could be seen in SEM images indicating regions where the nanorods did not grow. Nanowire coverage and morphology were dependent on the location of the metal disks within the sample holder relative to the evaporation source, and on the surface preparation of the substrates (particularly how smooth the surfaces were). Future work was to include other metal materials such as nickel and aluminum, and collaborative work on energy storage devices. SEM images of the resulting metal nanorod growth on the surfaces of the disks are shown in *Figure 28*.



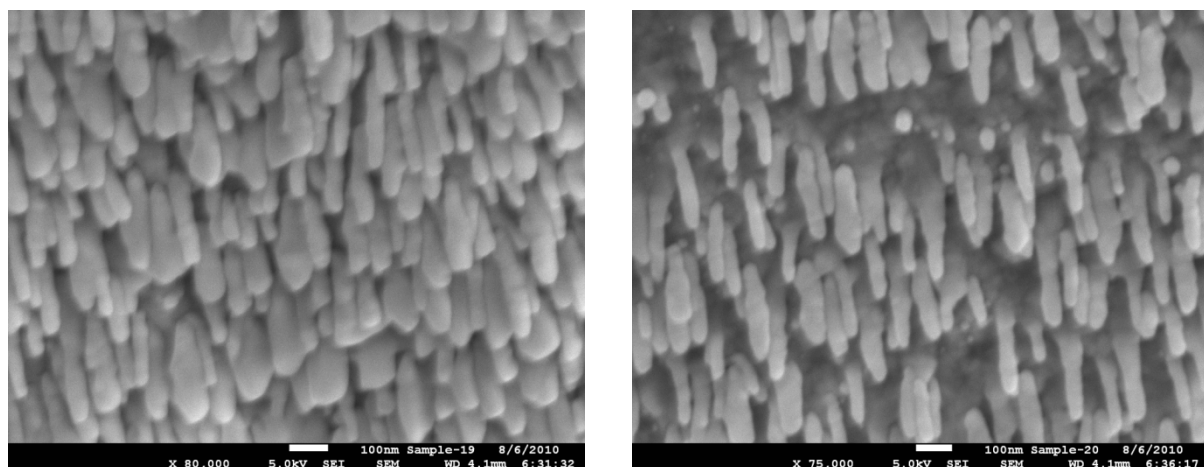


Figure 28. Silver nanorod growth on metal substrates to be used as an electrode for carbon nanoparticle decoration and supercapacitor applications (scale bars are 1 μ m in the top two images, and 100nm for the bottom two images).

The grown silver nanorods are approximately 30-100nm in diameter, and approximately 200-300nm in length. Surface coverage of the nanorod formations is not uniform but shows regions where the nanorods are not found. This also depends on the location of the metal disks within the sample holder. Other metal disks closer to the evaporation source showed only initial growth or no growth as indicated in *Figure 29*.

The process of optimizing the deposition conditions of temperature and deposition rate to achieve more uniform coverage both within a given metal disk, as well as among all metal disks is being optimized so that nickel and aluminum metal nanorods can be made. Interaction with other groups to deposit high surface area carbon materials to finish the supercapacitor electrodes could not be completed before the end of the project.

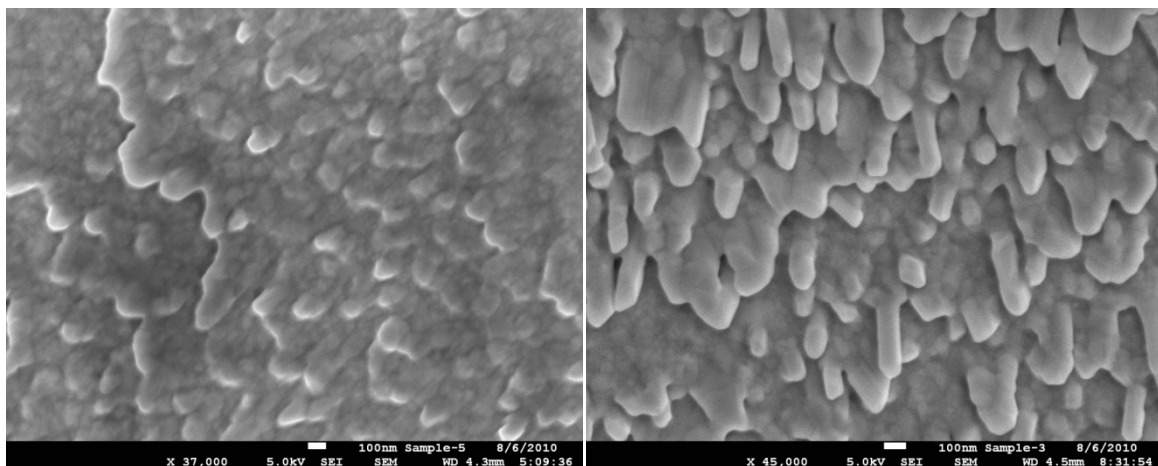


Figure 29. Coins placed closer to the evaporation source showed little, or no metal nanorod growth.

Summary. Reductions of the internal resistance of supercapacitors and lithium ion batteries would help decrease the time constants and increase the efficiency of such devices. The results completed under this project showed that the development of high surface area metal electrodes could be accomplished with these methods. Decoration of these metal nanowires with high surface area carbon materials such as carbon aerogels, nanoplatelet graphene, and/or silicon nanoparticles would be expected to boost the performance of these devices. The initial efforts toward such goals were achieved, laying the groundwork for a number of possible subsequent studies to be done.

5. Composites with Dielectric Properties and Capacitive Density for Applications as Embedded Capacitors - Martin C. Hawley

Energy storage and wireless energy transport could be key technologies to addressing the several major challenges in the coming decade. The focus of this work was based on improving materials for wireless energy transport.

Antennas used to provide energy for navigation, propulsion, etc. are limited due to “scan blindness”; that is, they work well when the radiated energy is incident normally on the antenna array, but their performance depreciates rapidly as the angle of incidence increases, a limitation that can be mitigated with newly designed materials like wide-angle impedance matching (WAIM) layers. Use of a magneto-dielectric material (material with an enhanced permittivity and permeability) would enhance both the span of angles with good transmission but also the spectral operational bandwidth.

Preliminary experimental approaches included investigating polymer composites with spherical iron oxide nanoparticles; very large loadings of iron oxide were necessary to increase the magnetic permeability, at the cost of material integrity. An alternative approach focused on using frequency selective surface (FSS) layers designed as periodic metallic arrays, acting as “inductive inclusions” within the polymer. Interactions between inclusions and a self inductance of the inclusions resulted in an enhanced magnetic response. The shape, dimension, and periodicity of the metallic elements of the array were variables for the final design and determined the effective properties and operational bandwidth for the composites. These materials were designed, fabricated, and characterized and shown to have a permittivity and permeability greater than 2, with very low loss, from 2-5GHz, and the scan angle dependence was minimal.

Objectives:

- Design of composites with the required dielectric properties and capacitive density for applications as embedded capacitors; composites may include metal

- oxide particle reinforcement and frequency selective surface layers (periodic metallic arrays)
- Fabrication and characterization of composites designed to have specific properties for embedded capacitor applications

Background

Energy storage is essential for such applications as cell phones, computers, transportation and load leveling for further development of renewable energy sources (wind and solar power). With all these applications, for success in commercialization, long life and low cost are essential; yet, these are not attainable with the current state of technology for batteries and capacitor storage systems. The key challenge in capacitor design is increasing the storage capacity as well as the efficiency while maintaining low weight and low cost [10, 11]. The current hurdles encountered with the capacitor components include limited substrate space, high cost, unreliable system performance, and low energy density. With increasing efforts focused on miniaturization of electronics, there is presently an ongoing transition from these discrete passive components to embedded passives, including embedded capacitors; which allow for improved reliability and performance with lower cost, size, and weight.

The goal of this research would be to design the composite material and thereby tailor the material properties for the application of embedded capacitors as well as to fabricate and characterize these composites to validate the design methodology. Specifically, these materials require high dielectric constant, low dielectric loss, low dissipation factor, increased capacitive density, wideband performance, and simple processability; however, currently, there are limited materials designed that satisfy these requirements. Therefore, efforts to improve the design methodology and fabrication of these composites are essential to transition from discrete capacitive components to embedded capacitors.

Embedded capacitors are configured similar to a parallel-plate capacitor with the capacitance be calculated using the following equation:

$$C = \frac{\epsilon_0 \epsilon_r A}{t}$$

where C is the capacitance (F), ϵ_0 is the relative permittivity of free space, ϵ_r is the dielectric constant of the material, A is the electrode area, and t is the thickness of the dielectric medium. Since the larger dielectric constant also increases the capacitance in a specific space; therefore, for applications that involve a constrained space, higher dielectric constants are favored. The dissipation factor is a measure of loss-rate of the power and is expressed as a ratio of resistive power to the capacitive power, also called the loss tangent [12, 13].

Description of Research Tasks:

Task 1: Selection of materials. The first phase of work will revolve around the design of materials with tailored dielectric properties. This will involve a focus on selection of polymers and inclusion materials. In the proposed project, we will use thermosetting polymers. The advantage of using thermosetting polymers in the event of using a layered composite is that one can make layered materials easily – by curing a layer and adding layers repeatedly to achieve the desired thickness. An epoxy that has been widely used in thermoset applications is diglycidyl ether of bisphenol A (DGEBA) and would work well for creating the layered composites; however, a similar epoxy resin of a lower viscosity would be better for those samples with layers including dopants or inclusions. For this reason, DGEBA could be used instead of DGEBA so that when inclusions are used in certain layers, dispersion will be easier to achieve. The dielectric constant of the epoxy resin can be increased by combining additives like metal acetylacetonate (metal acac), which has been shown to increase ϵ' for the polymer matrix before addition of a ceramic filler [9]. Nanomaterials or micromaterials are ideal for dopants since they allow for a thinner dielectric thickness and hence an increased capacitance density. Using metallic fillers would be an ideal solution; however, the increased conductivity will also lead to an increased dielectric loss. Metal oxides or core-shell dopants with a non-metallic shell and metallic core would be possible solutions to this problem [10]. Ferroelectric ceramics and other materials with a high dielectric constant require a high temperature for processing (like sintering), so these are not ideal for embedded capacitor applications. Surface modification of the dopants will play an important role not only in dispersion but in the resulting dielectric properties, specifically by reducing the dielectric loss.

Task 2: Utilization of simulation and design tools for composite design. Preliminary studies have been conducted in developing models for extracting effective medium properties for composites using numerical models. A numerical approach is used to compute reflection and transmission and use algorithms for extracting effective permittivity and magnetic permeability. This has been done for three types of composites that comprise of (i) a set of layers and (ii) cylindrical rods, and (iii) spheres [14]. A thorough understanding of how the size and distribution of various filler materials affects the dielectric constant and dielectric loss factor will be developed. An interesting approach to creating a layered composite would be to use the idea of frequency selective surfaces at the interfaces of the layers. A frequency selective surface (FSS) is a periodic array of conducting patches or aperture elements. The frequency-filtering property of the FSS comes from the planar periodic structure; the elements reflect the incident microwave for a specific frequency range. This property is dependent on the element shapes, periodicity, and dielectric property of the substrate. An incident wave to the FSS layer will cause an induced current in each element,

which act as either capacitors or inductors (depending on the shape). These currents result in a scattered magnetic/electric field. The design of the frequency selective surface is highly dependent on the desired reflection and transmission characteristics as well as the desired bandwidth for varying angle of incidence [15]. A combination of layers including particle inclusions and FSS layers at the interface can further enhance the dielectric properties of the material while keeping the dielectric loss very low. Furthermore, combining the idea of FSS layers and layers with metallic or metal oxide fillers would further enhance the permittivity without necessarily requiring very high loadings.

Task 3: Fabrication and characterization of composites. During the second year of work, the major focus will be fabrication of composites based on the designs developed in previous tasks and further design efforts with new geometries. Challenges to be expected during fabrication include achieving an adequate dispersion of dopants, a good adhesion between the filler and the polymer matrix. The frequency selective layers will be etched on a polymer substrate; the resulting patterned layers will be cured layer by layer with epoxy as the adhesive or compression molded with polypropylene layers filled with metal oxide particle reinforcement. Polyethylene films (~125 μm thick) have been successfully coated with silver (~100 nm thick layer). Photolithography has been successfully used to pattern the silver coated polymer films. Characterization will play a key role in future phases of this project. Dielectric characterization will be the primary analysis, to study both frequency and temperature dependence of both dielectric constant and dielectric loss factor. Capacitance and dissipation factor will also be investigated as a function of temperature and frequency.

Summary of Hawley Group Scientific Progress and Accomplishments.

By increasing the effective permeability (magnetic properties) and permittivity (dielectric properties), materials for antennas and other wireless energy transport can be improved to increase bandwidth performance as well as reduce scan angle “blindness.” However, naturally occurring magneto-dielectric materials are often either non-magnetic at frequencies greater than 1 GHz or exhibit large loss at these frequencies. Other challenges with these materials include their high mass density, which can require external biasing for operation.

I. Magneto-Dielectric Materials for Wireless Energy Transport

The conventional approach of macroscopic composites with magnetic reinforcement material (iron oxide nanocomposites) resulted in the need for a volume fraction of 40% or higher, leading to brittle materials. Such performance can be attributed to the geometry of the inclusions, which does not allow for a large magnetization in the composite; therefore, the permeability is near unity and the material is non-magnetic. Furthermore, the spherical ferrimagnetic particles used in this study have a demagnetization factor of 1/3, meaning that they must be very tightly packed in order to result in a significant increase in permeability.

A secondary approach to designing the magneto-dielectric composites utilized the idea of periodic arrays of metallic patches, which can be designed to act as “inductive” inclusions, thereby enhancing the properties for the material and is shown in *Figure 30* below.

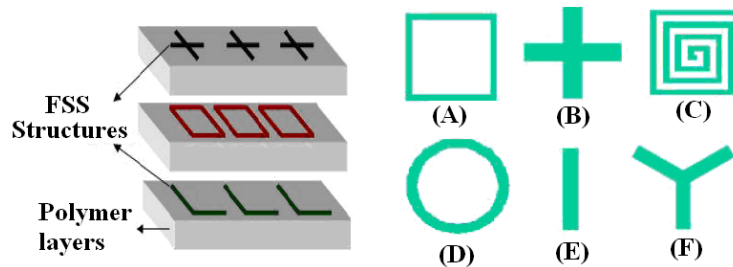


Figure 30. Illustration of Periodic FSS Layers

Engineered inductive inclusions were designed through one or more frequency selective surface, resulting in an “artificial” magnetic material with low mass density and controlled loss for frequencies greater than 2GHz).

Magneto-dielectrics for Energy Transport. Initial work was carried out to improve material properties for magneto-dielectrics that would result in a wide scan angle performance, optimal for use in WAIM materials for applications used in energy transport. The goal

properties for this application would be a relative permittivity and permeability both near 2 with low loss (below 10^{-2}). The composite geometry and FSS array layout are shown in *Figure 31*. Polymer layers were made of epoxy, while the elements on the array were silver.

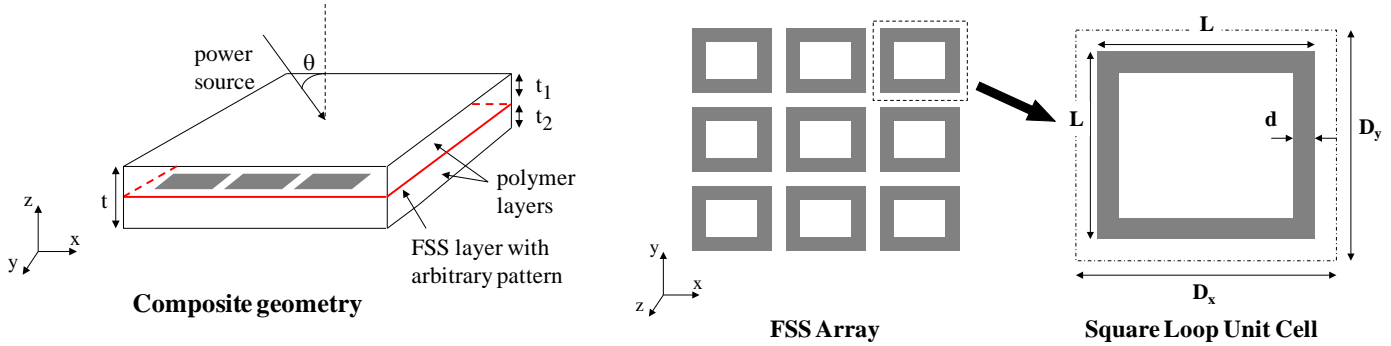


Figure 31. Illustration of Composite Geometry and FSS Arrays

For the initial modelling, Ansoft Designer and Ansoft HFSS were software used for simulation of the composite geometries. These software packages use method of moments and finite element methods, respectively, to solve electromagnetics problems; the geometries for the composites are meshed adaptively for a range of frequencies

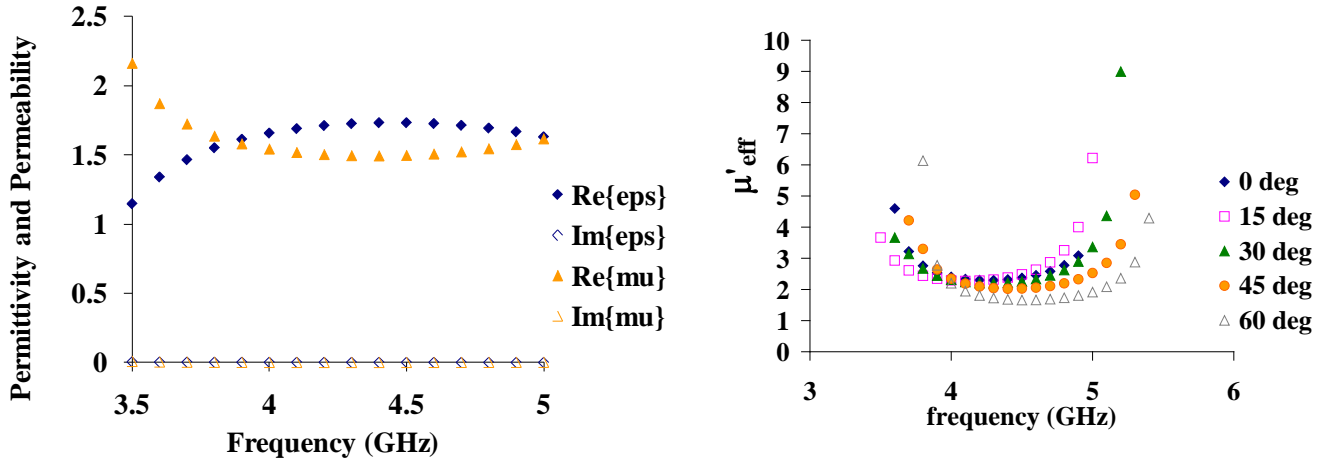


Figure 32. Permittivity and Permeability Illustrations

For the examples shown in *Figure 32*, the square loops were 5mm (L) and the unit cell was 5.5mm (D_x , D_y), with 10mm polymer layers (t_1 and t_2). The permittivity and permeability were both raised to the same extent, and the scan angle dependence was minimal (right). Materials were also fabricated using a photolithographic process to verify the modeling results.

What makes these designs novel is that the enhanced effective permeability is greater than 1; whereas, past work in metamaterials design involved designing artificial dielectrics (non-magnetic), dissipative materials like left-handed or double negative (DNG) materials, and other related technologies. The permeability and permittivity are both greater than 2 for frequencies from 2-5 GHz, with loss below 10^{-3} with minimal dependence on scan angle (results shown in *Figure 32*).

Another novel aspect of these designs is that with permittivity and permeability both increased to the same extent, impedance matching becomes much easier for application purposes. The FSS layered composites were fabricated and characterized using a waveguide to measure the reflection and transmission to compare to modeled results. The measurements correlated well with the modeled results.

Future Impact and Outlook. There are several design challenges associated with advancing electromagnetic materials for applications including wireless technologies or energy transport, for example. The work presented here illustrates an approach to designing materials that can circumvent some of the current design difficulties. This approach offers wide flexibility in the magneto-dielectric design space, since the possibility for shapes or patterning is infinite.

Future work may involve optimization schemes to fine tune the FSS elements' shape. By incorporating some of the concepts and results from earlier work at lower frequencies by using spherical ferromagnetic inclusions, a wider bandwidth can be achieved. This would require a co-design of layers and inclusions, so that their complementary effects will meet the overall design goal. Another aspect of the design approach presented here that offers more flexibility for the designer is the possibility of incorporating multiple FSS layers but to use alternate shapes on the multiple FSS layers. For example, by combining dipoles and loops, both the capacitance and inductance can be enhanced.

With a similar approach, the same methodology shown above can be used to tailor the properties of the material for other applications. Ultra-high dielectric properties can be achieved with appropriately designed FSS layers, which will be the focus of future work. These materials would be high permittivity, low loss (dissipation), and wideband, and would play a significant role in enhancing the performance of embedded capacitors or other energy storage materials.

6. Graphene Nanoplatelets (GnP) for Applications in Lithium Ion Batteries and Supercapacitors - Jeffrey Sakamoto

Objectives:

- Design, synthesize and characterize GnP-carbon (and metal) composite materials
- Evaluate GnP-carbon composite materials for potential use in lithium batteries and super capacitors

Background: Over the past decade several companies, government agencies and research groups have characterized the low temperature performance of Li-Ion batteries for space and terrestrial applications. It is agreed that the performance of Li-Ion batteries significantly decreases below -20 °C. Belt et al. evaluated several commercially available SAFT batteries using the FreedomCar performance criteria [16]. Although the commercially available batteries met the majority of the requirements, the cold cranking goal was not achieved at -30C. Jansen et al. characterized several Li-Ion cells using a SnSi microreference electrode to improve electrochemical measurement resolution at low temperatures [17]. The use of the reference electrode allowed characterization of the individual anode and cathode impedance contributions as a function of temperature. Although they did not conclude that Li-diffusivity in the graphite-based anodes limited low temperature performance, they did suggest using higher surface area anode materials, which is taken into consideration in our Technical Approach below.

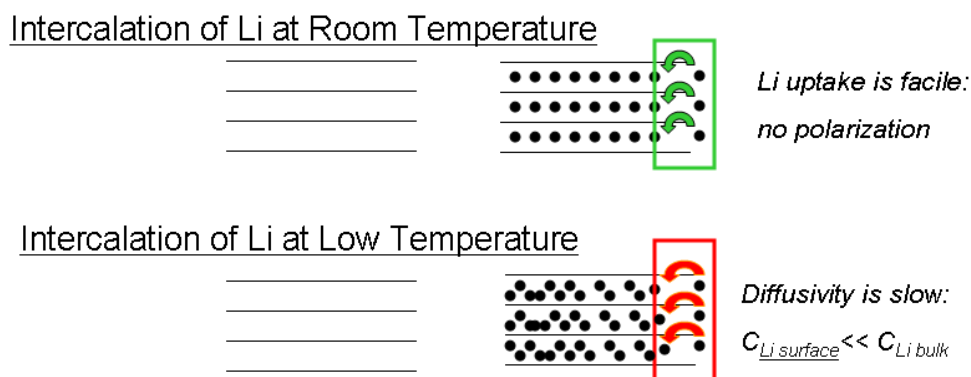


Figure 33. Li diffusivity during de-intercalation from graphite is slow below -20 °C, thus causing cell polarization.

The majority of groups, however, agree that Li-diffusivity in carbonaceous anodes primarily limits low temperature Li-ion battery performance. Essentially, each transport mechanism that occurs during charging/discharging was investigated independently (Fig.

9). Temperature sensitive mechanisms such as electrolyte conductivity, SEI impedance, and anode and metal oxide cathode capacity were characterized in full and half cells. For the most part, most groups agree that properly selected electrolytes have adequate conductivity at -40C. Similarly, Li diffusivity in the SEI and metal oxide cathode capacity do not limit low temperature performance. It is believed that the significant decrease in Li diffusivity in the anode results in cell polarization, thus limiting capacity at low temperatures. Huang et al. found that over 80% of the carbonaceous anode discharge capacity is available at -40C using 0.285 mA/cm² [18]. However, charge acceptance at -40C was negligible and was likely due to polarization that resulted from significant reduction in Li diffusivity. Zhang et al report that 12% of the room temperature charge/discharge capacity at 0.1 mA/cm² is retained at -20C in commercially available cells using graphite anodes [19]. Likewise, Zhang,[20] Fan[21] and Cousseau et al. [22] agree that Li diffusivity in the carbonaceous anode is the primary mechanism that limits low temperature performance. Interestingly, Cousseau (SAFT) et al report high discharge capacities at low temperatures. However, the high discharge capacities at low temperatures (-40C) were achieved by self-heating causing cells to generate enough thermal energy to heat the cells from -40C to +0C. Although this technique may improve low temperature capacity, it is not clear if the FreedomCar L-HPPC requirements were met. According to the FreedomCar requirement, 20% of the 25C discharge power capability (for example 5kW at low temperature available from a battery rated at 25kW at 25C) must be available for 2 second pulse power discharge at low temperatures [23]. This is also referred to as the Low Hybrid Pulse Power Characteristic (L-HPPC) requirement. At present, no Li-Ion battery technology exists (aerospace or terrestrial) that can meet the L-HPPC requirement. *One of our goals is to develop new carbonaceous anode materials, and possibly combine them with state-of-the-art materials, in an effort to improve the charge acceptance performance of Li-Ion batteries that can broaden the Army's battlefield requirements.*

Preliminary collaboration between the Drzal and Sakamoto groups has indicated that exfoliated graphite nanoplatelets (GnP) have potential for use in electrochemical applications. Initial characterization indicates that GnP can be used as an effective, low-cost conductive additive and as an electrochemically active anode material. The Drzal group has established a method for synthesizing high surface area GnP with the ability to modify the surface chemistry. Modifying the surface area can result in unique electrical and electrochemical properties such as reduced initial capacity loss (due to the solid electrolyte interphase formation) and higher specific capacitance (Farads/gram). Thus, efforts to integrate GnP into novel battery and super capacitor electrodes will be pursued. Specifically, the synthesis of GnP-carbon aerogel nanocomposite electrodes and GnP-carbon aerogel-metal [24] composites will be investigated for use as electrodes for lithium, lithium-air batteries [25] and super capacitors [26, 27]. *Our other goal is to explore new*

GnP-carbon-metal composite materials for potential use in electrochemical energy storage technologies.

Overall there are two aspects to this effort. First, the Sakamoto group has experience with characterizing and improving the charge acceptance of Li-ion batteries. It is believed that the Army can directly benefit from the charge acceptance activity if improvements can be made to this end. Second, it is believed that the fundamental materials research conducted in this effort could have broader impacts with regard to other electrochemical technologies such as Li-air batteries and super capacitors.

Description of Research Tasks:

Task 1. In research task 1, the primary emphasis will be on synthesizing new GnP-carbon composite materials and characterizing their physical and electrochemical properties. Sol-gel synthesis will be used to make prepare GnP-carbon composite materials, which entails casting liquid precursor (along with other constituents such as GnP), allowing the sol to gel and supercritical drying (achieved in a 16-L autoclave). The Sakamoto group also has a BET to measure surface area and porosity as well as a lithium battery glovebox with 34-channels for characterizing electrochemical properties.

Task 2. In research task 2, the primary emphasis will be on taking the appropriate materials from task 1 and integrating them into electrochemical energy storage prototypes such as Li-Ion batteries, Li-air batteries and super capacitors. The goal of this task is to test the novel composite materials in a relevant environment.

Summary of Sakamoto Group Scientific Progress and Accomplishments.

The Sakamoto group investigated the synthesis, processing, and characterization of ceramic electrolytes for use in advanced batteries. Initially, the focus was on developing new synthesis and processing techniques based on the ceramic electrolyte $\text{Li}_{0.33}\text{La}_{0.57}\text{TiO}_3$ (LLTO-perovskite). A novel solution-based (sol-gel) technique was developed to synthesize LLTO and was also modified to prepare $\text{Li}_4\text{Ti}_5\text{O}_{12}$ aerogel/graphene nanocomposite anodes. The novel sol-gel process also served as the genesis for a new material breakthrough; $\text{Li}_7\text{La}_3\text{Zr}_2\text{O}_{12}$ (LLZO) with the mineral name garnet. By modifying the stoichiometry and by replacing Ti in LLTO with Zr, the Sakamoto group developed a new ceramic electrolyte membrane technology, based on LLZO, exhibiting the unprecedented combination of high ionic conductivity ($\sim 1\text{mS/cm}$ at 298K), stability against Li and air. The Ti in LLTO is not stable against reduction against Li, but Zr is. It is believed that this membrane technology can enable several technologies such as solid-state, Li-air and Li-sulfur batteries.

The Sakamoto group tailored the sol-gel process to produce nanometer scale powders, with high phase purity. Densification of the powders into membranes (99% dense) was achieved through a novel induction hot pressing technique to rapidly heat LLZO powders, to limit Li loss, while applying pressure to enhance sintering.

I. Synthesis of Exfoliated Graphite Nanoplatelet (GnP) Composite Carbon Aerogels.

Exfoliated graphite nanoplatelet (GnP)/carbon aerogel composites were prepared. GnP was used as an electrical wiring and mechanical reinforcement additive. The GnP/carbon aerogel composites are prepared by the poly-condensation of phloroglucinol and furfural with GnP at room temperature, followed by supercritical drying and subsequent pyrolysis in inert atmosphere. The surface areas are typically in the 800 m²/g range in which most of the porosity is in the 2-10 nm range. The electrochemical properties were investigated using a three-electrode electrochemical cell and the electrical conductivity was measured using the 4-probe method. It was found that GnP acts as an effective conductive additive and can further enhance the electrical conductivity of carbon aerogel. Cyclic voltammograms were conducted between 1 and 1000 mV/s to evaluate the capacitance as a function of ionic adsorption/desorption rate. Compared to the pure carbon aerogel electrodes, the GnP/carbon aerogel electrodes were able to maintain capacitance at the higher sweep

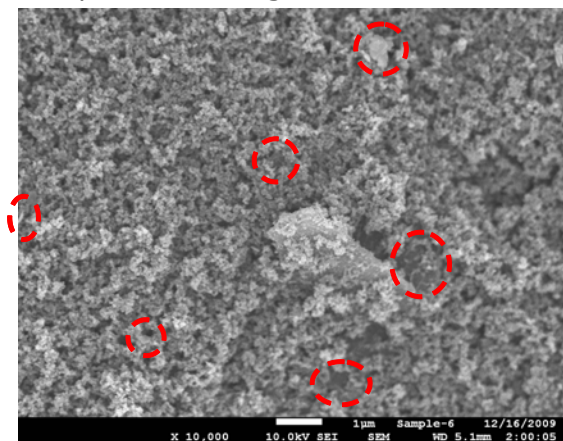


Figure 34. SEM of carbon aerogel with 2 wt% GnP. The red circles highlight the GnP embedded in the carbon aerogel

while electrons are shuttled through the electrode without occluding or slowing the formation of Li₂O.

rates. It is believed that increasing the electrical conductivity while maintaining the same level of accessible porosity can enhance the power density of capacitors.

Carbon aerogel is known to have ultrahigh porosity, thus it is a suitable candidate for use in super and ultracapacitors. Because of its high surface area, it can also be considered as a catalyst support for lithium-air batteries.

Catalysts such as nanophase MnO₂ particles can be dispersed in a carbon aerogel matrix such that air readily permeates the highly porous network,

However, it is also known that carbon aerogel can be relatively weak or brittle. Thus, the integration of GnP into carbon aerogel was investigated to improve both electrical conductivity as well as mechanical integrity. A range of GnP volume fractions were studied to include 0, 1, 2, 5, and 10wt%. It was determined that for an addition of 2 wt% GnP to carbon aerogel, a 40% increase in electrical conductivity was achieved. Furthermore, the 2

wt% GnP to carbon aerogel compressive rupture strength was increased by factor of three compared to pure carbon aerogel.

II. Synthesis and Characterization of Sol-Gel Derived Ceramic Oxides for Lithium-Air Batteries. Ceramic electrolytes are attractive candidates for lithium-air batteries, because they are structurally robust and recent progress has identified some with ionic conductivities comparable to that of liquid electrolytes. Specifically, $(\text{Li},\text{La})\text{TiO}_3$ (LLTO) has shown promise as a candidate ceramic electrolyte for lithium-air batteries. LLTO has the perovskite atomic structure, which is cubic in nature, thus it has isotropic physical properties. Although LLTO has shown promise, there are several challenges that must be addressed before it is integrated into lithium-air batteries. First, the ionic conductivity has been shown to be sensitive to porosity in that a few percent porosity can dramatically reduce lithium-ion transport. Thus, advanced nanophase processing of LLTO powders is necessary to facilitate sintering and purity. Second, to reduce cell impedance, the thickness of LLTO electrolyte layers must be relatively thin (10 to 100 micron range), which may impose a mechanical reliability concern for long-term usage. Thus, a relationship between the microstructure, processing, and the resulting mechanical properties must be clearly understood to enable the fabrication of robust, free-standing films of LLTO.

Two approaches for synthesizing LLTO have been investigated. First, an approach involving high energy ball milling (HEBM) of bulk scale LLTO precursors has been investigated. Nanophase lanthia, titania and bulk scale lithium carbonate were milled in a HEBM apparatus. The purpose for considering nanophase precursors is two-fold, i.e. it will facilitate mixing and can enhance sintering by virtue of its scale. The milled precursors were then hot pressed at 1050C in argon to convert the metastable mixture into LLTO and have been prepared for characterization (ionic conductivity, nanoindentation and density measurements) to determine the effects of sintering conditions on the mechanical and physical properties. The second approach for synthesizing LLTO involves sol-gel synthesis. Through our investigation using HEBM synthesis, it was determined that contamination from the metal milling vials and inconsistent mixing would compromise the LLTO phase purity. Thus, it is believed that the sol-gel synthetic approach can achieve a higher degree of stoichiometry and phase purity. A new sol-gel recipe for synthesizing LLTO has been developed, which involves the use of lithium acetate dihydrate, lanthanum nitrate hexahydrate, titanium isopropoxide and ethanol as the diluting solvent. Combining these liquid precursors under controlled conditions, creates a rigid and transparent gel network. Efforts are under way to dry, calcine and sinter the sol-gel derived LLTO.

The ARO CAESRT support was instrumental in establishing a new field of research in the Sakamoto group at MSU. The support enabled the development of a flexible solution-based

synthetic technique to prepare complex oxide ceramic electrolytes and graphene composite electrodes for Li batteries. The flexibility offered by the new synthetic technique enabled numerous investigation into a new, complex electrolyte based on $\text{Li}_7\text{La}_3\text{Zr}_2\text{O}_{12}$ (LLZO) with the mineral name garnet. Mechanisms were discovered that stabilize the fast ion conducting form of LLZO. The mechanism which was verified experimentally, involves the super-valent substitution of cations to create Li vacancies and disorder in the Li sublattice. The end result is a ceramic electrolyte that has the unprecedented combination of high ionic conductivity ($\sim 1\text{mS/cm}$ at 298K), stability against Li and air. We also developed a process for sintering the LLZO powders, prepared by the solution-based synthetic technique, involving a custom built induction hot press. The sintering process achieved ultra-high density LLZO membranes (99%) for transport measurements and Li cycling experiments. Essentially, the combination of synthesis, doping and sintering allowed the Sakamoto group to significantly advance the understanding of a new ceramic electrolyte that can enable solid-state, Li-air and Li-sulfur batteries.

7. Novel Management and Control Approaches for Battery Systems - Fang Z. Peng

Objectives:

- To identify and address the management and control issues of the existing energy storage systems and provide guidance and improvement goals for new materials and technologies for energy storage

Description of Research Tasks:

Task 1. Identification and investigation of management and control issues of the existing energy storage devices. The most important performance parameters about energy storage devices are energy density, power density, and lifetime. For example, a same type of battery can be designed and manufactured for higher energy density with less power density and vice versa. Depending on the application, the most important battery characteristic may differ. A hybrid use of high-energy battery and high-power battery or a combination of battery and super-capacitor may be more suited for certain applications. For increased capacity and higher operation voltage, battery cells or super-capacitors need to be connected in series. Series-connected cells require good management and control because cell-capacity matching and cell-balancing circuitry are often required to assure that each cell reaches the same float voltage and the same level of charge. Battery lifetime depends on battery chemistry, depth of discharge, battery temperature and battery capacity termination level. Charging speed and voltage profile, depth of discharge, battery temperature and battery capacity termination level are extremely sensitive to batteries. All

these issues make it very important to have a good and intelligent battery management and control for longer lifetime, prevention of permanent capacity loss and degradation, and so on. In this task, we will investigate how to boost battery life, charging methods, run-time versus battery life, charge and voltage balancing for series connection of batteries or super-capacitors.

Task 2. Investigation and development of system-level (circuitry and control) solutions for better management and control of batteries and super-capacitors. When battery cells and/or super-capacitors are assembled/connected together to power the load and for charging purpose, cell-capacity matching and cell-voltage/charge balancing circuitry are required to assure that each cell reaches the same float voltage and the same level of charge. In addition, temperature has to be closely control and monitored. Many existing solutions are either high cost or low performance. Low-performance solutions often lead to limited charge/discharge depth, de-rating (or over-sizing) of batteries and super-capacitors, and reduced lifetime. We will develop low-cost and high-performance circuitry and intelligent control to boost battery life, perform charging according to optimum charging profile, optimize run-time versus battery life according to application needs, and balance cell-charge and voltage.

Task 3. Preparation of experimental testing and verification of management and control of energy storage systems. We will use our extensive power electronics expertise at MSU to design and implement low-cost and high-performance management and control solutions developed for batteries and super-capacitors. To prove the concept, experimental testing and validation set-ups will be drafted and prepared. The experimental set-ups will be used for testing and evaluation of new material devices.

Summary of Peng Group Scientific Progress and Accomplishments.

The focus of this project is to make battery cells fail safe (no fire or explosion), maintain operation with cell failures, and extend battery life and depth of charge/discharge via power electronics circuits. A battery balancing (equalization) and bypassing circuit is one way to ensure safe, uninterruptable, long life-time operation of serially connected battery cells even when some cells fail. It is essential to a battery pack's performance, efficiency, and reliability. The issues of battery balance circuits have been investigated. The existing circuits cannot achieve these goals. New balancing and bypassing circuits have been proposed and implemented to achieve these goals. In particular, the proposed circuits can maintain the continuous operation even if when battery cells fail and provide the original rated voltage of a whole battery pack by bypassing and voltage boosting of the proposed circuit.

I. Balancing and Bypassing Circuits to Provide Fail Safe Battery System Operation

Specifically several problems and solutions have been investigated for different batteries, with a focus on Li-ion batteries; combined with testing on a 360 V 45 Ah commercial battery pack for hybrid electric buses. In addition, a comprehensive study has been performed on methods to increase battery utilization, cycle life and calendar life; compared and simulated some of the battery cell balance circuits; experimentally evaluated one balance circuit; proposed the improved candidate circuits and control method for the next step.

One of our goals for this joint project is to identify and address the issues of existing energy storage systems. This year, we have been investigating the following aspects: the characteristics of different batteries; the problems of using low-voltage battery cells in a high voltage battery pack; the present circuits and charge methods to increase the battery capacity utilization and lifetime; the defective cell bypass and other protective/prognosis methods to ensure a reliable long-term operation; the hybrid combination of batteries and supercapacitors to optimize the dynamic performance, design and cost of the battery pack; high efficient bidirectional dc-dc converter topologies for the voltage boost.

So far, the research has been focused on circuits for battery cell balance and the protection in the event of defective cell(s). A large number of low-voltage battery cells are connected in series when a sufficient voltage is desired. The serial cells inevitably exhibit the diversity due to the chemical and electrical characteristics and the thermal environment variety in the entire battery pack. As time goes by, repetitive process of continuous high rate charge/discharge can make some of the cells exhibit different SOC and eventually become overcharged/over-discharged. The commercial solution merely protects cells from overcharge via dissipative current shunt, not suitable for the elevated power rating of military hybrid electric vehicles. Since it cannot achieve real cell equalization, it leads to the shallow SOC range, the low effective energy density (1/6th), the limited charge/discharge speed, the constrained energy transfer from the regenerating break, and the shortened battery pack lifetime. Plus, it is not able to handle the any defective cell(s) that present high impedance or even open-circuit.

When cell balance circuits are applied, the individual cell currents are automatically distributed according to their output capacity, as formulated in (1). The cells with higher internal voltage and lower internal resistance undertake more current and thereby more output power. Moreover, less power loss will be dissipated on the cells with larger internal resistance, compared the simple overcharge “balance” method. Thus, the life time of the cells can be prolonged.

$$I_{Bj} = (V_{sj} - V_o / n) / R_{sj} \quad (j = 1, \dots, n) \quad (1)$$

where the terminal voltage of each cell is equalized to V_o/n for n cells; V_{sj} and R_{sj} are the internal voltage and resistance of individual cells, considering the simple battery dc model.

One of the experimental results is shown in *Figure 35* for charge/discharge with/without a 5-cell modular buck-boost balance circuit.. Each battery cell is a 21 Ah lithium ion polymer battery model HA055275. The discharge current is around 0.34~0.42 C (with a resistive load), and the charge current is 0.24 C. Two battery cells had much higher internal impedances than the others. When they get discharged, they present around 200 mV lower terminal voltage than the other cells and reach the end of discharge earlier. An over-100mV overcharge or over-discharge can lead to significant capacity loss and lifetime reduction.

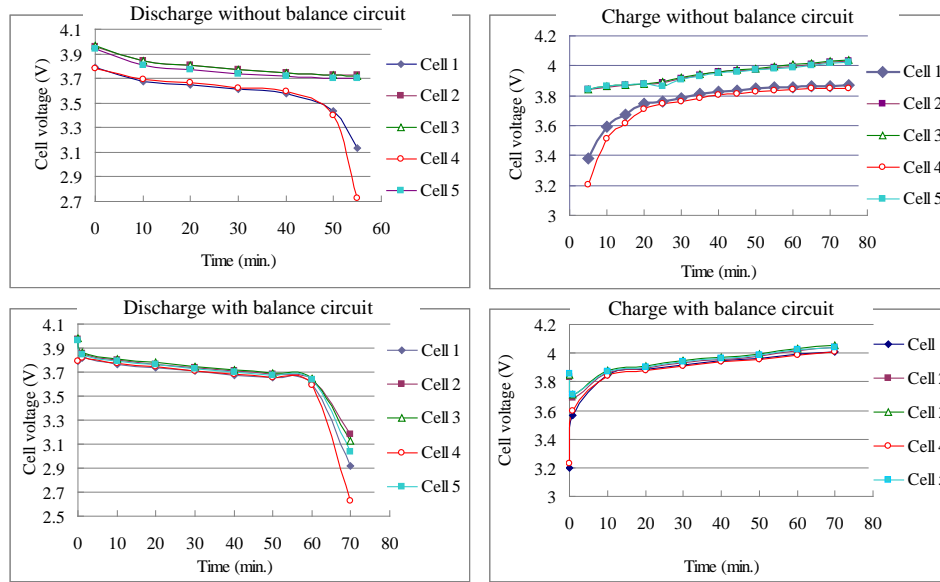


Figure 35. Test results for battery cell charge/discharge with/without balance circuit

Once the balance circuit kicks on, the five discharge curves get closer. Besides, analysis and tests were performed for the defective cell bypass functionality using the same balance circuit. The test configuration is illustrated in Figure 36. As can be seen from Table 5, even if one cell is open circuit, the serial string still can power the load thanks to the balance circuit. The test data indicate that the balance circuit is effective to balance the cell voltages and to bypass the defective cells, if any cells deviate from the others.

Many issues were identified that prevent the existing balance circuits from integrating with the batteries: the circuit complexity and power rating, low efficiency, the poor reliability and high cost. Hence, improved solutions will be implemented in the future research.

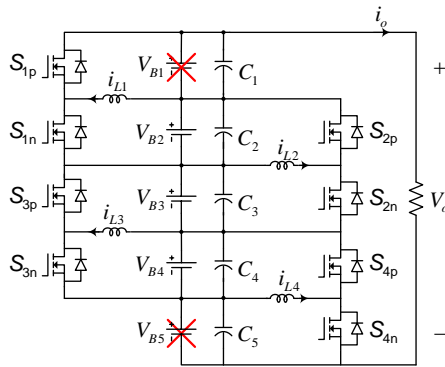


Figure 36. Test configuration of the defective cell bypass using the modular buck-boost balance circuit

Table 4. Test Data With Two Defective Cells

Terminal voltage (V)		Cell current (A)	
V_{B1}	2.732	I_{B1}	0
V_{B2}	3.61	I_{B2}	7.1
V_{B3}	3.936	I_{B3}	7.4
V_{B4}	3.618	I_{B4}	7.1
V_{B5}	2.76	I_{B5}	0
Output voltage (V)		Output current (A)	
V_o	16.656	I_o	4.2

Several cell voltage balancing and faulty cell bypassing circuits have been proposed and investigated. One of them is a magnetically coupled half-bridge balancing circuit, which is connected to a pair of battery cells in parallel. Charge is transferred directly from strong cells to weak ones with phase-shift control. Experiments demonstrated that the circuit was cost-effective and was able to achieve cell balancing and defective cell tolerance with evenly distributed current stress, which prevents defective cell from overheating and fire. The proposed circuit has a lower component count and lower device ratings than its counterparts. Another proposed circuit is a modularized buck-boost + Cuk converter. The proposed buck-boost + Cuk converter can balance the series battery cells with minimum number of switching devices and passive components. Furthermore, it is modular, easy to add on to any number of series cells. Both control and circuit are simple and straightforward.

8. Online And Precise Health Monitoring of Batteries Under Thermal Abuse Conditions - Elias Strangas

Objectives:

- Determine modes of operation and failure, and characteristics of fault severity in a variety of applications representing diverse load characteristics
- Develop and demonstrate methods to characterize the signatures of impending faults
- Implement techniques for fault diagnosis and prognosis of energy storage systems

Background:

Electric energy storage systems applied to hybrid electric vehicles and to safety applications are sensitive to the characteristics of the applications. Often it takes more than

one type of energy storage components to meet the application demands, e.g. ultracapacitors and lithium-ion. The reasons of such division are primarily energy density and rate of charge or discharge. Power surges, energy loss distribution and temperature fluctuations often have detrimental effects on the performance and life of the energy storage systems.[28,29]

These facts lead to a number of considerations, most importantly appropriate application of a mix of energy storage and fault diagnosis and failure prognosis. This first part, appropriate design and application of a storage system, requires an adequate understanding of the macroscopic characteristics of each component, and an analysis of the system operation. [30, 31] Secondly, recognizing that the storage system is in a state that can be considered a precursor to a fault, and predicting the remaining life of the storage system (subjected to expected operating conditions) are vital tasks, the methods that are used range from basic estimation of the Thevenin model of the system to the signal processing of the current signatures and the use of complex models such as Hidden Markov models. [32,33]

We are interested in two groups of characteristics of the energy storage components: steady state and transient. These are of interest for both the healthy and fault modes.

Healthy Mode Operation. Both types of devices, batteries and supercapacitors, can be modeled electrically through a complex version of a Thevenin equivalent circuit, usually as a ladder circuit of capacitors and resistors. Such models are needed used to study the transient behavior of healthy systems during fast charging and discharging and help determine the principle of operation and the appropriate split of storage in a hybrid vehicle between batteries and supercapacitors. [34,35]

Although analytical models are available, [36, 37] the parameters of the models can and should be determined or verified experimentally. In our laboratory we have inverters and regenerative loads of several kW ratings to perform these tests on small devices. Furthermore, as a test bed for a large system we plan to use two setups:

1. The baseline and prototype hybrid electric buses designed through our current project. At present the operational baseline bus uses only lithium-ion batteries of 45Ah, 360V (16kWh), but the prototype bus will use batteries along with supercapacitors.
2. The hybrid breadboard powertrain that is under construction to be used at MSU. The dynamometer testing setup will be ready in October 2009 and available in November for this project. The present battery system is the same 16kWh as the baseline bus

Fault Diagnosis and Prognosis. Faults in both batteries and supercapacitors can have a number of causes and manifestations. The two major causes are overcharging and internal faults, although others are possible. Both causes lead to degradation of performance and eventual open or short circuit. They present themselves as changes of the parameters of the equivalent circuit and as short transients on the terminal current and voltages. [38,39,40,41]

We plan to develop methods to recognize and categorize faults from the steady state parameter characterization and from the transient signature analysis. To do so we will use minimally invasive electrical tests, like injecting a low power frequency in the system and measuring the system response, and non-invasive time-frequency analysis on the voltage and current under normal load conditions. Starting from the characterization of faults we will use prognosis methods like Hidden Markov Models to study the progression of faults and estimate remaining useful life.

To minimize cost extensive testing will be conducted in small components using artificially introduced faults as well as faults created through thermal and electrical stresses. Full size systems will also be tested, with the careful introduction of components previously tested and characterized.

Description of Research Tasks:

Task 1. Study the characteristics of existing, experimental and commercially available, energy storage devices and the way that they can be used in standard applications with different steady state and transient demands. Develop models beyond what is available, including a mix of devices.

Task 2. Study the characteristics of the energy storage devices developed in this project and the way that they can be used in standard applications with different steady state and transient demands. Evaluate their performance in complex systems.

Task 3. Identify failure modes in existing and proposed energy storage systems and their manifestation in steady state performance and in transient resulting from internal intermittent fault precursors. Develop theoretical and simulation models and validate with experiments are possible, using naturally occurring and/or artificially induced faults.

Task 4. Develop failure models and appropriate algorithms for fault prognosis and diagnosis, implement them and apply them as possible on collected data.

Summary of Strangas Group Scientific Progress and Accomplishments

The objective of this work was to perform online and precise health monitoring of batteries under thermal abuse conditions. Thermal abuse creates various faults in the battery which change the battery's response to the load and charger. A faulty battery's current signal differs from a healthy one in normal cycling operation. This difference is not readily distinguishable in the time domain signal whereas using time-frequency representations such as wavelet transforms, the health informative features embedded in the current signal can be extracted. The features extracted from the healthy and faulty batteries were categorized using a classification algorithm and state-of-health of each battery is determined.

I. Healthy Mode Operation

The most common faults in batteries are caused by stresses such as aging, high and low temperatures, overcharging, overdischarging and high currents. These stresses cause negative impacts on the cells major characteristics such as calendar life, cycle life, capacity, power, and self-discharge; and in high intensities lead to catastrophic failures such as fire and explosion. The ultimate reliability goal for the battery-powered devices is precise and online health monitoring (i.e., estimation of state-of-health (SOH)) of the batteries using current, voltage and temperature readings over time. Health condition of a cell is a fault diagnosis problem in which given the current, voltage and temperature readings over time, fault(s) created in the batteries is(are) diagnosed and their impacts on the cell performance are determined.

High and low temperatures stresses are the most eminent stresses for batteries in many applications. If the lithium-ion batteries operating or storage temperature exceeds the safe temperature range specified by the battery manufacturer (i.e., about -20°C to 50°C), faults will be created in the batteries. The more the thermal abuse, the higher the fault severity. For instance, 80°C exposure creates various faults in the battery which weaken the battery's performance but, at higher temperatures (i.e., $> 120^{\circ}\text{C}$) faults lead to catastrophic failures. Although many studies have been performed to indicate the SOH status based on chemical analysis, columbic efficiency and batteries models developed using impedance measurement, Kalman filter or sliding-mode observers, several shortcomings have been identified. The chemical analysis are hard to apply to electrical circuits. Model-based methods suffer from the model inaccuracies and also are not precise in conditions that are different from the training set. The impedance measurement method shows good accuracy but is very expensive to implement and also should be performed offline which is not feasible in many applications. The Kalman filter method should be performed in the zero-

mean noise environment and the computational burden is high due to complex matrix operations.

The objective of this work is to perform online and precise health monitoring of batteries under thermal abuse conditions. Thermal abuse creates various faults in the battery which change the battery's response to the load and charger. A faulty battery's current signal differs from a healthy one in normal cycling operation. The difference can be in the form of high frequency noise on the current signal. Using time-frequency representations (TFRs) such as wavelet transform, features embedded in the TFRs of the current signal of the batteries with different SOH (i.e., exposed to different levels of thermal abuse) will be extracted. The extracted features are expected to be discriminative in an n-dimensional space. The discriminative features will be categorized using different classification algorithms. The categorization aids us to determine the SOH of the batteries exposed to different levels of thermal abuse.

A computer-controlled heating-cooling chamber was employed to apply high temperature stresses to the batteries. The chamber's temperature was controllable manually and automatically. A constant-current computer-controlled battery cycler (charger-discharger) consisting of a Printed-Circuit-Board, power converters, two DC power supplies, a data acquisition card and a PC with LabVIEW software was designed, installed and used. A protocol for cyclical thermal aging of batteries was designed and implemented.

The current signal of a faulty battery differs from a healthy one in normal cycling operation. This difference is not readily distinguishable in the time domain, whereas using time-frequency representations such as wavelet transforms, the health informative features embedded in the current signal can be extracted.

II. Fault Diagnosis And Prognosis

Healthy mode operation We tested a limited number of batteries. First the data (i.e., 40 samples taken at 500kHz and 100kHz from each of the 6 healthy and thermally stressed batteries) was divided into training and testing sets and the health informative features were extracted from the current signals using the wavelet packet transform (WPT) and stationary wavelet transform (SWT), and classified via k- nearest-neighbor (k-NN) classifier. Since not much data for training and testing were available, leave-one-out cross-validation approach is opted. Both the SWT and WPT performance are 100% for all samples. The developed method, although promising, was never fully tested, as the project ended before a large number of samples were obtained.

PUBLICATIONS

1. J. Wolfenstine, H. Jo, Y-H. Cho, I. David, P. Askeland, E. D. Case, H. Kim, H. Choe and J. Sakamoto, A preliminary investigation of fracture toughness of $\text{Li}_7\text{La}_3\text{Zr}_2\text{O}_{12}$ and its comparison to other solid Li-ion conductors, *Mater. Lett.* Accepted Jan 2013.
2. E. Rangasamy, J. Wolfenstine, J. Allen and J. Sakamoto, The effect of 24c-site (A) cation substitution on the tetragonal-cubic phase transition in $\text{Li}_{7-x}\text{La}_{3-x}\text{A}_x\text{Zr}_2\text{O}_{12}$ garnet-based ceramic electrolyte, *J. Power Sources*, Accepted December (2012).
3. D-Y. Kim, J-C. Yang, H-W. Kim and G. M. Swain, "The Voltammetric Response and Electrocapacitance of sp^3 -bonded Carbon Powders in an Aqueous Electrolyte and an Ionic Liquid: Comparisons with Conventional sp^2 -bonded Powders," submitted to *Chemistry of Materials*.
4. J. Wang, D-Y. Kim, J-C. Yang, H-W. Kim and G. M. Swain, "Electrolyte and Temperature Effects on Electron Transfer Kinetics of $\text{Fe}(\text{CN})_6^{3-/4}$ at Boron-Doped Diamond Thin-Film Electrodes," in preparation for submission to *J. Am. Chem. Soc.*
5. D-Y. Kim, J-C. Yang, H-W. Kim and G. M. Swain, "Electron Transfer Kinetics of Ferrocene Carboxylic Acid at Boron-Doped Diamond Electrodes: A Comparison of an Aqueous Electrolyte and an Ionic Liquid," in preparation for submission to *J. Electrochem. Soc.*
6. D-Y. Kim, A. Yoonyoung Cho and G. M. Swain, "Double-Layer Capacitance and Electron Transfer Kinetics at Chemically Modified Graphene and HOPG," in preparation for submission to *Langmuir*.
7. S. Biswas, and L. T. Drzal, "Multilayered Nano-Architecture of Variable Sized Graphene Nanosheets for Enhanced Supercapacitor Electrode Performance" ACS Applied Materials & Interfaces, ID: am-2010-00343a , Published July 10, 2010.
8. S. Biswas and L. T. Drzal, "Multilayered Nano Architecture Of Graphene Nanosheets And Polypyrrole Nanowires For High Performance Supercapacitor Electrodes" Chem Materials, DOI:10.1021/cm101132g Published September 30 (2010).
9. S. Biswas and L. T. Drzal, "Effect of Reduction of Oxygen Functional Groups at the Edges of Graphene Nanosheets on Electrical and Capacitative Properties" in preparation 2010.
10. S. Biswas and L. T. Drzal, "Self Assembly of Highly Hydrophilic Nanosheets of Manganese Dioxide at the Liquid-Liquid Interface for Electrochemical Energy Storage Applications" in preparation 2010.
11. J. Sakamoto, H. J. Kim, R. Maloney, I. Do, H. Fukushima, and L. T. Drzal, "Synthesis of exfoliated graphite nanoplatelet (GnP) composite carbon aerogels for use in supercapacitors," Spring 2010, Materials Research Society Meeting in San Francisco, CA.
12. Strangas, E.; Aviyente, S.; Zaidi, S.; Neely, J.; , "The Effect of Failure Prognosis and Mitigation on the Reliability of Permanent Magnet AC Motor Drives," *IEEE Transactions on Industrial Electronics*, , vol. PP, no.99, pp.1, 2011 2012 IEMDC conference.
13. E. Strangas, XXth International Conference on Electrical Machines (ICEM'2012) Palais des Congrès et des Expositions de Marseille France, September 2-5,2012. Fault Diagnosis, Prognosis and Reliability of Electrical Drives.

14. Weigui Ji, Xi Lu, Yuan Ji, Yingbin Tang, Feng Ran, and Fang Zheng Peng, "Low cost battery equalizer using buck-boost and series LC converter with synchronous phase-shift control," Applied Power Electronics Conference and Exposition (APEC), 2013 Twenty-Eighth Annual IEEE, March 2013.
15. X. Lu, W. Qian, F. Z. Peng, "Modularized buck-boost + Cuk converter for high voltage series connected battery cells", *IEEE Applied Power Electronics Conference and Exposition*, Orlando, FL, Mar. 2012, pp. 2272-2278.
16. W. Qian, J. Cintron-Rivera, S. Han, X. Lu and F. Z. Peng, "Management and control of energy storage systems," presentation at *the Joint 2010 IEEE Nanotechnology Materials and Devices Conference and 1st IEEE International Symposium on Energy, Environment, Safety and Security*, Monterey, CA, USA, Oct., 2010.

STUDENTS SUPPORTED

Baker (Chemistry): Hui Zhao, Gregory Spahlinger

Drzal (Chemical Engineering and Materials Science): Sanjib Biswas, Anchita Monga, Deb Kumar Saha

Swain (Chemistry): Hyoun Woo Kim, PhD, Ju Chan Yang, Grad., Anna Y. Cho, UG

Hogan (Electrical Engineering): Chun-I Wu, PhD., Karl Dersch (technician),

Hawley (Chemical Engineering and Materials Science): Susan Farhat

Sakamoto (Chemical Engineering and Materials Science): Hyun Joong Kim, PhD., Ezhiyl Rangasamy, Grad

Peng (Electrical Engineering): Wei Qian, Xi Lu, Shuai Jiang, Jorge Cintron-Rivera, UG summer

Strangas (Electrical Engineering): Ramin Amiri

TECHNOLOGY TRANSFER

- Commercial development of Graphene Nanoplatelets (xGnP) for use in Li Ion batteries and Supercapacitors is being developed through XG Sciences. (Drzal)
- Oak Ridge National Lab: Dr. N. Dudney Battery and Neutron Diffraction Groups (Sakamoto)
- Naval Research Lab (Dr. M. Johannes: theoretical physicist) (Sakamoto)
- Research sponsorship by GM and NSF (Strangas)
- Proposal Awarded from TARDEC, "Ceramic electrolyte membrane technology: enabling revolutionary electrochemical energy storage" PI Jeff Sakamoto, Co-I Eldon Case (MSU).
- Proposal submitted to ARO, "Joint experimental and theoretical investigations into a new class of ceramic electrolyte enabling all solid state and inorganic energy storage" PI Jeff Sakamoto, Co-I Michelle Johannes (NRL).
- J. Sakamoto, E. Rangasamy, H. Kim, R. Maloney, Y. Kim, "Methods of making and using oxide ceramic solids and products and devices related thereto", Filed non-Provisional Patent, 3000.048US1, TEC2011-0073-01US, MSU (2012). This patent

protects the technology supporting a recent award from TARDEC to advance the TRL: Proposal Awarded from TARDEC, "Ceramic electrolyte membrane technology: enabling revolutionary electrochemical energy storage" PI Jeff Sakamoto, Co-I Eldon Case (MSU).

REFERENCES

1. K.-M. Lina, K.-H. Changa, C.-C. Hua, Y.-Y. Li, "Mesoporous RuO₂ for the Next Generation Supercapacitors with an Ultrahigh Power Density," *Electrochimica Acta*, vol. 54, pp. 4574–4581, (2009).
2. J. Liu, Y. Li, X. Huang, "ZnO Nanoneedle Arrays Directly Grown on Bulk Nickel Substrate for Li Ion Battery Electrodes with Improved Performance," *2008 2nd IEEE International Nanoelectronics Conference (INEC 2008)*.
3. H. Wang, Q. Pan, Y. Cheng, J. Zhao, G. Yin, "Evaluation of ZnO Nanorod Arrays with Dandelion-like Morphology as Negative Electrodes for Lithium-Ion Batteries," *Electrochimica Acta*, vol. 54, pp. 2851–2855, (2009).
4. H. J. Fan, Y. Yang, M. Zacharias, "ZnO-based Ternary Compound Nanotubes and Nanowires," *Journal of Materials Chemistry*, vol. 19, pp. 885–900, (2009).
5. H. Kim, J. Cho, "Hard Templating Synthesis of Mesoporous and Nanowire SnO₂ Lithium Battery Anode Materials," *Journal of Materials Chemistry*, vol. 18, pp. 771–775, (2008).
6. J. Liu, Y. Li, X. Huang, R. Ding, Y. Hu, J. Jiang, L. Liao, "Direct Growth of SnO₂ Nanorod Array Electrodes for Lithium-Ion Batteries," *Journal of Materials Chemistry*, vol. 19, pp. 1859–1864, (2009).
7. M.-S. Park, G.-X. Wang, Y.-M. Kang, D. Wexler, S.-X. Dou, H.-K. Liu, "Preparation and Electrochemical Properties of SnO₂ Nanowires for Application in Lithium-Ion Batteries," *Angewandte Chemie International Version*, vol. 46, pp. 750–753, (2007).
8. C. K. Chan, H. Peng, G. Liu, K. McIlwrath, X. F. Zhang, R. A. Huggins, Y. Cui, "High-Performance Lithium Battery Anodes Using Silicon Nanowires," *Nature Nanotechnology*, vol. 3, pp. 31–35, (2008).
9. C. K. Chan, X. F. Zhang, Y. Cui, "High Capacity Li Ion Battery Anodes Using Ge Nanowires," *Nano Letters*, vol. 8, no. 1, pp. 307–309, (2008).
10. Whittingham, M. "Materials Challenges Facing Electrical Energy Storage." *MRS Bulletin*. 33: 411–420. 2008.
11. Lu, J. and C. Wong. "Recent Advances in High-k Nanocomposite Materials for Embedded Capacitor Applications." *IEEE Transactions on Dielectrics and Electrical Insulation*. 15 (5). 2008.
12. Rao, Y., et al. "Novel Polymer-Ceramic Nanocomposites Based on High Dielectric Constant Epoxy Formula for Embedded Capacitor Application." *Journal of Applied Polymer Science*. 83: 1084–1090. 2002.
13. Rao, Y. and C. Wong. "Material Characterization of a High Dielectric Constant Polymer-Ceramic Composite for Embedded Capacitor for RF Applications." *Journal of Applied Polymer Science*. 92: 2229–2231. 2004.
14. Killips, D. Composite material design and characterization for RF applications. Ph.D Thesis, Michigan State University, 2007.
15. Munk, B. Frequency Selective Surfaces: Theory and Design. John Wiley & Sons. 2000.
16. J.R. Belt, C.D. Ho, T.J. Miller, M.A. Habib, T.Q. Duong, *J. Power Sources* **142** (2005) 354–360
17. A.N. Jansen, D.W. Dees, D.P. Abraham, K. Amine, G.L. Henriksen, *J. Power Sources* **174** (2007) 373–379.

-
18. C.-K. Huang, J. S. Sakamoto, J. Wolfenstine, R. Surampudi, *J. Electrochem. Soc.*,
 19. J. Fan, S. Tan, *J. Electrochem. Soc.* **153** (2006) A1081-A1092.
 20. S.S. Zhang, K. Xu, T.R. Jow, *Electrochim. Acta* **48** (2002) 241-246.
 21. J. Fan, S. Tan, *J. Electrochem. Soc.* **153** (2006) A1081-A1092.
 22. J. Cousseau, C. Siret, P. Biensan, M. Broussely, *J. Power Sources* **162** (2006) 790-796.
 23. "FreedomCar Battery Test Manual For Power-Assist Hybrid Electric Vehicles", DOE/ID-11069, available at <http://www.uscar.org> (2003).
 24. J. Hassoun, G. Derrien, S. Panero and B. Scrosati, *Adv. Mater.*, **20** (2008) 3169-3175
 25. <http://www.epsrc.ac.uk/PressReleases/oxlithbattery.htm>
 26. K. Kang, B. Lee, J. Lee, *Carbon*, **47**, (2009) 1171-1180.
 27. S. Sepehri, B. Garcia, Q. Zhang, G. Cao, *Carbon*, **47** (2009) 1436-1443.
 28. Miller, J.M.; McCleer, P.J.; Everett, M.; Strangas, E.G.; Ultracapacitor Plus Battery Energy Storage System Sizing Methodology for HEV Power Split Electronic CVT's, ISIE 2005. Proceedings of the IEEE International Symposium on Industrial Electronics, 2005. Volume 1, June 20-23, 2005, Page(s):317 – 324.
 29. Schaltz, E.; Khaligh, A.; Rasmussen, P.O.; Investigation of battery/ultracapacitor energy storage rating for a Fuel Cell Hybrid Electric Vehicle IEEE Vehicle Power and Propulsion Conference, 2008. VPPC '08. 3-5 Sept. 2008, Page(s):1 – 6.
 30. Lijun Gao; Dougal, R.A.; Shengyi Liu; Power enhancement of an actively controlled battery/ultracapacitor hybrid, IEEE Transactions on Power Electronics Volume 20, Issue 1, Jan. 2005, Page(s):236 – 243.
 31. Yuchen Lu; Hess, H.L.; Edwards, D.B.; Adaptive Control of an Ultracapacitor Energy Storage System for Hybrid Electric Vehicles, IEEE International Electric Machines & Drives Conference, 2007, IEMDC '07. Volume 1, 3-5 May 2007, Page(s):129 – 133.
 32. Gualous H.; Louahlia-Gualous, H.; Gallay, R.; Miraoui, A.; Supercapacitor Thermal Modeling and Characterization in Transient State for Industrial Applications, IEEE Transactions on Industry Applications, Volume 45, Issue 3, May-June 2009 Page(s):1035 – 1044.
 33. El Brouji, H.; Vinassa, J.-M.; Briat, O.; Lajnef, W.; Bertrand, N.; Woirgard, E.; Parameters evolution of an ultracapacitor impedance model with ageing during power cycling tests IEEE Power Electronics Specialists Conference, 2008, PESC 2008.
 34. Alcicek, G.; Gualous, H.; Venet, P.; Gallay, R.; Miraoui, A.; Experimental study of temperature effect on ultracapacitor ageing 2007 European Conference on Power Electronics and Applications, 2-5 Sept. 2007, Page(s):1 – 7
 35. Yu Zhang; Zhenhua Jiang; Xunwei Yu; Control Strategies for Battery/Supercapacitor Hybrid Energy Storage Systems, IEEE Energy 2030 Conf, 2008. ENERGY 2008. 17-18 Nov. 2008:1 – 6.
 36. Marie-Francoise, J.-N.; Gualous, H.; Berthon, A.; Supercapacitor thermal- and electrical-behaviour modelling using ANN, IEE Proceedings -Electric Power Applications, Volume 153, Issue 2, 2 March 2006, Page(s):255 – 262.
 37. Belyakov, Alexey I.; Sojref, Dalik A.; High power supercapacitor's solutions for reliable power supply, International Conference on Power Engineering, Energy and Electrical Drives, 2009. 18-20 March 2009 Page(s):348 – 352.
 38. Loud, J.; Nilsson, S.; Yanqing Du; On the testing methods of simulating a cell internal short circuit for lithium ion batteries, The Seventeenth Annual Battery Conference on Applications and Advances, 15-18 Jan. 2002, Page(s):205 – 208.
 39. Laidig, M.R.; Wurst, J.W.; Technology implementation of stationary battery failure prediction. Proceedings of the Ninth Annual Battery Conference on Applications and Advances. 11-13 Jan. 1994, Page(s):168 – 172.

-
40. Gun, J.-P.; Fiorina, J.N.; Fraisse, M.; Mabboux, H.; Increasing UPS battery life main failure modes, charging and monitoring solutions. 19th International Telecommunications Energy Conference, 1997. INTELEC 97, 19-23 Oct. 1997, Page(s):389 – 396.
 41. Yamaguchi, Y.; Hirakawa, K.; Hojo, E.; Nakayama, Y.; Life performance and failure mode analysis of improved, large VRLA batteries, used in a 20 kW load-leveling installation. Twenty-Third International Telecommunications Energy Conference, 2001. INTELEC 2001.